

**Mathematical Models for  
Rain-wind Induced Vibrations  
of Simple Structures**



# Mathematical Models for Rain-wind Induced Vibrations of Simple Structures

Proefschrift

ter verkrijging van de graad van doctor  
aan de Technische Universiteit Delft,  
op gezag van de Rector Magnificus prof.dr.ir. J. T. Fokkema,  
voorzitter van het College voor Promoties,  
in het openbaar te verdedigen  
op woensdag 30 juni 2004 te 10.30 uur

door

**HARTONO**

Magister Sains Matematika  
Institut Teknologi Bandung, Indonesië

geboren te Kediri, Indonesië.

*Dit proefschrift is goedgekeurd door de promotor:*

Prof. dr. ir. A.W. Heemink

*Toegevoegd promotor:* Dr. ir. W.T. van Horsen

*Samenstelling promotiecommissie:*

Rector magnificus,	voorzitter
Prof. dr. ir. A.W. Heemink,	Technische Universiteit Delft, promotor
Dr. ir. W.T. van Horsen,	Technische Universiteit Delft, toegevoegd promotor
Prof. I.V. Andrianov,	Pridneprovska State Academy
Prof. dr. ir. P.G. Bakker,	Technische Universiteit Delft
Prof. dr. H.G. Meijer,	Technische Universiteit Delft
Prof. dr. E. Soewono,	Bandung Institute of Technology
Prof. dr. F. Verhulst,	Rijks Universiteit Utrecht

Hartono

Mathematical Models for Rain-wind Induced Vibrations of Simple Structures.

Thesis Delft University of Technology.

With summary in Dutch.

ISBN 90-xxxx-xxx-x

Copyright ©2004 by Hartono

All rights reserved. No part of the material protected by this copyright notice may be reproduced or utilized in any form or by any means, electronic or mechanical, including photocopying, recording or by any information storage and retrieval system, without written permission from the copyright holder.

Printed by [OPTIMA] Grafische Communicatie, Rotterdam

*To my family*

# Contents

<b>1</b>	<b>Introduction</b>	<b>1</b>
<b>2</b>	<b>Higher Order Averaging</b>	<b>3</b>
2.1	Introduction . . . . .	3
2.2	Existence and Stability of Periodic Solutions . . . . .	4
2.3	Higher Order Averaging for Linear Equations . . . . .	10
2.4	Application . . . . .	12
2.4.1	THE CASE $m = \omega$ . . . . .	13
2.4.2	THE CASE $m \neq \omega$ . . . . .	19
2.5	Conclusion . . . . .	19
<b>3</b>	<b>Time-periodic Damping</b>	<b>21</b>
3.1	Introduction . . . . .	21
3.2	Coexistence of Time Periodic Solutions and the Stability Diagram . .	22
3.3	An application in the theory of rain-wind induced vibrations. . . . .	28
3.3.1	The Model Equation for Rain-Wind Induced Vibrations of a Prototype Oscillator . . . . .	30
3.3.2	The non-linear model . . . . .	35
3.4	Conclusions and Remarks . . . . .	38
3.5	Appendix . . . . .	39
<b>4</b>	<b>Rain-wind Induced Vibrations</b>	<b>45</b>
4.1	Introduction . . . . .	45
4.2	A model equation with time-varying mass and lift and drag forces . .	46
4.3	The non-linear model . . . . .	51
4.3.1	Fixed position of water ridge and time-varying mass . . . . .	51
4.3.2	Constant mass and varying position of water ridge . . . . .	54
4.3.3	Mass and position of water ridge vary both with time . . . . .	56
4.4	Conclusions . . . . .	61
4.5	Appendix . . . . .	62
<b>5</b>	<b>A Seesaw Oscillator</b>	<b>67</b>
5.1	Introduction . . . . .	67

5.2	Derivation of the equation of motion . . . . .	68
5.3	Case I : $q_1 < 0$ and $q_2 < 0$ . . . . .	71
5.4	Case II : $q_1 < 0$ and $q_2 > 0$ . . . . .	74
5.5	Conclusion . . . . .	75
<b>Summary</b>		<b>81</b>
<b>Samenvatting</b>		<b>83</b>
<b>Acknowledgments</b>		<b>85</b>
<b>Curriculum Vitae</b>		<b>87</b>

# List of Figures

1.1	Cross section of the spring and the seesaw type model. . . . .	1
2.1	Stability diagrams for the periodic solutions of equation (2.4.1) for $m = \omega = 1$ . In the shaded regions the periodic solutions are unstable. . . . .	15
2.2	Curves on which the eigenvalues of (2.4.8) and (2.4.9) are zero and on both sides of the curves the eigenvalues are purely imaginary. . . . .	17
2.3	Stability diagrams for the periodic solutions of equation (2.4.1) for $m = \omega = 3$ . In the shaded regions the periodic solutions are unstable. . . . .	19
3.1	In the shaded regions the trivial solution is unstable. On the curves separating the white and shaded regions periodic solution exist. Figure 3.1a the Mathieu stability diagram. Figure 3.1b the new stability diagram. . . . .	24
3.2	Stability diagram of equation (3.2.17) for various values of $b$ . The shaded regions are areas of instability. When $b = 0$ the instability areas have disappeared for $\lambda = 4n^2$ . . . . .	29
3.3	Cross-section of the cylinder-spring system, fluid flow with respect to the cylinder and wind forces on the cylinder . . . . .	31
3.4	Separation of the instability tongue: Figure 3.4a: $a_o = 0$ , Figure 3.4b: $a_o \neq 0$ . . . . .	34
3.5	Orbits of equation (3.3.22) for $A=0$ , $A=0.1$ , $A=0.1420$ and $A=0.25$ . Vertical axis is $\bar{y}_2$ and horizontal axis is $\bar{y}_1$ . . . . .	37
3.6	Curve relation between $\bar{y}_1$ and $\eta$ after using Gröbner basis algorithm. Vertical axis is $\bar{y}_1$ and horizontal axis is $\eta$ . . . . .	38
3.7	Orbits of equation (3.3.27) for $A = 0.1$ and $\eta = 0.1$ , $\eta = 0.2$ . Vertical axis is $\bar{y}_2$ and horizontal axis is $\bar{y}_1$ . . . . .	38
4.1	Cross-section of the cylinder-spring system, fluid flow with respect to the cylinder and wind forces on the cylinder . . . . .	47
4.2	Aerodynamic drag and lift coefficients . . . . .	48
4.3	Inside the cone and hyperboloid the critical point is stable . . . . .	50
4.4	The phase portrait of (4.3.3) for $a_2 = 0.6$ and $a_2 = 4$ , $b_2 = 0$ , $\eta = 0$ , $C_{L3} = 2$ , $C_{L1} = -6$ , $C_{D_o} = 1/2$ , $\beta/\omega = 2$ and $K = 1$ . . . . .	52



4.5	The phase portraits of equation (4.3.3) for several values of $\eta$ , the detuning parameter, $a_2 = 4$ , $b_2 = 0$ , $C_{L_3} = 2$ , $C_{L_1} = -6$ , $C_{D_o} = 1/2$ , $\beta/\omega = 2$ and $K = 1$ . . . . .	52
4.6	Relation between $r$ and $\eta$ of formula (4.3.10). . . . .	54
4.7	4.7a. Critical points $(0, \bar{y}_2)$ of (4.3.11) as a function of $A$ for $\eta = 0$ . 4.7b. The phase portrait of (4.3.11) for $A = 0.1$ and $\eta = 0$ . . . . .	55
4.8	Relation between $\bar{y}_2$ and $\eta$ by using a Gröbner basis algorithm. . . . .	55
4.9	Orbits of equation (4.3.11) for $A = 0.1$ and $\eta = 0.1$ , $\eta = 0.2$ . . . . .	55
4.10	Critical points $(\bar{y}_1, \bar{y}_2)$ of system (4.3.12) as a function of $A$ where $d_1 = 0$ , $a_2 = 4$ , $b_2 = 0$ and $\eta = 0$ . . . . .	57
4.11	The phase portraits of equation (4.3.12) for several values of $A$ , the amplitude of the variation of the position of the water ridge. The variation of the mass of rainwater has in this case a constant amplitude $a_2 = 4$ , $b_2 = 0$ . . . . .	57
4.12	Critical points $(\bar{y}_1, \bar{y}_2)$ of system (4.3.12) as a function of $a_2$ , where $c_1 = A = 0.1$ , $d_1 = 0$ , $b_2 = 0$ and $\eta = 0$ . . . . .	59
4.13	The phase portraits of system (4.3.12) for several values of $a_2$ , the amplitude of the variation of the mass of rain water. The variation of the position of the water ridge has constant amplitude $A = 0.1$ . . . . .	59
4.14	The phase portraits of equation (4.3.12) for several values of $\eta$ , the detuning parameter, $a_2 = 4$ , $b_2 = 0$ , $C_{L_3} = 2$ , $C_{L_1} = -6$ , $C_{D_o} = 1/2$ , $\beta/\omega = 2$ , $K = 1$ and $A = 0.1$ . . . . .	61
5.1	The cross-section of the seesaw oscillator, the fluid flow with respect to the cylinder, and the definitions of the angles $\alpha$ , $\alpha_s$ , and $\theta$ . . . . .	68
5.2	The aerodynamic torsion coefficient $C_M(\alpha)$ . . . . .	70
5.3	Critical points $(\bar{y}_1, \bar{y}_2)$ of system (5.2.14) as function of $A$ , where $\mu = 1$ , $c_1 = -3$ , $c_3 = 2$ , $\beta_\theta = 1$ and $\eta = 0$ . . . . .	72
5.4	The phase portraits of system (5.2.14) for several values of $A$ , and $\mu = 1$ , $c_1 = -3$ , $c_3 = 2$ , $\beta_\theta = 1$ and $\eta = 0$ . . . . .	72
5.5	Critical points $(\bar{y}_1, \bar{y}_2)$ of system (5.2.14) as a function of $\eta$ , where $\mu = 1$ , $c_1 = -3$ , $c_3 = 2$ , $\beta_\theta = 1$ and $A = 0.1$ . . . . .	73
5.6	The phase portraits of system (5.2.14) for several values of $\eta$ , where $\mu = 1$ , $c_1 = -3$ , $c_3 = 2$ , $\beta_\theta = 1$ and $A = 0.1$ . . . . .	73
5.7	Critical points $(\bar{y}_1, \bar{y}_2)$ of system (5.2.14) as a function of $A$ where $\mu = 1$ , $c_1 = -3$ , $c_3 = 2$ , $\beta_\theta = 1$ and $\eta = 0.3$ . . . . .	74
5.8	Critical points $(\bar{y}_1, \bar{y}_2)$ of system (5.2.14) as a function of $A$ where $\mu = 1$ , $c_1 = -3$ , $c_3 = 2$ , $\beta_\theta = 1$ and $\eta = 1$ . . . . .	74
5.9	Critical points $(\bar{y}_1, \bar{y}_2)$ of system (5.2.14) as a function of $A$ , where $\mu = 1$ , $c_1 = -2$ , $c_3 = 2$ , $\beta_\theta = 2$ and $\eta = 0$ . . . . .	75
5.10	Critical points $(\bar{y}_1, \bar{y}_2)$ of system (5.2.14) as a function of $A$ , where $\mu = 1$ , $c_1 = -2$ , $c_3 = 2$ , $\beta_\theta = 2$ , $\eta = 3$ . . . . .	75
5.11	The phase portraits of system (5.2.14) for $\mu = 1$ , $c_1 = -2$ , $c_3 = 2$ , $\beta_\theta = 2$ , and for different values of $A$ and $\eta$ . . . . .	76

# List of Tables

2.1	The first order averaged equation for (2.4.1) and its critical points for the case $m = \omega$ , $\mathbf{z}$ is a $2 \times 1$ column vector. . . . .	14
3.1	Comparison of the values of $\lambda$ in equation (3.2.3) obtained with the numerical method and the perturbation method for $\epsilon = 1$ . For this value (of $\lambda$ ) equation (3.2.3) has periodic solution. . . . .	26
4.1	The number of critical points and their stability of system (4.3.12) for several values of $A$ and $a_2$ , where $A$ = the amplitude of the variation of the position of the water ridge, $a_2$ = the amplitude of the variation of the mass of rain water, s = stable and u = unstable, c.p.= critical point, o.n.s.=origin is not a solution. . . . .	60

# Chapter 1

## Introduction

The aim of this thesis is to get a better insight in the mechanisms of rain-wind induced vibrations of elastic structures such as cables or bridges. The Erasmus bridge in Rotterdam and the Meikonishi bridge in the Nagoya harbor in Japan are examples of such elastic structures. The cables of these bridges are stable under dry wind conditions (no rain), but can become unstable when it is raining (see also [13]). This instability mechanism is due to the presence of a water rivulet along the surface of the cable. This mechanism was studied experimentally by Hikami [13], Matsumoto and others [17, 18]. Another instability mechanism can be caused by torsional flutter as for instance described in [21]. This instability mechanism might have been the cause of the collapse of the Tacoma Narrows bridge. In this thesis the vibrations are described in an ODE (that is, ordinary differential equation) setting. The first instability mechanism can then be described by spring type oscillators, and the torsional instability mechanism can be modelled by seesaw type oscillator (see Figure 1.1). The last 15 years a lot of researchers ( Van der Beek, Van der Burgh,

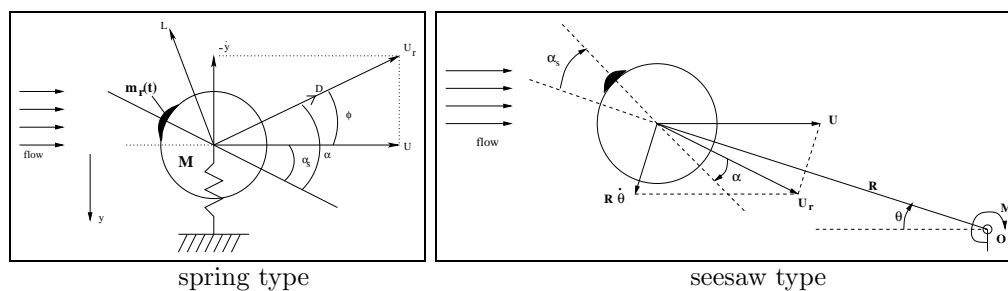


**Figure 1.1:** Cross section of the spring and the seesaw type model.

Van Horsen, Haaker, Waluya, Lumbantobing ( see [27, 31, 8, 34, 15] ) studied these type of oscillators for which the rivulet of water had a fixed position on the surface of the oscillators. In this thesis it is assumed that the position of the water rivulet on the surface of the oscillator varies harmonically in time. The equations that will

be derived in this thesis are the form

$$\ddot{z} + z = \epsilon H(z, \dot{z}, t), \quad \dot{\phantom{z}} = \frac{d}{dt} \quad (1.0.1)$$

where  $z = z(t)$  and  $\epsilon$  is a small parameter. First order or higher order averaging techniques, strained parameters methods, and numerical methods are used to determine the behaviour of the solutions of (1.0.1). Phase plane plots of the averaged equations will be presented by using the software package DSTOOLS, and a Gröbner basis algorithm in the software package Maple will be used to determine the critical points of the averaged equations.

The existence and the stability of periodic solutions of (1.0.1) by using a second order averaging technique (when the vector field by first order averaging vanishes) will be studied in chapter 2. Also generalizations to higher order will be considered. A special averaging algorithm for the computation of higher order approximations of the fundamental matrix of linear equations with periodic coefficients will be presented. As an application the existence and stability of periodic solutions of the following inhomogeneous second order equation with time-dependent damping coefficients will be studied in detail

$$\ddot{x} + (c + \epsilon \cos 2t)\dot{x} + (m^2 + \alpha)x + A \cos \omega t = 0, \quad (1.0.2)$$

where  $c, \alpha$ , and  $A$  are of  $O(\epsilon)$ ,  $0 < \epsilon \ll 1$ , and where  $m$  and  $\omega$  are positive integers. In chapter 3 the following second order differential equation with a time-dependent damping coefficient

$$\ddot{x} + (\epsilon \cos 2t)\dot{x} + \lambda x = 0 \quad (1.0.3)$$

will be studied. In fact (1.0.3) is a special case of (1.0.2). In particular the coexistence of the periodic solutions corresponding to vanishing domains of instability is investigated. It will also be shown that (1.0.3) can be used to study the linear stability properties for rain-wind induced vibrations of the oscillator of spring-type. In chapter 4 a nonlinear equation is derived to study the rain-wind induced vibrations of an oscillator of spring-type. As will be shown the presence of raindrops in the wind-field may have an essential influence on the dynamic stability of the oscillator. In this model equation the influence of the variation of the mass of the oscillator due to incoming flow of raindrops hitting the oscillator and a mass flow which is blown and shaken off, is investigated. The time-varying mass is modelled by a time harmonic function whereas simultaneously also time-varying lift and drag forces are considered.

Finally in chapter 5 a nonlinear equation will be derived to study the rain-wind induced vibrations of an oscillator of see-saw type. The model equations will be derived under the assumption that the position of the rivulet of water on the surface of the oscillator varies harmonically in time. In the last two chapters the existence and the stability of time-periodic solutions or of time-modulated solutions will be investigated. Several Hopf and saddle-node bifurcations will occur when the amplitude of the movement of the water rivulet on the oscillator is varied.

# Chapter 2

## Higher Order Averaging : periodic solutions, linear systems and an application <sup>†</sup>

**Abstract.** Existence and stability of periodic solutions by using second order averaging when the vector field by first order averaging vanishes, will be studied in this chapter as well as its generalization to higher order. A special averaging algorithm for the computation of higher order approximations of the fundamental matrix of linear equations with periodic coefficients is given. As an application the existence and stability of periodic solutions of an inhomogeneous second order equation with time-dependent damping coefficient are studied.

### 2.1 Introduction

The averaging method is a well-known method for the construction of approximations for solutions of initial value problems for a class of non-linear differential equations, as well as for finding periodic solutions. Usually the respective algorithm is concerned with first or second order approximations. Little attention has been paid to problems where third and higher order approximations have to be considered. Particularly for the construction of stability diagrams of linear equations with time varying coefficients like equations of Hill's type, these higher order approximations are relevant. For the construction of third and higher order approximations we will study two aspects in more detail: the existence of periodic solutions, in particular when from first and second order averaging no conclusions about existence of periodic solutions can be drawn and the algorithm for the construction of the approximations. The well-known theorem on the existence of time periodic solutions is based on the existence of critical points of the autonomous system obtained by

---

<sup>†</sup>This chapter is a revised version of [10], Higher Order Averaging : periodic solutions, linear systems and an application, *Nonlinear Analysis*, 52:1327-1346, 2003.

(first order) averaging. This theorem will be extended to the case that the system obtained by (first order) averaging vanishes identically. The algorithm for higher order averaging is straight forward: however because of the complexity little attention has been paid in applications. As is well-known the averaging method is of an asymptotic nature the respective asymptotic series may not converge. The situation for linear systems with time-varying coefficients is quite different. Consider a linear system of the form:

$$\dot{\mathbf{x}} = \epsilon \mathbf{A}(t, \epsilon) \mathbf{x}, \quad (2.1.1)$$

where  $\mathbf{A}(t, \epsilon)$  is  $T$ -periodic in  $t$  and  $\epsilon$  a small parameter. The averaging algorithm is concerned with the computation of the fundamental matrix  $\Phi(t, \epsilon)$  which can be represented (Floquet) by:

$$\Phi(t, \epsilon) = \mathbf{P}(t, \epsilon) e^{\mathbf{B}(\epsilon)t}, \quad (2.1.2)$$

where  $\mathbf{P}(t, \epsilon)$  is a  $T$ -periodic matrix and  $\mathbf{B}(\epsilon)$  a constant matrix. The algorithm implies the computation of approximations of  $\mathbf{P}(t, \epsilon)$  and  $\mathbf{B}(\epsilon)$  to any order of  $\epsilon$ . In the case that  $\mathbf{A}(t, \epsilon)$  is an analytic function in  $\epsilon$  for  $|\epsilon| < \epsilon_0$  one may assume that, as  $\mathbf{P}(t, \epsilon)$  and  $\mathbf{B}(\epsilon)$  are also analytic functions in  $\epsilon$  on the same interval, the power series for  $\mathbf{P}(t, \epsilon)$  and  $\mathbf{B}(\epsilon)$  obtained by the algorithm converge.

The organization of this chapter is as follows. In section 2 a theorem is discussed on the existence and stability of periodic solutions by using second order averaging when the vector field by first order averaging vanishes and a generalization of this theorem to higher order is presented. The approximations of the fundamental matrix of linear equations with periodic coefficients by using a special averaging algorithm are given in the section 3. At the end of this chapter an example, taken from [9], concerning the existence and stability of periodic solutions of an inhomogeneous second order equation with time-dependent damping coefficient is given.

## 2.2 Existence and Stability of Periodic Solutions

The existence and stability of periodic solutions by using first order averaging, has been studied extensively and can be found for instance in [20, 32]. In this section the existence and stability of periodic solutions (by using the second order averaging) in the case that the averaged vector field (to first order) vanishes, is investigated. A theorem on the validity of approximations for initial value problems in the case that the vector field by first order averaging vanishes is recalled.

*Theorem 1.2.1*

Consider the initial value problems :

$$\begin{cases} \dot{\mathbf{x}} = \epsilon \mathbf{f}(t, \mathbf{x}) + \epsilon^2 \mathbf{g}(t, \mathbf{x}) + \epsilon^3 \mathbf{R}(t, \mathbf{x}, \epsilon), \\ \mathbf{x}(0) = \mathbf{x}_0 \end{cases} \quad (2.2.1)$$

with

$$\mathbf{f}^o(\mathbf{y}) = \frac{1}{T} \int_0^T \mathbf{f}(s, \mathbf{y}) ds \equiv \mathbf{0}$$

and

$$\begin{cases} \dot{\mathbf{u}} = \epsilon^2 \mathbf{f}_1^o(\mathbf{u}) + \epsilon^2 \mathbf{g}^o(\mathbf{u}), \\ \mathbf{u}(0) = \mathbf{x}_o, \end{cases} \quad (2.2.2)$$

with  $\mathbf{f}, \mathbf{g} : [0, \infty) \times D \rightarrow \mathbb{R}^n$ ,  $\mathbf{R} : [0, \infty) \times D \times (0, \epsilon_o] \rightarrow \mathbb{R}^n$ , where  $D$  is a bounded domain in  $\mathbb{R}^n$ ,

$$\mathbf{f}_1^o(\mathbf{y}) = \frac{1}{T} \int_0^T \mathbf{f}_1(s, \mathbf{y}) ds, \quad \mathbf{g}^o(\mathbf{y}) = \frac{1}{T} \int_0^T \mathbf{g}(s, \mathbf{y}) ds,$$

$$\mathbf{f}_1(t, \mathbf{x}) = \frac{\partial \mathbf{f}(t, \mathbf{x})}{\partial \mathbf{x}} \mathbf{u}_1(t, \mathbf{x}) \quad \text{and} \quad \mathbf{u}_1(t, \mathbf{x}) = \int_0^t \mathbf{f}(s, \mathbf{x}) ds.$$

Suppose

1.  $\mathbf{f}, \mathbf{g}$  and  $\mathbf{R}$  are Lipschitz-continuous in  $\mathbf{x}$  on  $D$ ;  $\mathbf{f}, \mathbf{g}, \mathbf{R}$  are continuous in  $t$ ;
2.  $\mathbf{f}, \mathbf{g}$  and  $\mathbf{R}$  are  $T$ -periodic in  $t$ ,  $\mathbf{R}$  is bounded by a constant independent of  $\epsilon$  for  $\mathbf{x} \in D$ ;
3.  $\mathbf{u}(t)$  belongs to an interior subset of  $D$  on the time scale  $\frac{1}{\epsilon^2}$ ;
4. the vector fields  $\mathbf{f}, \mathbf{g}, \mathbf{R}, \partial \mathbf{f} / \partial \mathbf{x}, \partial^2 \mathbf{f} / \partial \mathbf{x}^2, \partial \mathbf{g} / \partial \mathbf{x}, \partial \mathbf{R} / \partial \mathbf{x}$  are defined continuous and bounded by a constant  $M$  (independent of  $\epsilon$ ) in  $[0, \infty) \times D, 0 \leq \epsilon \leq \epsilon_o$ ;

then

$$\mathbf{x}(t) = \mathbf{u}(t) + O(\epsilon),$$

on the time scale  $\frac{1}{\epsilon^2}$ .

A proof of this theorem can be found in [25].

The following theorem is related to the above one and is concerned with the existence of periodic solutions for the case that the vector field in first order averaging vanishes.

*Theorem 1.2.2*

Let  $\mathbf{f}^1 = \mathbf{f}_1^o + \mathbf{g}^o$  then equation (2.2.2) can be written as

$$\dot{\mathbf{u}} = \epsilon^2 \mathbf{f}^1(\mathbf{u}) \quad (2.2.3)$$

Suppose  $\mathbf{p}_o$  is a critical point of (2.2.3) and

$$|\partial \mathbf{f}^1(\mathbf{u}) / \partial \mathbf{u}|_{\mathbf{u}=\mathbf{p}_o} \neq 0, \quad (2.2.4)$$

then there exists a  $T$ -periodic solution  $\psi(t, \epsilon)$  of equation (2.2.1) which is close to  $\mathbf{p}_o$  such that

$$\lim_{\epsilon \rightarrow 0} \psi(t, \epsilon) = \mathbf{p}_o.$$

Further if  $\mathbf{f}^1$  is continuously differentiable in  $\mathbf{u}$  and the eigenvalues of the matrix  $\partial \mathbf{f}^1(\mathbf{p}_o) / \partial \mathbf{u}$  all have negative real parts, the corresponding periodic solution  $\psi(t, \epsilon)$  is asymptotically stable for  $\epsilon$  sufficiently small. If one of the eigenvalues has a positive real part,  $\psi(t, \epsilon)$  is unstable.

A proof of this theorem is a slight modification of the proofs of theorem 11.5 and 11.6 in [32]. To prove this theorem we need the following proposition and the Lipschitz's continuity of  $\mathbf{f}$ . As is well known the function  $\mathbf{f}(t, \mathbf{x})$  with  $\mathbf{f} : \mathbb{R}^{n+1} \rightarrow \mathbb{R}^n$ ,  $|t - t_o| \leq a$ ,  $\mathbf{x} \in \mathbf{D} \subset \mathbb{R}^n$ ; satisfies the Lipschitz condition with respect to  $\mathbf{x}$  if in  $[t_o - a, t_o + a] \times \mathbf{D}$

$$\|\mathbf{f}(t, \mathbf{x}_1) - \mathbf{f}(t, \mathbf{x}_2)\| \leq L\|\mathbf{x}_1 - \mathbf{x}_2\|,$$

with  $\mathbf{x}_1, \mathbf{x}_2 \in \mathbf{D}$  and  $L$  a constant. Furthermore,  $L$  is called a Lipschitz constant.

*Proposition.* Suppose that the functions  $\mathbf{f}$  and  $\mathbf{g}$  are Lipschitz continuous in  $\mathbf{x}$  and  $\alpha, \beta$  are real constants. Let  $\mathbf{f}^o$  be the average of  $\mathbf{f}$  over  $t$  i.e.  $\mathbf{f}^o(\mathbf{x}) = 1/T \int_0^T \mathbf{f}(t, \mathbf{x}) dt$  where in the general case  $\mathbf{f}^o(\mathbf{x})$  is not identical zero and

$$U(t, \mathbf{x}) = \int_0^t [\mathbf{f}(s, \mathbf{x}) - \mathbf{f}^o(\mathbf{x})] ds.$$

Then the functions  $\alpha\mathbf{f} + \beta\mathbf{g}$ ,  $\mathbf{f} \cdot \mathbf{g}$ , and  $U(t, \mathbf{x})$  are Lipschitz continuous in  $\mathbf{x}$ .

Proof of theorem 1.2.2. Consider the equation :

$$\dot{\mathbf{x}} = \epsilon\mathbf{f}(t, \mathbf{x}) + \epsilon^2\mathbf{g}(t, \mathbf{x}) + \epsilon^3\mathbf{R}(t, \mathbf{x}, \epsilon), \quad (2.2.5)$$

$\mathbf{f}$ ,  $\mathbf{g}$  are  $T$ -periodic in  $t$ . Introduce a "near-identity transformation"

$$\mathbf{x} = \mathbf{z} + \epsilon\mathbf{u}_1(t, \mathbf{z}) + \epsilon^2\mathbf{u}_2(t, \mathbf{z}). \quad (2.2.6)$$

Substituting (2.2.6) into (2.2.5) considering  $\mathbf{f}^o(\mathbf{x}) \equiv \mathbf{0}$  and choosing  $\mathbf{u}_1$  and  $\mathbf{u}_2$  as follows:

$$\mathbf{u}_1(t, \mathbf{z}) = \int_0^t \mathbf{f}(s, \mathbf{z}) ds, \quad \mathbf{u}_2(t, \mathbf{z}) = \int_0^t [\mathbf{g}(s, \mathbf{z}) + \frac{\partial \mathbf{f}}{\partial \mathbf{z}} \cdot \mathbf{u}_1 - \mathbf{f}^1] ds,$$

$$\mathbf{f}^1(\mathbf{z}) = \frac{1}{T} \int_0^T [\mathbf{g}(s, \mathbf{z}) + \frac{\partial \mathbf{f}}{\partial \mathbf{z}} \cdot \mathbf{u}_1] ds,$$

one obtains the transformed equation ( up to order  $\epsilon^3$  )

$$\dot{\mathbf{z}} = \epsilon^2\mathbf{f}^1(\mathbf{z}) + \epsilon^3\bar{\mathbf{R}}(t, \mathbf{z}, \epsilon), \quad (2.2.7)$$

where

$$\bar{\mathbf{R}}(t, \mathbf{z}, \epsilon) = \frac{\partial \mathbf{f}}{\partial \mathbf{z}} \cdot \mathbf{u}_2 + \frac{\partial \mathbf{g}}{\partial \mathbf{z}} \cdot \mathbf{u}_1 - \frac{\partial \mathbf{u}_1}{\partial \mathbf{z}} \cdot \mathbf{f}^1 + \quad (2.2.8)$$

$$\mathbf{G} + \mathbf{R}(t, \mathbf{z}, 0) + O(\epsilon),$$

in which  $\mathbf{G}$  is a vector with the  $k$ -th component  $\mathbf{G}_k$  as follows:

$$\mathbf{G}_k = \frac{1}{2} \sum_{i=1}^n u_{1i}^2 \frac{\partial^2 f_k}{\partial z_i^2} + \sum_{i \neq j}^n u_{1i} u_{1j} \frac{\partial^2 f_k}{\partial z_i \partial z_j},$$

$u_{1i}$  is  $i$ -th component of  $\mathbf{u}_1$ ,  $f_k$  is  $k$ -th component of  $\mathbf{f}$ , and  $z_i$  is  $i$ -th component of  $\mathbf{z}$ . The periodicity of  $\mathbf{f}$  and  $\mathbf{g}$  with respect to  $t$  implies the periodicity of  $\mathbf{u}_1$ ,  $\mathbf{u}_2$ , and



$\bar{\mathbf{R}}$ .

Introduce an initial value  $\mathbf{z}(0) = \mathbf{z}_o$  for equation (2.2.7). As an equivalent integral equation one obtains:

$$\mathbf{z}(t) = \mathbf{z}_o + \epsilon^2 \int_0^t [\mathbf{f}^1(\mathbf{z}) + \epsilon \bar{\mathbf{R}}] ds.$$

It may be clear that the solution of this equation depends on  $\epsilon$  as well as on  $\mathbf{z}_o$  i.e.  $\mathbf{z}(t) = \mathbf{z}(t, \epsilon, \mathbf{z}_o)$ .

Further, one can calculate  $\mathbf{z}(t+T)$  as follows :

$$\begin{aligned} \mathbf{z}(t+T) &= \mathbf{z}_o + \epsilon^2 \int_0^{t+T} [\mathbf{f}^1(\mathbf{z}) + \epsilon \bar{\mathbf{R}}] ds \\ &= \mathbf{z}_o + \epsilon^2 \int_0^T [\mathbf{f}^1(\mathbf{z}) + \epsilon \bar{\mathbf{R}}] ds + \epsilon^2 \int_T^{t+T} [\mathbf{f}^1(\mathbf{z}) + \epsilon \bar{\mathbf{R}}] ds. \end{aligned} \quad (2.2.9)$$

To have a time periodic solution for  $\mathbf{z}(t)$  with period  $T$  one should have  $\mathbf{z}(t) = \mathbf{z}(t+T)$  from which it follows that:

$$\mathbf{h}(\mathbf{z}_o, \epsilon) = \int_0^T [\mathbf{f}^1(\mathbf{z}) + \epsilon \bar{\mathbf{R}}] ds = \mathbf{0}.$$

As  $\mathbf{z} = \mathbf{z}(t, \mathbf{z}_o, \epsilon)$  one obtains for  $t = 0$ :  $\mathbf{z}(0, \mathbf{z}_o, \epsilon) = \mathbf{z}_o$  and when  $\epsilon$  equals zero one finds that  $\mathbf{z}(t, \mathbf{z}_o, 0) = \mathbf{z}_o$ . So evidently  $\mathbf{h}(\mathbf{p}_o, 0) = \mathbf{0}$ , and

$$\begin{aligned} \mathbf{h}(\mathbf{z}_o, 0) &= \int_0^T \mathbf{f}^1(\mathbf{z}(s, \mathbf{z}_o, 0)) ds \\ &= \int_0^T \mathbf{f}^1(\mathbf{z}_o) ds \\ &= T \mathbf{f}^1(\mathbf{z}_o). \end{aligned} \quad (2.2.10)$$

From (2.2.4) it follows that

$$|\partial \mathbf{h}(\mathbf{z}_o, 0) / \partial \mathbf{z}_o|_{\mathbf{z}_o = \mathbf{p}_o} \neq 0. \quad (2.2.11)$$

Finally according to the Implicit Function Theorem there exist a unique function  $\mathbf{p} : (-\epsilon_o, \epsilon_o) \rightarrow \mathbb{R}^n$  with  $\mathbf{p}(0) = \mathbf{p}_o$  and  $\mathbf{h}(\mathbf{p}(\epsilon), \epsilon) = \mathbf{0}$  for  $\epsilon \in (-\epsilon_o, \epsilon_o)$ . So  $\mathbf{h}(\mathbf{z}_o, \epsilon) = \mathbf{0}$  has unique solution  $\mathbf{z}_o(\epsilon)$  and  $\mathbf{z}_o(\epsilon) \rightarrow \mathbf{p}_o$  when  $\epsilon \rightarrow 0$ . Thus the transformed equation (2.2.7) has a  $T$ -periodic solution with initial value  $\mathbf{z}_o(\epsilon)$ . Suppose the solution is  $\psi_1(\mathbf{z}_o(\epsilon), t)$ . As  $\mathbf{u}_1$  and  $\mathbf{u}_2$  are time periodic, the original equation (2.2.1) has a  $T$ -periodic solution, that is

$$\psi(\mathbf{z}_o(\epsilon), t) = \psi_1 + \epsilon \mathbf{u}_1(t, \psi_1) + \epsilon^2 \mathbf{u}_2(t, \psi_1), \quad (2.2.12)$$

and satisfies  $\psi \rightarrow \mathbf{p}_o$  when  $\epsilon \rightarrow 0$ .

To study the stability of this periodic solution one can show that its stability depends on the stability of the periodic solution of the transformed system. First, set  $\mathbf{z} = \psi_1 + \mathbf{w}$ . Differentiating this term and substituting into (2.2.7) gives :

$$\begin{aligned} \dot{\mathbf{w}} + \dot{\psi}_1 &= \epsilon^2 \mathbf{f}^1(\psi_1 + \mathbf{w}) + \epsilon^3 \bar{\mathbf{R}}(t, \psi_1 + \mathbf{w}, \epsilon) \\ &= \epsilon^2 \mathbf{f}^1(\psi_1) + \epsilon^2 \frac{\partial \mathbf{f}^1(\psi_1)}{\partial \mathbf{w}} \mathbf{w} + \\ &\quad \epsilon^3 \bar{\mathbf{R}}(t, \psi_1, \epsilon) + \epsilon^3 \frac{\partial \bar{\mathbf{R}}(\psi_1)}{\partial \mathbf{w}} \mathbf{w} + O(\mathbf{w}^2). \end{aligned} \quad (2.2.13)$$

As is known  $\psi_1(t, \epsilon)$  is a periodic solution of the transformed equation (2.2.7), so

$$\dot{\psi}_1 = \epsilon^2 \mathbf{f}^1(\psi_1) + \epsilon^3 \bar{\mathbf{R}}(t, \psi_1, \epsilon), \quad (2.2.14)$$

and it follows that

$$\begin{aligned} \dot{\mathbf{w}} &= \epsilon^2 \frac{\partial \mathbf{f}^1(\psi_1)}{\partial \mathbf{w}} \mathbf{w} + \epsilon^3 \frac{\partial \bar{\mathbf{R}}(\psi_1)}{\partial \mathbf{w}} \mathbf{w} + O(\mathbf{w}^2) \\ &= \epsilon^2 \frac{\partial \mathbf{f}^1(\mathbf{p}_o)}{\partial \mathbf{w}} \mathbf{w} + \epsilon^2 \left[ \frac{\partial \mathbf{f}^1(\psi_1)}{\partial \mathbf{w}} - \frac{\partial \mathbf{f}^1(\mathbf{p}_o)}{\partial \mathbf{w}} \right] \mathbf{w} + \epsilon^3 \frac{\partial \bar{\mathbf{R}}(\psi_1)}{\partial \mathbf{w}} \mathbf{w} + O(\mathbf{w}^2). \end{aligned} \quad (2.2.15)$$

Assume that  $\frac{\partial \mathbf{f}^1}{\partial \mathbf{w}}$  and  $\frac{\partial \bar{\mathbf{R}}}{\partial \mathbf{w}}$  continuous, and define the continuous function  $\mathbf{K}(t, \epsilon)$  by:

$$\mathbf{K}(t, \epsilon) = \frac{\partial \mathbf{f}^1(\psi_1)}{\partial \mathbf{w}} - \frac{\partial \mathbf{f}^1(\mathbf{p}_o)}{\partial \mathbf{w}}.$$

As is known  $\psi_1(t, \epsilon) \rightarrow \mathbf{p}_o$  when  $\epsilon \rightarrow 0$ , so  $\mathbf{K}(t, \epsilon) \rightarrow 0$  when  $\epsilon \rightarrow 0$ . Secondly, consider the linear part of equation (2.2.15)

$$\dot{\bar{\mathbf{w}}} = \epsilon^2 \left[ \frac{\partial \mathbf{f}^1(\mathbf{p}_o)}{\partial \bar{\mathbf{w}}} + \mathbf{K}(t, \epsilon) + \epsilon \frac{\partial \bar{\mathbf{R}}(\psi_1)}{\partial \bar{\mathbf{w}}} \right] \bar{\mathbf{w}}. \quad (2.2.16)$$

Suppose that  $\alpha_j$ ,  $j = 1, 2, \dots, n$  are the eigenvalues of matrix  $\frac{\partial \mathbf{f}^1(\mathbf{p}_o)}{\partial \mathbf{w}}$ . Then the characteristic exponents of equation (2.2.16)  $\lambda_j(\epsilon)$ ,  $j = 1, 2, \dots, n$  can be considered as single-valued continuous functions of  $\epsilon$  with  $\lambda_j(0) = \alpha_j$ . So if  $Re(\alpha_j) < 0$  (respectively  $Re(\alpha_j) > 0$ ) then there exists a positive  $\epsilon_o$  such that  $Re(\lambda_j(\epsilon)) < 0$  (respectively  $Re(\lambda_j(\epsilon)) > 0$ ) for all  $|\epsilon| \leq \epsilon_o$ . In other words, the sign of the real part of the characteristic exponent is equal to the sign of the real parts of the eigenvalues of the matrix  $\frac{\partial \mathbf{f}^1(\mathbf{p}_o)}{\partial \mathbf{w}}$  for  $\epsilon$  sufficiently small. We now apply theorem 7.2 in [32] page 86, saying that if  $Re(\lambda_j) < 0$  then the trivial solution  $\mathbf{w} = \mathbf{0}$  of equation (2.2.15) is asymptotically stable. But the trivial solution  $\mathbf{w} = \mathbf{0}$  corresponds with  $\mathbf{z} = \psi_1$ , so one can deduce that  $\psi_1$  is asymptotically stable. According to the Floquet theorem, every fundamental matrix  $\Phi(t, \epsilon)$  of equation (2.2.16) can be written as  $\Phi(t, \epsilon) = \mathbf{P}(t, \epsilon)e^{\mathbf{B}(\epsilon)t}$ , and the eigenvalues of matrix  $\mathbf{B}(\epsilon)$  are the characteristic exponents of equation (2.2.16). If one transforms the variable  $\mathbf{w}$  to a new variable  $\mathbf{v}$ , according  $\mathbf{w} = \mathbf{P}(t, \epsilon)\mathbf{v}$ , then the equation (2.2.15) becomes:

$$\dot{\mathbf{v}} = \epsilon^2 \mathbf{B}(\epsilon)\mathbf{v} + O(\mathbf{v}^2). \quad (2.2.17)$$

Now theorem 7.3 in [32] page 88 can be applied, yielding that if at least one of the  $Re(\lambda_j)$  is positive then the solution  $\mathbf{v} = \mathbf{0}$  of equation (2.2.17) is unstable. The trivial solution  $\mathbf{v} = \mathbf{0}$  corresponds with the trivial solution  $\mathbf{w} = \mathbf{0}$ , and the trivial solution  $\mathbf{w} = \mathbf{0}$  corresponds with the solution  $\mathbf{z} = \psi_1$ . Thus in other words one can conclude that  $\psi_1$  is unstable.

Now it will be shown that if  $\psi_1$  is a stable periodic solution of system (2.2.7) then  $\psi$  is also a stable periodic solution of the original system (2.2.1). Suppose  $\eta(t)$  is a solution of (2.2.1), then  $\eta(t)$  can be written as

$$\eta(t) = \eta_1(t) + \epsilon \mathbf{u}_1(t, \eta_1) + \epsilon^2 \mathbf{u}_2(t, \eta_1), \quad (2.2.18)$$

where  $\eta_1(t)$  is some solution in (2.2.7).

According to the fourth assumption of the theorem and the proposition above it can be concluded that  $\mathbf{u}_1$  and  $\mathbf{u}_2$  satisfy the Lipschitz condition. Thus from (2.2.12) and (2.2.18) it follows that,

$$\begin{aligned} \|\psi(t) - \eta(t)\| &\leq \|\psi_1(t) - \eta_1(t)\| + \epsilon \|\mathbf{u}_1(t, \psi_1) - \mathbf{u}_1(t, \eta_1)\| + \\ &\quad \epsilon^2 \|\mathbf{u}_2(t, \psi_1) - \mathbf{u}_2(t, \eta_1)\| \\ &\leq N(\epsilon) \|\psi_1(t) - \eta_1(t)\|. \end{aligned} \quad (2.2.19)$$

Hence the stability of  $\psi$  follows from the stability of  $\psi_1$ .

The result obtained above can be extended to more general cases. As has been shown when the vector field  $\mathbf{f}(t, \mathbf{x})$  vanishes by first order averaging one has to consider second order averaging. In a similar way when higher order averaging, say  $n$ -th order averaging yields the trivial vector field one has to consider  $(n + 1)$ -th order averaging and has to determine critical points of the  $(n + 1)$ -th order non-trivial vector field.

Consider the initial value problem for the system

$$\dot{\mathbf{x}} = \epsilon \mathbf{f}_1(t, \mathbf{x}) + \cdots + \epsilon^k \mathbf{f}_k(t, \mathbf{x}) + \epsilon^{k+1} \hat{\mathbf{f}}(t, \mathbf{x}, \epsilon), \quad \mathbf{x}(0) = \mathbf{x}_o, \quad (2.2.20)$$

where  $\mathbf{f}_1, \cdots, \mathbf{f}_k, \hat{\mathbf{f}}$  are  $T$ -periodic in  $t$ . By substituting the "near identity" transformation

$$\mathbf{x} = \mathbf{y} + \epsilon \mathbf{u}_1(t, \mathbf{y}) + \cdots + \epsilon^k \mathbf{u}_k(t, \mathbf{y}) \quad (2.2.21)$$

into (2.2.20) one obtains the following transformed system :

$$\dot{\mathbf{y}} = \epsilon \mathbf{g}_1(\mathbf{y}) + \cdots + \epsilon^k \mathbf{g}_k(\mathbf{y}) + \epsilon^{k+1} \hat{\mathbf{g}}(t, \mathbf{y}, \epsilon). \quad (2.2.22)$$

By neglecting the last term of (2.2.22) one finds the averaged system :

$$\dot{\mathbf{w}} = \epsilon \mathbf{g}_1(\mathbf{w}) + \cdots + \epsilon^k \mathbf{g}_k(\mathbf{w}). \quad (2.2.23)$$

The term  $\mathbf{g}_1$  in the averaged equation is the average of  $\mathbf{f}_1$  in equation (2.2.20), the term  $\mathbf{g}_2$  depends not only on  $\mathbf{f}_2$  but also on  $\mathbf{f}_1$  and  $\mathbf{u}_1$ . The term  $\mathbf{g}_2$  is the average of  $\mathbf{f}_2$  plus the average of the multiplication of the derivative of  $\mathbf{f}_1$  with  $\mathbf{u}_1$ . The term  $\mathbf{g}_j$  is the average of  $\mathbf{f}_j$  plus the average of some multiplication of  $\mathbf{f}_m$  with  $\mathbf{u}_m$  where  $m < j$  and their derivatives. The higher the index  $i$  of the term  $\mathbf{g}_i(\mathbf{w})$  the more complicated this term becomes.

*Theorem 1.2.3.*

Assume that the vector field in (2.2.20) is smooth and periodic in  $t$ . Let  $\mathbf{K}$  be a compact subset of  $\mathbb{R}^n$  and let  $\mathbf{W}$  be a larger compact subset containing  $\mathbf{K}$  in its interior. Let  $\epsilon_o$  be such that the near identity transformation (2.2.21) is valid (invertible) for  $\mathbf{y}$  in  $\mathbf{W}$  and  $0 \leq \epsilon < \epsilon_o$ . Suppose that  $\mathbf{g}_1, \cdots, \mathbf{g}_{k-1}$  in the averaged system (2.2.23) are identically zero. The solution of the

$$d\mathbf{z}/d\tau = \mathbf{g}_k(\mathbf{z}), \quad \mathbf{z}(0) = \mathbf{x}_o, \quad \tau = \epsilon^k t \quad (2.2.24)$$

remains in  $\mathbf{K}$  in  $0 \leq \tau \leq C$ . Then there exist constants  $c$  and  $\epsilon_1$  such that

$$\|\mathbf{x}(t, \mathbf{x}_o, \epsilon) - \mathbf{z}(t, \mathbf{x}_o, \epsilon)\| < c\epsilon \quad \text{for } 0 \leq t \leq C/\epsilon^k, \quad 0 < \epsilon \leq \epsilon_1, \quad (2.2.25)$$

for all  $\mathbf{x}_o$  in  $\mathbf{K}$ . Furthermore, if  $\mathbf{p}$  is a critical point of

$$\dot{\mathbf{z}} = \epsilon^k \mathbf{g}_k(\mathbf{z}) \quad (2.2.26)$$

and

$$|\partial \mathbf{g}_k(\mathbf{z}) / \partial \mathbf{z}|_{\mathbf{z}=\mathbf{p}} \neq 0, \quad (2.2.27)$$

then there exist a periodic solution of (2.2.20) in the  $\epsilon$ -neighbourhood of  $\mathbf{p}$ . Besides that if  $\partial \hat{\mathbf{g}}_{k+1}(\mathbf{z}) / \partial \mathbf{z}$  is continuous, then this periodic solution is asymptotically stable if all of the eigenvalues of the matrix  $\partial \mathbf{g}_k(\mathbf{p}) / \partial \mathbf{z}$  have negative real part and unstable if there exist at least one eigenvalue of that matrix with positive real part.

*Remarks.* The first part of this theorem is generalization of *Theorem 1.2.1*, resulting in approximations on longer time scales. For more general results on higher order averaging one can consult [4], where, however, approximations are studied on a  $1/\epsilon$  time scale. The second part of this theorem seems not to be known that is this theorem gives conditions for the existence and the stability of periodic solution of the original equation depending on a higher order term of which the determinant of the matrix obtained by linearization in the neighbourhood of the critical point does not vanish. To prove the first part of this theorem one can use the method used in the proof of *Theorem 1.2.1*. The proof of the second part of *Theorem 1.2.3* can be given on the basis of the principles given in the proof of *Theorem 1.2.2*.

## 2.3 Higher Order Averaging for Linear Equations

In general solutions of systems of linear differential equation with time-periodic coefficients are not always periodic. The Floquet theorem shows that the fundamental matrix of this system can be written as a product of a periodic matrix with an exponential matrix. As is known there are no general methods to calculate this fundamental matrix. In this section an example will be given how to approximate solutions of systems of linear differential equations with time-periodic coefficients by using higher order averaging.

Consider the equation

$$\dot{\mathbf{x}} = (\epsilon \mathbf{A}_1(t) + \epsilon^2 \mathbf{A}_2(t) \cdots + \epsilon^n \mathbf{A}_n(t)) \mathbf{x}, \quad (2.3.1)$$

where  $\mathbf{A}_i(t)$ ,  $i = 1, 2, \dots, n$  are  $T$ -periodic  $n \times n$ -matrices in  $t$  and  $\mathbf{x}$  is a column vector. According to the Floquet theorem the fundamental matrix of equation (2.3.1) can be written as follows :

$$\mathbf{P}(t, \epsilon) e^{\mathbf{B}(\epsilon)t}, \quad (2.3.2)$$

where  $\mathbf{P}(t, \epsilon)$  is a  $n \times n$ -matrix,  $T$ -periodic in  $t$  and  $\mathbf{B}(\epsilon)$  is a  $n \times n$  constant matrix depending on  $\epsilon$ . As the right hand side of equation (2.3.1) is linear, the "near identity" transformation can be chosen in linear form as follows:

$$\mathbf{x} = (\mathbf{I} + \epsilon \mathbf{V}_1(t) + \epsilon^2 \mathbf{V}_2(t) + \cdots + \epsilon^n \mathbf{V}_n(t)) \mathbf{y}. \quad (2.3.3)$$

By substitution of (2.3.3) into (2.3.1) one obtains the transformed system

$$\dot{\mathbf{y}} = \mathbf{F}^{-1}(\mathbf{A}\mathbf{F} - \dot{\mathbf{F}})\mathbf{y}, \quad (2.3.4)$$

where  $\mathbf{A}$ ,  $\mathbf{F}$  and  $\mathbf{F}^{-1}$  are

$$\begin{aligned} \mathbf{A} &= \epsilon \mathbf{A}_1(t) + \epsilon^2 \mathbf{A}_2(t) + \cdots + \epsilon^n \mathbf{A}_n(t), \\ \mathbf{F} &= \mathbf{I} + \epsilon \mathbf{V}_1(t) + \epsilon^2 \mathbf{V}_2(t) + \cdots + \epsilon^n \mathbf{V}_n(t), \\ \mathbf{F}^{-1} &= \mathbf{I} + \sum_{j=1}^{\infty} (-1)^j [\sum_{i=1}^n \epsilon^i \mathbf{V}_i(t)]^j. \end{aligned} \quad (2.3.5)$$

If one chooses :

$$\begin{aligned} \mathbf{V}_1(t) &= \int_0^t [\mathbf{A}_1(s) - \mathbf{A}^{(0)}] ds, & \mathbf{A}^{(0)} &= \frac{1}{T} \int_0^T \mathbf{A}_1(t) dt, \\ \mathbf{V}_2(t) &= \int_0^t [\mathbf{A}_1(s) \mathbf{V}_1(s) + \mathbf{A}_2(s) - \mathbf{V}_1(s) \mathbf{A}^{(0)} - \mathbf{A}^{(1)}] ds, \\ & \mathbf{A}^{(1)} = \frac{1}{T} \int_0^T [\mathbf{A}_1(t) \mathbf{V}_1(t) + \mathbf{A}_2(t) - \mathbf{V}_1(t) \mathbf{A}^{(0)}] dt, \\ & \vdots \\ \mathbf{V}_n(t) &= \int_0^t \sum_{\substack{j=0 \\ i+j=n}}^{n-1} \mathbf{A}_i(s) \mathbf{V}_j(s) - \sum_{j=0}^{n-1} \mathbf{V}_j(s) \mathbf{A}^{(n-j-1)} ds, \\ \mathbf{V}_0 &= \mathbf{I}, \\ \mathbf{A}^{(n-1)} &= \frac{1}{T} \int_0^T \sum_{\substack{j=0 \\ i+j=n}}^{n-1} \mathbf{A}_i(t) \mathbf{V}_j(t) - \sum_{j=1}^{n-1} \mathbf{V}_j(t) \mathbf{A}^{(n-j-1)} dt, \end{aligned}$$

then one obtains the transformed equation (2.3.4) up to order  $\epsilon^{n+1}$  :

$$\begin{aligned} \dot{\mathbf{y}} &= (\epsilon \mathbf{A}^{(0)} + \epsilon^2 \mathbf{A}^{(1)} + \cdots + \epsilon^n \mathbf{A}^{(n-1)}) \mathbf{y} + O(\epsilon^{n+1}) \\ &= \left( \sum_{j=0}^{n-1} \epsilon^{j+1} \mathbf{A}^{(j)} \right) \mathbf{y} + O(\epsilon^{n+1}). \end{aligned} \quad (2.3.6)$$

Truncating the order  $\epsilon^{n+1}$  terms yields the averaged equation

$$\dot{\mathbf{z}} = \left( \sum_{j=0}^{n-1} \epsilon^{j+1} \mathbf{A}^{(j)} \right) \mathbf{z} \quad (2.3.7)$$

and its solution (with initial condition  $\mathbf{x}_o$ ) is

$$\mathbf{z} = \exp \left( \left[ \sum_{j=0}^{n-1} \epsilon^{j+1} \mathbf{A}^{(j)} \right] t \right) \mathbf{x}_o. \quad (2.3.8)$$

By substituting (2.3.8) into (2.3.3) the solution of equation (2.3.1) with initial condition  $\mathbf{x}_o$  can be approximated by  $\mathbf{x}_{app}$  i.e. :

$$\begin{aligned}\mathbf{x}_{app} &= \mathbf{z} + \left( \sum_{i=1}^n \epsilon^i \mathbf{V}_i(t) \right) \mathbf{z} \\ &= [\mathbf{I} + \left( \sum_{i=1}^n \epsilon^i \mathbf{V}_i(t) \right)] \exp \left( \left[ \sum_{j=0}^{n-1} \epsilon^{j+1} \mathbf{A}^{(j)} \right] t \right) \mathbf{x}_o.\end{aligned}\tag{2.3.9}$$

In other words, the fundamental matrix of (2.3.1),  $\mathbf{P}(t, \epsilon)e^{\mathbf{B}(\epsilon)t}$ , can be approximated by

$$[\mathbf{I} + \left( \sum_{i=0}^n \epsilon^i \mathbf{V}_i(t) \right)] \exp \left( \left[ \sum_{j=0}^{n-1} \epsilon^{j+1} \mathbf{A}^{(j)} \right] t \right).$$

Now it follows that if (2.3.1) and (2.3.7) have the same initial value then  $\|\mathbf{x} - \mathbf{x}_{app}\| = O(\epsilon^n)$  on a time scale  $1/\epsilon$ . This result is a special case of the  $n$ -th order averaging as given in [4], where the system

$$\dot{\mathbf{x}} = \epsilon \mathbf{f}(t, \mathbf{x}, \epsilon)\tag{2.3.10}$$

is considered. As this system is non-linear the near-identity transformation as well as the resulting  $n$ -th order averaged system are much more complicated. As will be shown in the following section the algorithm for linear systems as presented in this section can be applied straightforwardly to special examples yielding interesting results.

## 2.4 Application

In this section the theory of the previous sections is illustrated with an example. A special equation is studied by first and higher order averaging. It will be shown that higher order averaging is essential for obtaining interesting results. The periodic solutions of an inhomogeneous second order equation with time-dependent damping coefficient:

$$\ddot{x} + (c + \epsilon \cos(2t))\dot{x} + (m^2 + \alpha)x + A \cos(\omega t) = 0\tag{2.4.1}$$

are studied, where  $c, \alpha, \epsilon, A$  are small parameters and  $m, \omega$  positive integers. A rather special property of equation (2.4.1) is that the coefficient of  $\dot{x}$  is time dependent and it seems that only little attention has been paid in the literature to an equation of type (2.4.1). For  $m = 1$  and  $A = 0$  some results especially related to the stability of the trivial solution can be found in [2]. As will be shown in chapter 3 the equation (2.4.1) may be used as a model equation for the study of rain-wind induced vibrations of a special oscillator. In a more general context the homogeneous equation (2.4.1) may be considered as a variational equation for a corresponding non-linear equation with a periodic solution. The study of periodic solutions of equation (2.4.1) involves the existence of the periodic solutions as well as the construction of approximations. Also the stability of these periodic solutions will be studied. Because of the

presence of a number of small parameters in equation (2.4.1) the averaging method for the construction of approximations for the periodic solutions will be used. The parameters  $c, \alpha$  and  $A$  are considered to be small implying that they are expressed in the characteristic small parameter  $\epsilon$  of the problem:

$$\begin{aligned} c &= \epsilon c_1 + \epsilon^2 c_2 + \epsilon^3 c_3, \\ \alpha &= \epsilon \alpha_1 + \epsilon^2 \alpha_2 + \epsilon^3 \alpha_3, \\ A &= \epsilon A_1 + \epsilon^2 A_2 + \epsilon^3 A_3, \end{aligned} \tag{2.4.2}$$

where  $c_i, \alpha_i$  and  $A_i, i = 1, 2, 3$  are of  $O(1)$ . Note that throughout the analysis the parametric excitation  $\epsilon \cos 2t$  remains of  $O(\epsilon)$ .

For  $m, \omega \in \{1, 2, 3\}$ , it will be shown that an  $O(1)$ -periodic solution exists if  $m = \omega$  and if  $m \neq \omega$  the periodic solution is of order  $\epsilon$ . Further, if  $c = O(\epsilon)$ ,  $\alpha = O(\epsilon)$ , and  $A = O(\epsilon)$ , for  $m = \omega = 1$  both stable and unstable periodic solutions exist but for  $m = \omega = 2, 3$  only stable periodic solutions are found. For the case that  $c = O(\epsilon^2)$ ,  $\alpha = O(\epsilon^2)$ , and  $A = O(\epsilon^2)$ , for  $m = \omega = 2, 3$  only stable periodic solutions are found. But for  $m = 3$  and  $\alpha = \frac{9}{64}\epsilon^2 + O(\epsilon^3)$ ,  $c = O(\epsilon^3)$ ,  $A = O(\epsilon^3)$  both stable and unstable periodic solutions exist. The stability of the periodic solutions follows from stability diagrams related to equation (2.4.1) with  $A \equiv 0$ . According to the Floquet theorem the homogeneous equation has unbounded solutions when  $c$  is negative, so in this section we only consider the cases  $c = 0$  and  $c$  positive.

### 2.4.1 THE CASE $m = \omega$

#### Application of the averaging method: first order approximation

For the cases  $c, \alpha, A$  are  $O(\epsilon)$ , the averaging method can be used to analyze the stability diagram of equation (2.4.1). To obtain the standard form for the application of the averaging method one can put

$$c = c_1 \epsilon, \quad \alpha = \alpha_1 \epsilon, \quad A = A_1 \epsilon, \tag{2.4.3}$$

and transform  $x$  and  $\dot{x}$  to the new variables  $y_1$  and  $y_2$  by:

$$\begin{aligned} x &= y_1 \cos(mt) + \frac{1}{m} y_2 \sin(mt), \\ \dot{x} &= -m y_1 \sin(mt) + y_2 \cos(mt). \end{aligned} \tag{2.4.4}$$

The standard form is:

$$\begin{pmatrix} \dot{y}_1 \\ \dot{y}_2 \end{pmatrix} = \epsilon \begin{pmatrix} a_{11}(t) & a_{12}(t) \\ a_{21}(t) & a_{22}(t) \end{pmatrix} \begin{pmatrix} y_1 \\ y_2 \end{pmatrix} + \epsilon \begin{pmatrix} \frac{A_1}{m} \sin(mt) \cos(\omega t) \\ -A_1 \cos(mt) \cos(\omega t) \end{pmatrix}, \tag{2.4.5}$$

where

$$\begin{aligned} a_{11}(t) &= -\sin^2(mt)(c_1 + \cos(2t)) + \frac{\alpha_1}{2m} \sin(2mt), \\ a_{12}(t) &= \frac{1}{2m} \sin(2mt)(c_1 + \cos(2t)) + \frac{\alpha_1}{m^2} \sin^2(mt), \\ a_{21}(t) &= \frac{m}{2} \sin(2mt)(c_1 + \cos(2t)) - \alpha_1 \cos^2(mt), \\ a_{22}(t) &= -\cos^2(mt)(c_1 + \cos(2t)) - \frac{\alpha_1}{2m} \sin(2mt). \end{aligned}$$

*	The first order averaged equation and its critical points
m=1	$\dot{\mathbf{z}} = \epsilon \begin{pmatrix} \frac{1}{4} - \frac{1}{2}c_1 & \frac{1}{2}\alpha_1 \\ -\frac{1}{2}\alpha_1 & -\frac{1}{4} - \frac{1}{2}c_1 \end{pmatrix} \mathbf{z} + \epsilon \begin{pmatrix} 0 \\ -\frac{1}{2}A_1 \end{pmatrix},$ $\left( \frac{-\alpha_1 A_1}{\alpha_1^2 + c_1^2 - \frac{1}{4}}, \frac{(\frac{1}{2} - c_1) A_1}{\alpha_1^2 + c_1^2 - \frac{1}{4}} \right)$
m=2	$\dot{\mathbf{z}} = \epsilon \begin{pmatrix} -\frac{1}{2}c_1 & \frac{1}{8}\alpha_1 \\ -\frac{1}{2}\alpha_1 & -\frac{1}{2}c_1 \end{pmatrix} \mathbf{z} + \epsilon \begin{pmatrix} 0 \\ -\frac{1}{2}A_1 \end{pmatrix},$ $\left( \frac{-\frac{1}{4}A_1\alpha_1}{c_1^2 + \frac{1}{4}\alpha_1^2}, \frac{-A_1 c_1}{c_1^2 + \frac{1}{4}\alpha_1^2} \right)$
m=3	$\dot{\mathbf{z}} = \epsilon \begin{pmatrix} -\frac{1}{2}c_1 & \frac{1}{9}\alpha_1 \\ -\frac{1}{2}\alpha_1 & -\frac{1}{2}c_1 \end{pmatrix} \mathbf{z} + \epsilon \begin{pmatrix} 0 \\ -\frac{1}{2}A_1 \end{pmatrix},$ $\left( \frac{-2\alpha_1 A_1}{2\alpha_1^2 + 9c_1^2}, \frac{-9A_1 c_1}{2\alpha_1^2 + 9c_1^2} \right)$

**Table 2.1:** The first order averaged equation for (2.4.1) and its critical points for the case  $m = \omega$ ,  $\mathbf{z}$  is a  $2 \times 1$  column vector.

For  $m = 1, 2$ , and  $3$  the averaged equation of (2.4.5) and its critical points are presented in Table 2.1.

The critical points of the averaged equation in table 2.1 correspond with an  $O(1)$  time periodic solution of equation (2.4.5). The stability of these solutions follows from the eigenvalues of the coefficient matrix as can easily be verified. For  $m = 1$  and given  $c$  positive, after rescaling the parameters, the eigenvalues of the coefficient matrix become:

$$\lambda_{1,2} = \frac{1}{\epsilon} \left( -\frac{c}{2} \pm \frac{1}{2} \sqrt{\frac{1}{4}\epsilon^2 - \alpha^2} \right).$$

According to the character of the eigenvalues the  $\alpha - \epsilon$  plane can be divided into two regions (see Figure 2.1b) by the curves  $\alpha = \pm \sqrt{\frac{1}{4}\epsilon^2 - c^2}$ . On this curve the determinant of the coefficient matrix is equal to zero, implying that the averaged equation does not have an isolated critical point. In region I the real part of the eigenvalues are negative, thus in this region the periodic solutions are stable. In the region II the periodic solutions are unstable because in this region the eigenvalues are real-valued, one positive and one negative.

In case  $c = 0$  the  $\alpha - \epsilon$  plane divided into two regions (see Figure 2.1a) by the lines  $\alpha = \pm \frac{1}{2}\epsilon$ . In the region II the periodic solutions are unstable because the eigenvalues



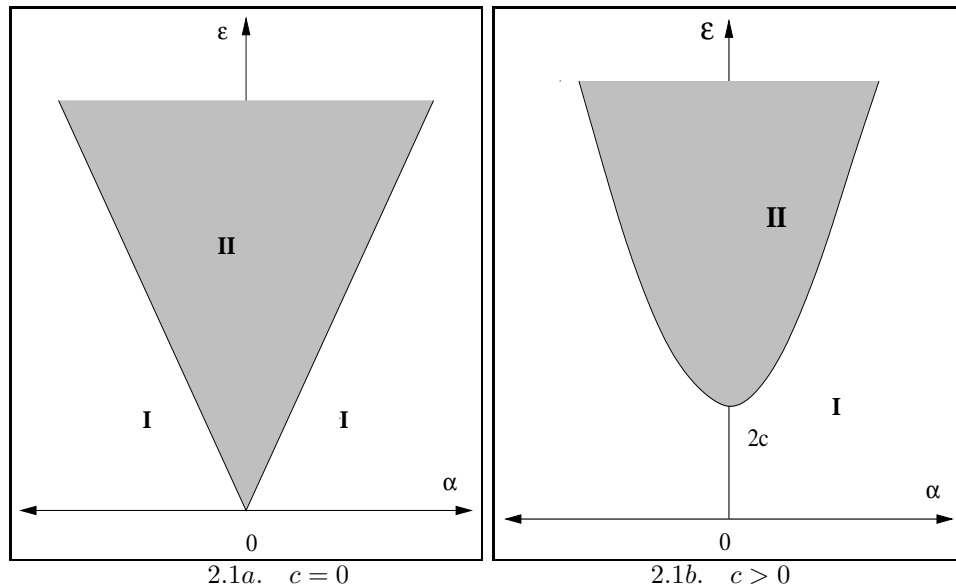


**Figure 2.1:** Stability diagrams for the periodic solutions of equation (2.4.1) for  $m = \omega = 1$ . In the shaded regions the periodic solutions are unstable.

are real-valued, one positive and one negative. In region I the eigenvalues are purely imaginary.

For  $m = 2$  and  $m = 3$ , and given  $c$  positive the determinant of the coefficient matrix is not equal to zero. In these cases there exists one critical point and the eigenvalues of the coefficient matrix are complex-valued with negative real part implying that equation (2.4.1) has always stable periodic solutions.

### Application of the averaging method to second order

By applying first order averaging for  $m = 2$  and  $m = 3$  one finds a critical point and hence a periodic solution depending on the parameters  $c_1$  (damping),  $\alpha_1$  (detuning) and  $A_1$  (forcing). In the  $\alpha - \epsilon$  plane one does not find a stability diagram similar to the ones in Figure 2.1. i.e. for  $c_1 > 0$  the critical point is locally but also globally stable. Higher order averaging will not affect this qualitative picture because of the dominant  $O(\epsilon)$  terms involving damping ( $c_1 > 0$ ) in the averaged equations. By reducing the order of magnitude of the damping and forcing as well as the detuning up to  $O(\epsilon^2)$  but keeping the parametric excitation at  $O(\epsilon)$  one may find a region of instability. This can be achieved by considering the expansion

$$\begin{aligned} c &= \epsilon c_1 + \epsilon^2 c_2 + \epsilon^3 c_3 + \dots, \\ \alpha &= \epsilon \alpha_1 + \epsilon^2 \alpha_2 + \epsilon^3 \alpha_3 + \dots, \\ A &= \epsilon A_1 + \epsilon^2 A_2 + \epsilon^3 A_3 + \dots \end{aligned} \tag{2.4.6}$$

and setting  $c_1 = \alpha_1 = A_1 = 0$ . As the second order averaging are applied, one can truncate the expansion :

$$c = \epsilon^2 c_2, \quad \alpha = \epsilon^2 \alpha_2, \quad A = \epsilon^2 A_2. \tag{2.4.7}$$

For  $m = 2$ , substitution of (2.4.7) and (2.4.4) into (2.4.1) yields after second order averaging :

$$\dot{\mathbf{z}} = \epsilon^2 \begin{pmatrix} -\frac{1}{2}c_2 & \frac{1}{8}(\alpha_2 - \frac{1}{6}) \\ -\frac{1}{2}(\alpha_2 - \frac{1}{6}) & -\frac{1}{2}c_2 \end{pmatrix} \mathbf{z} + \epsilon^2 \begin{pmatrix} 0 \\ -\frac{1}{2}A_2 \end{pmatrix}. \quad (2.4.8)$$

The critical point of (2.4.8) is

$$\left( \frac{-\frac{1}{16}A_2(\alpha_2 - \frac{1}{6})}{\frac{1}{4}c_2^2 + \frac{1}{16}(\alpha_2 - \frac{1}{6})^2}, \frac{-\frac{1}{4}A_2c_2}{\frac{1}{4}c_2^2 + \frac{1}{16}(\alpha_2 - \frac{1}{6})^2} \right).$$

The determinant of the coefficient matrix in (2.4.8) is  $|\mathbf{B}_2| = \frac{1}{4}c_2^2 + \frac{1}{16}(\alpha_2 - \frac{1}{6})^2$  and its eigenvalues are :

$$\lambda_{1,2} = -\frac{c_2}{2} \pm \frac{1}{2} \sqrt{-\frac{1}{16}(\alpha_2 - \frac{1}{6})^2}.$$

By rescaling the parameters, the determinant and the eigenvalues become  $\frac{1}{\epsilon^4}(\frac{1}{4}c^2 + \frac{1}{16}(\alpha - \frac{1}{6}\epsilon^2)^2)$  and

$$\lambda_{1,2} = \frac{1}{\epsilon^2} \left( -\frac{c}{2} \pm \frac{1}{2} \sqrt{-\frac{1}{16}(\alpha - \frac{1}{6}\epsilon^2)^2} \right),$$

respectively.

For given  $c_2$  positive,  $|\mathbf{B}_2|$  is never zero and its eigenvalues are complex-valued with negative real part for  $\alpha_2 \neq \frac{1}{6}$ . Thus (2.4.1) has stable periodic solutions.

But for the case  $c_2 = 0$  the eigenvalues are purely imaginary and equal zero when  $\alpha_2 = \frac{1}{6}$ . In this case the  $\alpha - \epsilon$  plane can be divided in two regions separated by the curve  $\alpha = \frac{1}{6}\epsilon^2$ . On this curve the averaged equation does not have a critical point (see Figure 2.2a) implying that no periodic solutions are found in second order approximation.

In a similar way for  $m = 3$ , by using second order averaging one obtains :

$$\dot{\mathbf{z}} = \epsilon^2 \begin{pmatrix} -\frac{1}{2}c_2 & \frac{1}{18}(\alpha_2 - \frac{9}{64}) \\ -\frac{1}{2}(\alpha_2 - \frac{9}{64}) & -\frac{1}{2}c_2 \end{pmatrix} \mathbf{z} + \epsilon^2 \begin{pmatrix} 0 \\ -\frac{1}{2}A_2 \end{pmatrix}. \quad (2.4.9)$$

The critical point of (2.4.9) is

$$\left( \frac{-\frac{1}{36}A_2(\alpha_2 - \frac{9}{64})}{\frac{1}{4}c_2^2 + \frac{1}{36}(\alpha_2 - \frac{9}{64})^2}, \frac{-\frac{1}{4}c_2A_2}{\frac{1}{4}c_2^2 + \frac{1}{36}(\alpha_2 - \frac{9}{64})^2} \right).$$

The determinant of the coefficient matrix of (2.4.9) is  $\frac{1}{4}c_2^2 + \frac{1}{36}(\alpha_2 - \frac{9}{64})^2$  and its eigenvalues are :

$$\lambda_{1,2} = -\frac{c_2}{2} \pm \frac{1}{2} \sqrt{-\frac{1}{9}(\alpha_2 - \frac{9}{64})^2}.$$

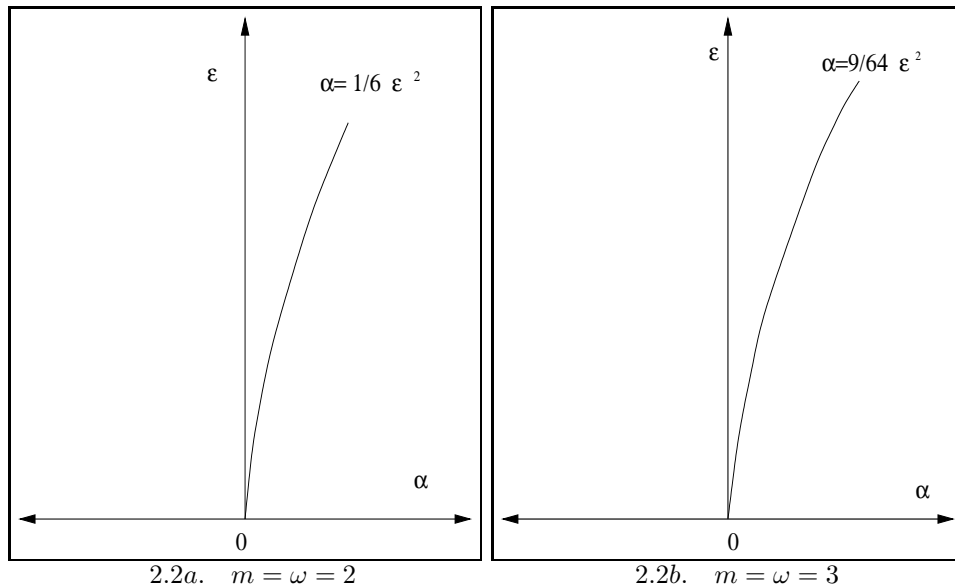


**Figure 2.2:** Curves on which the eigenvalues of (2.4.8) and (2.4.9) are zero and on both sides of the curves the eigenvalues are purely imaginary.

By rescaling the parameters, the eigenvalues and the determinant become  $\frac{1}{\epsilon^4}(\frac{1}{4}c^2 + \frac{1}{36}(\alpha - \frac{9}{64}\epsilon^2)^2)$  and

$$\lambda_{1,2} = \frac{1}{\epsilon^2} \left( -\frac{c}{2} \pm \frac{1}{2} \sqrt{-\frac{1}{9}(\alpha - \frac{9}{64}\epsilon^2)^2} \right),$$

respectively.

The situation for  $m = 3$  is qualitatively the same as the situation for  $m = 2$ . The curve on which the equation (2.4.9) does not have a critical point is, however, slightly different i.e.  $\alpha = \frac{9}{64}\epsilon^2$  (see Figure 2.2b).

### Application of the averaging method to third order

In this subsection the case  $m = 2, 3$  by using third order averaging are investigated. When the averaging method to second order is used to investigate the cases  $m = 2$  and  $m = 3$ , two curves are obtained in the  $\alpha - \epsilon$  plane that are  $\alpha = \frac{1}{6}\epsilon^2$  and  $\alpha = \frac{9}{64}\epsilon^2$  respectively, on which curves the averaged equation does not have critical points. However, for  $m = 3$  one can obtain an interesting result when one reduces the order of magnitude of the parameters  $c$  (damping) and  $A$  (forcing) up to  $O(\epsilon^3)$  i.e.  $c = \epsilon^3 c_3$ ,  $A = \epsilon^3 A_3$ . It turns out that for the detuning one should consider  $\alpha = \frac{9}{64}\epsilon^2 + \epsilon^3 \alpha_3$ . As will be shown the curve  $\alpha = \frac{9}{64}\epsilon^2$  will split in two curves  $\alpha = \frac{9}{64}\epsilon^2 \pm \frac{3}{512}\epsilon^3$  for  $c = 0$ , defining a domain of instability which has not been found by second order averaging and scaling of the parameters.

In case  $m = 2$ , to eliminate the order  $\epsilon$  and  $\epsilon^2$  effects one sets  $c_1 = \alpha_1 = c_2 = A_1 = A_2 = 0$  and  $\alpha_2 = \frac{1}{6}$ . Thus the expansions in the series (2.4.6) up to order  $\epsilon^3$  are :

$$c = \epsilon^3 c_3, \quad \alpha = \frac{1}{6}\epsilon^2 + \epsilon^3 \alpha_3, \quad A = \epsilon^3 A_3. \quad (2.4.10)$$

By substituting (2.4.10) and (2.4.4) into (2.4.1) one obtains after third order averaging :

$$\dot{\mathbf{z}} = \epsilon^3 \begin{pmatrix} -\frac{1}{2}c_3 & \frac{1}{8}\alpha_3 \\ -\frac{1}{2}\alpha_3 & -\frac{1}{2}c_3 \end{pmatrix} \mathbf{z} + \epsilon^3 \begin{pmatrix} 0 \\ -\frac{1}{2}A_3 \end{pmatrix}. \quad (2.4.11)$$

The equation (2.4.11) does not have a critical point if and only if  $c_3 = \alpha_3 = 0$ . Thus for  $m = 2$  the curve on which the equation (2.4.11) does not have a critical point is  $\alpha = \frac{1}{6}\epsilon^2$  (the same result was obtained by using the averaging method to second order).

In order to eliminate order  $\epsilon$  and  $\epsilon^2$  effects in case  $m = 3$  one sets  $c_1 = \alpha_1 = c_2 = A_1 = A_2 = 0$  and  $\alpha_2 = \frac{9}{64}$ . Thus the expansions in the series (2.4.6) up to order  $\epsilon^3$  are :

$$c = \epsilon^3 c_3, \quad \alpha = \frac{9}{64}\epsilon^2 + \epsilon^3 \alpha_3, \quad A = \epsilon^3 A_3. \quad (2.4.12)$$

By substituting (2.4.12) and (2.4.4) into (2.4.1) one obtains after third order averaging :

$$\dot{\mathbf{z}} = \epsilon^3 \begin{pmatrix} -\frac{1}{2}c_3 + \frac{1}{1024} & \frac{1}{18}\alpha_3 \\ -\frac{1}{2}\alpha_3 & -\frac{1}{2}c_3 - \frac{1}{1024} \end{pmatrix} \mathbf{z} + \epsilon^3 \begin{pmatrix} 0 \\ -\frac{1}{2}A_3 \end{pmatrix}. \quad (2.4.13)$$

After rescaling the parameters the determinant of the coefficient matrix  $\mathbf{B}_3$  of equation (2.4.13) becomes :

$$|\mathbf{B}_3| = \frac{1}{36} \left( \alpha - \frac{9}{64}\epsilon^2 \right)^2 - \frac{1}{4} \left( \frac{\epsilon^6}{512^2} - c^2 \right),$$

and its eigenvalues are

$$\lambda_{1,2} = \frac{1}{\epsilon^3} \left( -\frac{c}{2} \pm \frac{1}{2} \sqrt{\frac{\epsilon^6}{512^2} - \frac{1}{9} \left( \alpha - \frac{9}{64}\epsilon^2 \right)^2} \right).$$

The existence of an isolated critical point of equation (2.4.13) corresponds with the existence of a periodic solution of equation (2.4.1), and the stability of this periodic solution depends on the eigenvalues of matrix  $\mathbf{B}_3$ . Equation (2.4.13) has an isolated critical point if  $|\mathbf{B}_3| \neq 0$ , and does not have a critical point if  $|\mathbf{B}_3| = 0$ . In the  $\alpha - \epsilon$  plane,  $|\mathbf{B}_3| = 0$  corresponds with the curve :

$$\alpha = \frac{9}{64}\epsilon^2 \pm \frac{3}{512} \sqrt{\epsilon^6 - (512c)^2}. \quad (2.4.14)$$

Given  $c$  positive, this curve divides the  $\alpha - \epsilon$  plane into two regions, that are region I and II (see Figure 2.3b). In region I the real part of the eigenvalues are negative, and in the region II the eigenvalues are real-valued, one positive and one negative. So the periodic solution of (2.4.1) is stable in region I but unstable in region II.

In the case  $c = 0$ , the  $\alpha - \epsilon$  plane is divided into two regions by the curves  $\alpha = \frac{9}{64}\epsilon^2 \pm \frac{3}{512}\epsilon^3$  ( see Figure 2.3a ).

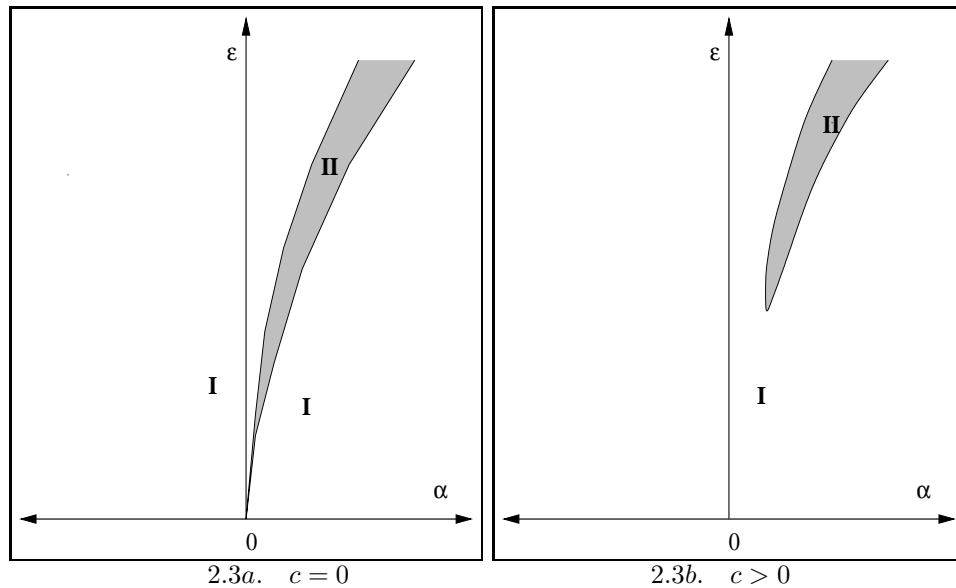


**Figure 2.3:** Stability diagrams for the periodic solutions of equation (2.4.1) for  $m = \omega = 3$ . In the shaded regions the periodic solutions are unstable.

### 2.4.2 THE CASE $m \neq \omega$

In case  $m = \omega$ , the general form of the averaged equation can be written as  $\dot{\mathbf{z}} = \mathbf{C}\mathbf{z} + \mathbf{b}$ , where  $\mathbf{b}$  is  $2 \times 1$  column vector which depends on the parameter  $A$ . However, for the case  $m \neq \omega$  the parameter  $A$  does not occur in the averaged equation, and the general form of the averaged equation is  $\dot{\mathbf{z}} = \mathbf{C}\mathbf{z}$ . Thus the only isolated critical point of this system is the origin. This implies that the periodic solution of (2.4.5) is in an  $\epsilon$ -neighbourhood of the origin. In other words the amplitude of the periodic solution of equation (2.4.1) is of order  $\epsilon$ . The stability diagrams in Figure 2.1 - Figure 2.3 depend on the coefficient matrix  $\mathbf{C}$ , and on the curves, which separates region I and II, the determinant of the coefficient matrix  $\mathbf{C}$  is equal to zero. Because in both cases the same coefficient matrix is obtained the stability diagram also applies to the stability of the periodic solution of the inhomogeneous equation. The difference is only the order of magnitude of the amplitude of the periodic solution; in case  $m = \omega$  the amplitude is  $O(1)$  but in case  $m \neq \omega$  the amplitude is  $O(\epsilon)$ .

## 2.5 Conclusion

In this chapter the averaging method is studied for the case that all terms up to  $O(\epsilon^n)$  obtained by averaging vanish identically. When the first non identical zero term is of  $O(\epsilon^{n+1})$  the validity of asymptotic approximations for the initial value problems on a  $1/\epsilon^{n+1}$  time scale is established as well as conditions are given for the existence of time-periodic solutions. Moreover, the stability of these periodic solutions is investigated.

A special averaging algorithm is presented for time-periodic linear systems. The theory is illustrated with an example which clearly shows that for a relatively simple equation third order averaging is needed to prove existence of periodic solutions, to

establish their stability and to compute approximations.

# Chapter 3

## An Equation with a Time-periodic Damping Coefficient: stability diagram and an application <sup>†</sup>

**Abstract.** In this chapter the second order differential equation with a time-dependent damping coefficient will be studied. In particular the coexistence of periodic solutions corresponding with the vanishing of domains of instability is investigated. This equation can be considered as a model equation for the study of rain-wind induced vibrations of a special oscillator.

### 3.1 Introduction

In this chapter we consider an inhomogeneous second order differential equation with time-dependent damping coefficient i.e.

$$\ddot{x} + (c + \epsilon \cos(2t))\dot{x} + (m^2 + \alpha)x + A \cos(\omega t) = 0, \quad (3.1.1)$$

where  $c, \alpha, \epsilon, A$  are small parameters and  $m, \omega$  positive integers. A rather special property of equation (3.1.1) is that the coefficient of  $\dot{x}$  is time dependent. For  $m = 1$  and  $A = 0$  some results especially related to the stability of the trivial solution can be found in [2]. Further for the case  $c = 0$  and  $A = 0$  the equation (3.1.1) is a special case of Ince's equation (see [16], page 92 i.e.  $a = 0, d = 0$  and  $t \rightarrow t + \pi/4$ ). As is known, Ince's equation displays the phenomenon of coexistence of periodic solutions when  $m$  is an even integer. The coexistence of periodic solutions means that there are two linearly independent periodic solutions with the same period. Coexistence implies that domains of instability disappear or in other words that an instability

---

<sup>†</sup>This chapter is a revised and combined version of [11] and [29], A linear differential equation with a time-periodic damping coefficient: stability diagram and an application, to be published in *Journal of Engineering Mathematics*, 49(2):99-112, 2004 and Rain-wind induced vibrations of a simple oscillator, *International Journal of Non-Linear Mechanics*, 39:93-100, 2004.

gap closes. The coexistence of periodic solutions of this equation will be studied in this chapter. A stability diagram is presented and the strained parameter is used to obtain approximations for the transition and the coexistence curves for small values of  $\epsilon$ . Finally it is shown that (3.1.1) can be used as a model equation for the study of rain-wind induced vibrations of a special oscillator.

## 3.2 Coexistence of Time Periodic Solutions and the Stability Diagram

For the case  $c = A = 0$  and replacing  $m^2 + \alpha$  by  $\lambda$ , the equation (3.1.1) can be written as

$$\ddot{x} + \epsilon \cos(2t)\dot{x} + \lambda x = 0. \quad (3.2.1)$$

Transform  $x$  to the new variable  $y$  by

$$x = y \cdot e^{-\frac{1}{2} \int_0^t \epsilon \cos(2s) ds} \quad (3.2.2)$$

to obtain a new equation of Hill's type:

$$\ddot{y} + \left( \lambda - \frac{1}{8} \epsilon^2 + \epsilon \sin(2t) - \frac{1}{8} \epsilon^2 \cos(4t) \right) y = 0. \quad (3.2.3)$$

The standard form of Hill's equation (in [16]) is

$$\ddot{y} + [\lambda + Q(t)]y = 0, \quad (3.2.4)$$

where  $\lambda$  is a parameter and  $Q$  is a real  $\pi$ -periodic function in  $t$ . Apparently (3.2.3) is of type (3.2.4) where  $Q(t)$  depends additionally on a parameter  $\epsilon$ . The determination of the value of  $\lambda$  for which the equation (3.2.4) has a  $\pi$  or  $2\pi$  periodic solution can be related to the following theorem.

*Theorem* ([16], page 11).

To every differential equation (3.2.4), there belong two monotonically increasing infinite sequences of real numbers  $\lambda_0, \lambda_1, \lambda_2, \dots$  and  $\lambda'_1, \lambda'_2, \lambda'_3, \dots$  such that (3.2.4) has a solution of period  $\pi$  if and only if  $\lambda = \lambda_n, n = 0, 1, 2, \dots$  and a solution of period  $2\pi$  if and only if  $\lambda = \lambda'_n, n = 1, 2, 3, \dots$ . The  $\lambda_n$  and  $\lambda'_n$  satisfy the inequalities

$$\lambda_0 < \lambda'_1 \leq \lambda'_2 < \lambda_1 \leq \lambda_2 < \lambda'_3 \leq \lambda'_4 < \lambda_3 \leq \lambda_4 < \dots$$

and the relations

$$\lim_{n \rightarrow \infty} \lambda_n^{-1} = 0, \quad \lim_{n \rightarrow \infty} (\lambda'_n)^{-1} = 0.$$

The solutions of (3.2.4) are stable (that is, all solutions of (3.2.4) are bounded) in the open intervals

$$(\lambda_0, \lambda'_1), (\lambda'_2, \lambda_1), (\lambda_2, \lambda'_3), (\lambda'_4, \lambda_3), \dots$$

At the endpoints of these intervals the solutions of (3.2.4) are, in general, unstable. The solutions of (3.2.4) are stable for  $\lambda = \lambda_{2n+1}$  or  $\lambda = \lambda_{2n+2}$  if and only



if  $\lambda_{2n+1} = \lambda_{2n+2}$ , and they are stable for  $\lambda = \lambda'_{2n+1}$  or  $\lambda = \lambda'_{2n+2}$  if and only if  $\lambda'_{2n+1} = \lambda'_{2n+2}$ .

As described in [16], Hill's equation in general has only one periodic solution of period  $\pi$  or  $2\pi$ . If the Hill's equation has two linearly independent periodic solutions of period  $\pi$  or two linearly independent periodic solutions of period  $2\pi$ , we say that two such solutions *coexist*. And then every solution of this equation can be expressed into a linear combination of two these periodic solutions. The occurrence of coexisting periodic solutions is equivalent with the disappearance of intervals of instability. If for instance two linearly independent solutions of period  $\pi$  exist then the interval of instability  $(\lambda_{2n+1}, \lambda_{2n+2})$  disappears, because  $\lambda_{2n+1} = \lambda_{2n+2}$ .

Further in [14] a special case of  $Q(t)$  was studied, that is, if  $Q(t)$  in equation (3.2.4) has the form

$$Q(t) = \gamma + \dot{P}(t) + P^2(t), \quad (3.2.5)$$

where  $P(t)$  is  $\pi/2$ -anti-periodic i.e.  $P(t + \pi/2) = -P(t)$  then  $\lambda_{2n+1} = \lambda_{2n+2}$  for all  $n$ .

Clearly equation (3.2.3) is of the form (3.2.5) with  $P(t) = -\frac{1}{2}\epsilon \cos(2t)$  and  $\gamma = 0$ , and  $\cos(2t)$  is  $\pi/2$  anti-periodic. Thus coexistence in equation (3.2.3) exists for  $\lambda = \lambda_{2n+1} = \lambda_{2n+2}$ .

Unfortunately it is not known how to calculate exactly the values of  $\lambda$  for which equation (3.2.3) has a periodic solution. However, one can approximate the value of  $\lambda$  by the following method [5].

We consider a Fourier series representation of the periodic solution:

$$y = \frac{a_o}{2} + \sum_{n=1}^{\infty} (a_n \cos(nt) + b_n \sin(nt)). \quad (3.2.6)$$

Substituting (3.2.6) into (3.2.3) yields

$$\begin{aligned} & (\lambda - \frac{1}{8}\epsilon^2) \frac{a_o}{2} + \epsilon \frac{a_o}{2} \sin(2t) - \frac{1}{16}\epsilon^2 a_o \cos(4t) + \\ & \sum_{n=1}^{\infty} [(\lambda - \frac{1}{8}\epsilon^2 - n^2) a_n \cos(nt) + \\ & (\lambda - \frac{1}{8}\epsilon^2 - n^2) b_n \sin(nt)] + \\ & \frac{1}{2}\epsilon \sum_{n=1}^{\infty} [a_n \sin((n+2)t) - a_n \sin((n-2)t) \\ & - b_n \cos((n+2)t) + b_n \cos((n-2)t)] \\ & - \frac{1}{16}\epsilon^2 \sum_{n=1}^{\infty} [a_n \cos((n+4)t) + a_n \cos((n-4)t) + \\ & b_n \sin((n+4)t) + b_n \sin((n-4)t)] = 0. \end{aligned} \quad (3.2.7)$$

Equating the coefficients of sine and cosine terms to zero we have a system of infinitely many equations for  $a_n$  and  $b_n$ . This system can be split up into two independent systems which contain even indices and odd indices respectively as has been shown explicitly in the appendix. In this way we obtain two systems

$$\mathbf{A}(\lambda, \epsilon)\mathbf{v} = \mathbf{0}, \quad \text{and} \quad \mathbf{B}(\lambda, \epsilon)\mathbf{w} = \mathbf{0},$$

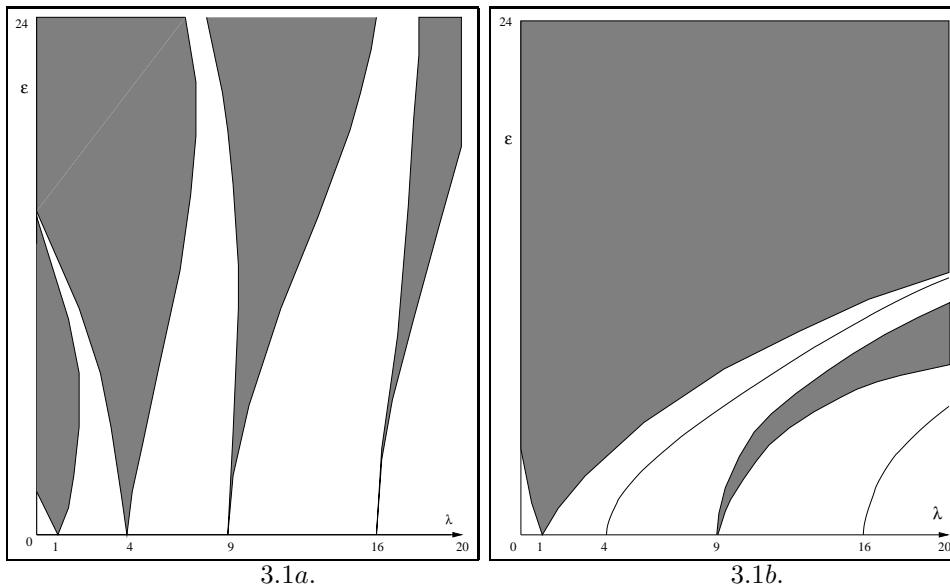


**Figure 3.1:** In the shaded regions the trivial solution is unstable. On the curves separating the white and shaded regions periodic solution exist. Figure 3.1a the Mathieu stability diagram. Figure 3.1b the new stability diagram.

where  $\mathbf{A}(\lambda, \epsilon), \mathbf{B}(\lambda, \epsilon)$  are square matrices of infinite dimension, and where  $\mathbf{v}$  and  $\mathbf{w}$  are infinite column vectors. The matrices  $\mathbf{A}$  and  $\mathbf{B}$  and the vectors  $\mathbf{v}$  and  $\mathbf{w}$  are also given in the appendix. The system  $\mathbf{B}(\lambda, \epsilon)\mathbf{w} = \mathbf{0}$  is related to the  $\pi$ -periodic solution(s) when  $y$  is expanded as

$$y = \frac{\hat{a}_0}{2} + \sum_{n=1}^{\infty} (\hat{a}_n \cos(2nt) + \hat{b}_n \sin(2nt)).$$

The other system,  $\mathbf{A}(\lambda, \epsilon)\mathbf{v} = \mathbf{0}$ , corresponds with the  $2\pi$ -periodic solution(s). To have a non trivial solution the determinant of  $\mathbf{A}$  or  $\mathbf{B}$  must be equal zero. These determinants define the curves in the  $\epsilon - \lambda$  plane on which periodic solutions exist. However, it is not possible to compute these curves exactly from the determinants as they are of infinite dimension. Hence we consider (3.2.6) and truncate the series up to 16 modes from which the determinants of finite dimension follow. Some remarks on the truncation errors are also given in the appendix. In these determinants we choose  $\epsilon$  in the interval  $(0, 24)$  arbitrary but fixed. Subsequently the determinants are evaluated, yielding an algebraic equation for  $\lambda$  which can be solved numerically. Along this way a stability diagram as depicted in Figure 3.1b is obtained. In a similar way the famous stability diagram of the Mathieu equation:

$$\ddot{y} + (\lambda + \epsilon \cos(2t))y = 0 \tag{3.2.8}$$

is obtained and presented in Figure 3.1a. One can observe remarkable differences between the two diagrams. Especially the curves starting in  $\lambda = 4n^2, n = 1, 2, 3, \dots$  on which two periodic solutions coexists are of interest.

In case  $\epsilon$  is small we can use the strained parameter method, as described in [22], to approximate the value of  $\lambda$  for which the equation (3.2.3) has periodic solutions. In this method we assume that  $\lambda$  can be expanded as

$$m^2 + \epsilon\alpha_1 + \epsilon^2\alpha_2 + \epsilon^3\alpha_3 + \dots, \quad (3.2.9)$$

where  $m$  is an integer number and the solution of (3.2.3) is expanded as

$$a_o \cos mt + b_o \sin mt + \epsilon y_1(t) + \epsilon^2 y_2(t) + \epsilon^3 y_3(t) + \dots \quad (3.2.10)$$

Substituting (3.2.10) into (3.2.3) and eliminating the secular terms gives the values of  $\alpha_i, i = 1, 2, 3, \dots$ . For instance, for  $m = 1$  we obtain  $a_o = -b_o$  and  $\lambda = \lambda'_1$  where

$$\begin{aligned} \lambda'_1 = & 1 - \frac{1}{2}\epsilon + \frac{3}{32}\epsilon^2 - \frac{3}{512}\epsilon^3 - \frac{3}{8192}\epsilon^4 + \frac{5}{141072}\epsilon^5 \\ & - \frac{17}{4194304}\epsilon^6 - \frac{7}{134217728}\epsilon^7 - \frac{1}{16777216}\epsilon^8 + O(\epsilon^9) \end{aligned} \quad (3.2.11)$$

or  $a_o = b_o$  and  $\lambda = \lambda'_2$  where

$$\begin{aligned} \lambda'_2 = & 1 + \frac{1}{2}\epsilon + \frac{3}{32}\epsilon^2 + \frac{3}{512}\epsilon^3 - \frac{3}{8192}\epsilon^4 - \frac{5}{141072}\epsilon^5 + \\ & \frac{17}{4194304}\epsilon^6 + \frac{7}{134217728}\epsilon^7 - \frac{1}{16777216}\epsilon^8 + O(\epsilon^9). \end{aligned} \quad (3.2.12)$$

But for  $m = 2$ , we obtain  $b_o = 0$  and  $\lambda = \lambda_1$  or  $a_o = 0$  and  $\lambda = \lambda_2$  where  $\lambda_1 = \lambda_2$  i.e. :

$$\lambda_1 = \lambda_2 = 4 + \frac{1}{6}\epsilon^2 - \frac{1}{3456}\epsilon^4 - \frac{1}{1244160}\epsilon^6 + \frac{11}{5733089280}\epsilon^8 + O(\epsilon^9). \quad (3.2.13)$$

The case  $m = 3$  is similar with  $m = 1$ , that is, one obtains  $a_o = b_o$  and  $\lambda = \lambda'_3$  where

$$\begin{aligned} \lambda'_3 = & 9 + \frac{9}{64}\epsilon^2 - \frac{3}{512}\epsilon^3 + \frac{9}{65536}\epsilon^4 + \frac{15}{524288}\epsilon^5 \\ & - \frac{141}{33554432}\epsilon^6 - \frac{21}{536870912}\epsilon^7 + \frac{4101}{68719476736}\epsilon^8 + O(\epsilon^9) \end{aligned} \quad (3.2.14)$$

or  $a_o = -b_o$  and  $\lambda = \lambda'_4$  where

$$\begin{aligned} \lambda'_4 = & 9 + \frac{9}{64}\epsilon^2 + \frac{3}{512}\epsilon^3 + \frac{9}{65536}\epsilon^4 - \frac{15}{524288}\epsilon^5 \\ & - \frac{141}{33554432}\epsilon^6 + \frac{21}{536870912}\epsilon^7 + \frac{4101}{68719476736}\epsilon^8 + O(\epsilon^9). \end{aligned} \quad (3.2.15)$$

The case  $m = 4$  is similar with  $m = 2$ . We obtain  $b_o = 0$  and  $\lambda = \lambda_3$  or  $a_o = 0$  and  $\lambda = \lambda_4$  with  $\lambda_3 = \lambda_4$  i. e.

$$\begin{aligned} \lambda_3 = \lambda_4 = & 16 + \frac{2}{15}\epsilon^2 + \frac{11}{108000}\epsilon^4 + \frac{1033}{1360800000}\epsilon^6 \\ & - \frac{60703}{31352832000000}\epsilon^8 + O(\epsilon^9). \end{aligned} \quad (3.2.16)$$

The approximations of  $\lambda'_1$  and  $\lambda'_2$  are given by (3.2.11) and (3.2.12) respectively. The approximation of  $\lambda_1$  and  $\lambda_2$  are the same and are given by (3.2.13). The expansions of  $\lambda'_3$  and  $\lambda'_4$  are given by (3.2.14) and (3.2.15) respectively, and finally the approximations of  $\lambda_3$  and  $\lambda_4$  are given by (3.2.16).

Numerical	Analytical
$\lambda'_1 = 0.5875\mathbf{666498}$	$0.5875\mathbf{55692}$
$\lambda'_2 = 1.5992\mathbf{09067}$	$1.5992\mathbf{11767}$
$\lambda_1 = 4.166376513$	$4.166376513$
$\lambda'_3 = 9.1349273\mathbf{78}$	$9.1349273\mathbf{83}$
$\lambda'_4 = 9.146588994$	$9.146588991$
$\lambda_3 = 16.13343594$	$16.13343594$

**Table 3.1:** Comparison of the values of  $\lambda$  in equation (3.2.3) obtained with the numerical method and the perturbation method for  $\epsilon = 1$ . For this value (of  $\lambda$ ) equation (3.2.3) has periodic solution.

The analytical results as obtained above are compared with the numerical results as presented in Figure 3.1b, for  $\epsilon = 1$  in Table 3.1 . One can observe a striking resemblance.

The occurrence of the coexistence of periodic solutions in equation (3.2.3) depends on the periodicity of the coefficient of the damping term. As is known in [14] coexistence occurs when the coefficient of the damping term is  $\pi/2$ -anti periodic. So, if one perturbs the period then the coexistence does not occur anymore as is shown in the following example.

Consider the equation

$$\ddot{x} + (\epsilon \cos(2t) + \epsilon b \cos t)\dot{x} + \lambda x = 0. \quad (3.2.17)$$

The period of the coefficient of the damping term is  $2\pi$  if  $b$  is not equal to zero, thus if one transform equation (3.2.17) into Hill's type then this equation does not satisfy (3.2.5) i.e.  $P(t + \pi/2) \neq -P(t)$  where  $P(t) = -\frac{1}{2}(\epsilon \cos 2t + \epsilon b \cos t)$ . So coexistence may not occur anymore, and the approximation of  $\lambda'_1, \lambda'_2, \lambda_1, \lambda_2, \lambda'_3, \lambda'_4, \lambda_3$  and  $\lambda_4$  (up to order  $O(\epsilon^9)$ ) are given by

$$\begin{aligned} \lambda'_1 = & 1 - \frac{1}{2}\epsilon + \left(\frac{3}{32} + \frac{1}{6}b^2\right)\epsilon^2 - \left(\frac{3}{512} + \frac{1}{36}b^2\right)\epsilon^3 - \left(\frac{3}{8192} + \frac{7}{576}b^2 + \frac{1}{864}b^4\right)\epsilon^4 \\ & + \left(\frac{5}{131072} + \frac{11}{3072}b^2 + \frac{47}{13824}b^4\right)\epsilon^5 \\ & + \left(\frac{17}{4194304} - \frac{39}{573440}b^2 - \frac{653}{4976640}b^4 - \frac{1}{77760}b^6\right)\epsilon^6 \\ & - \left(\frac{7}{134217728} + \frac{187403}{2890137600}b^2 + \frac{430961}{1194393600}b^4 + \frac{3877}{18662400}b^6\right)\epsilon^7 \\ & + \left(-\frac{1}{16777216} + \frac{6431}{2055208960}b^2 + \frac{1259837}{17836277760}b^4\right. \\ & \left. + \frac{10421}{627056640}b^6 + \frac{11}{89579520}b^8\right)\epsilon^8 + O(\epsilon^9), \end{aligned} \quad (3.2.18)$$

$$\begin{aligned}
 \lambda'_2 &= 1 + \frac{1}{2}\epsilon + \left(\frac{3}{32} + \frac{1}{6}b^2\right)\epsilon^2 + \left(\frac{3}{512} + \frac{1}{36}b^2\right)\epsilon^3 - \left(\frac{3}{8192} + \frac{7}{576}b^2 + \frac{1}{864}b^4\right)\epsilon^4 \\
 &+ \left(\frac{5}{131072} + \frac{11}{3072}b^2 + \frac{47}{13824}b^4\right)\epsilon^5 \\
 &+ \left(\frac{17}{4194304} - \frac{39}{573440}b^2 - \frac{653}{4976640}b^4 - \frac{1}{77760}b^6\right)\epsilon^6 \\
 &- \left(\frac{7}{134217728} + \frac{187403}{2890137600}b^2 + \frac{430961}{1194393600}b^4 + \frac{3877}{18662400}b^6\right)\epsilon^7 \\
 &+ \left(-\frac{1}{16777216} + \frac{6431}{2055208960}b^2 + \frac{1259837}{17836277760}b^4 + \frac{10421}{627056640}b^6\right. \\
 &\left. + \frac{11}{89579520}b^8\right)\epsilon^8 + O(\epsilon^9),
 \end{aligned} \tag{3.2.19}$$

$$\begin{aligned}
 \lambda_1 &= 4 + \left(\frac{1}{6} + \frac{2}{15}b^2\right)\epsilon^2 - \frac{1}{36}b^2\epsilon^3 + \left(-\frac{1}{3456} + \frac{1}{180}b^2 + \frac{11}{27000}b^4\right)\epsilon^4 \\
 &+ \left(-\frac{37}{64800}b^2 - \frac{1}{1350}b^4\right)\epsilon^5 \\
 &- \left(\frac{1}{1244160} + \frac{79}{6531840}b^2 + \frac{6397}{108864000}b^4 + \frac{1033}{85050000}b^6\right)\epsilon^6 \\
 &+ \left(\frac{1739}{232243200}b^2 + \frac{7639}{51030000}b^4 + \frac{409}{58320000}b^6\right)\epsilon^7 \\
 &+ \left(\frac{11}{5733089280} - \frac{67}{470292480}b^2 - \frac{19979}{261273600}b^4 - \frac{864931}{48988800000}b^6\right. \\
 &\left. - \frac{60703}{489888000000}b^8\right)\epsilon^8 + O(\epsilon^9),
 \end{aligned} \tag{3.2.20}$$

$$\begin{aligned}
 \lambda_2 &= 4 + \left(\frac{1}{6} + \frac{2}{15}b^2\right)\epsilon^2 + \frac{1}{36}b^2\epsilon^3 + \left(-\frac{1}{3456} + \frac{1}{180}b^2 + \frac{11}{27000}b^4\right)\epsilon^4 \\
 &+ \left(-\frac{37}{64800}b^2 - \frac{1}{1350}b^4\right)\epsilon^5 \\
 &- \left(\frac{1}{1244160} + \frac{79}{6531840}b^2 + \frac{6397}{108864000}b^4 - \frac{1033}{85050000}b^6\right)\epsilon^6 \\
 &- \left(\frac{1739}{232243200}b^2 + \frac{7639}{51030000}b^4 + \frac{409}{58320000}b^6\right)\epsilon^7 \\
 &+ \left(\frac{11}{5733089280} - \frac{67}{470292480}b^2 - \frac{19979}{261273600}b^4 - \frac{864931}{48988800000}b^6\right. \\
 &\left. - \frac{60703}{489888000000}b^8\right)\epsilon^8 + O(\epsilon^9),
 \end{aligned} \tag{3.2.21}$$

$$\begin{aligned}
 \lambda'_3 &= 9 + \left(\frac{9}{64} + \frac{9}{70}b^2\right)\epsilon^2 - \frac{3}{512}\epsilon^3 + \left(\frac{9}{65536} + \frac{9}{4480}b^2 + \frac{279}{1372000}b^4\right)\epsilon^4 \\
 &+ \left(\frac{15}{524288} - \frac{1311}{1254400}b^2 - \frac{3}{12800}b^4\right)\epsilon^5 \\
 &+ \left(-\frac{141}{33554432} + \frac{3207}{50462720}b^2 + \frac{17789}{351232000}b^4 + \frac{5953}{10084200000}b^6\right)\epsilon^6 \\
 &+ \left(-\frac{21}{536870912} + \frac{19287}{1284505600}b^2 - \frac{20945241}{786759680000}b^4 - \frac{93}{31360000}b^6\right)\epsilon^7 \\
 &+ \left(\frac{4101}{68719476736} - \frac{569953}{180858388480}b^2 + \frac{6165641}{1186883174400}b^4 + \frac{25654589}{28397107200000}b^6\right. \\
 &\left. + \frac{171697}{316240512000000}b^8\right)\epsilon^8 + O(\epsilon^9),
 \end{aligned} \tag{3.2.22}$$

$$\begin{aligned}
\lambda_4 = & 9 + \left(\frac{9}{64} + \frac{9}{70}b^2\right)\epsilon^2 + \frac{3}{512}\epsilon^3 + \left(\frac{9}{65536} + \frac{9}{4480}b^2 + \frac{279}{1372000}b^4\right)\epsilon^4 \\
& - \left(\frac{15}{524288} - \frac{1311}{1254400}b^2 - \frac{3}{12800}b^4\right)\epsilon^5 \\
& + \left(-\frac{141}{33554432} + \frac{3207}{50462720}b^2 + \frac{17789}{351232000}b^4 + \frac{5953}{10084200000}b^6\right)\epsilon^6 \\
& - \left(-\frac{21}{536870912} + \frac{19287}{1284505600}b^2 - \frac{20945241}{786759680000}b^4 - \frac{93}{31360000}b^6\right)\epsilon^7 \\
& + \left(\frac{4101}{68719476736} - \frac{569953}{180858388480}b^2 + \frac{6165641}{1186883174400}b^4 + \frac{25654589}{28397107200000}b^6\right. \\
& \left. + \frac{171697}{316240512000000}b^8\right)\epsilon^8 + O(\epsilon^9),
\end{aligned} \tag{3.2.23}$$

$$\begin{aligned}
\lambda_3 = & 16 + \left(\frac{2}{15} + \frac{8}{63}b^2\right)\epsilon^2 + \left(\frac{11}{108000} + \frac{1}{945}b^2 + \frac{59}{500094}b^4\right)\epsilon^4 - \frac{25}{127008}b^2\epsilon^5 + \\
& \left(\frac{1033}{1360800000} + \frac{58031}{5837832000}b^2 + \frac{19363}{1584297792}b^4 + \frac{19561}{218336039460}b^6\right)\epsilon^6 \\
& - \left(\frac{1}{529200}b^2 + \frac{61069}{6301184400}b^4 + \frac{1}{1411200}b^6\right)\epsilon^7 \\
& + \left(-\frac{60703}{31352832000000} + \frac{10021589}{73556683200000}b^2 + \frac{2034457}{41191742592000}b^4 + \right. \\
& \left. \frac{7397773}{74313648339840}b^6 + \frac{41146789}{110921694798942720}b^8\right)\epsilon^8 + O(\epsilon^9),
\end{aligned} \tag{3.2.24}$$

$$\begin{aligned}
\lambda_4 = & 16 + \left(\frac{2}{15} + \frac{8}{63}b^2\right)\epsilon^2 + \left(\frac{11}{108000} + \frac{1}{945}b^2 + \frac{59}{500094}b^4\right)\epsilon^4 + \frac{25}{127008}b^2\epsilon^5 + \\
& \left(\frac{1033}{1360800000} + \frac{58031}{5837832000}b^2 + \frac{19363}{1584297792}b^4 + \frac{19561}{218336039460}b^6\right)\epsilon^6 \\
& + \left(\frac{1}{529200}b^2 + \frac{61069}{6301184400}b^4 + \frac{1}{1411200}b^6\right)\epsilon^7 \\
& + \left(-\frac{60703}{31352832000000} + \frac{10021589}{73556683200000}b^2 + \frac{2034457}{41191742592000}b^4 + \right. \\
& \left. \frac{7397773}{74313648339840}b^6 + \frac{41146789}{110921694798942720}b^8\right)\epsilon^8 + O(\epsilon^9).
\end{aligned} \tag{3.2.25}$$

One can easily check that for  $b \rightarrow 0$  (3.2.18)-(3.2.25) reduce to (3.2.11)-(3.2.16). It can be shown that for  $b \neq 0$  the stability diagram of equation (3.2.17) has a similar geometry for  $\epsilon$  small as the stability diagram of the Mathieu equation (see Figure 3.1). The areas of instability depend on the parameter  $b$  in the damping term. As depicted in Figure 3.2 one may observe that when  $b$  tends to zero the areas of instability become narrower and finally when  $b$  equals zero the areas of instability vanish especially for  $\lambda = 4n^2$ ,  $n = 1, 2, 3, \dots$ . This phenomenon has been described for an equation which differs from the one presented in [23, 24].

### 3.3 An application in the theory of rain-wind induced vibrations.

In this section an application is given of the results obtained above. The application is concerned with the rain-wind induced vibrations of a simple one degree of free-

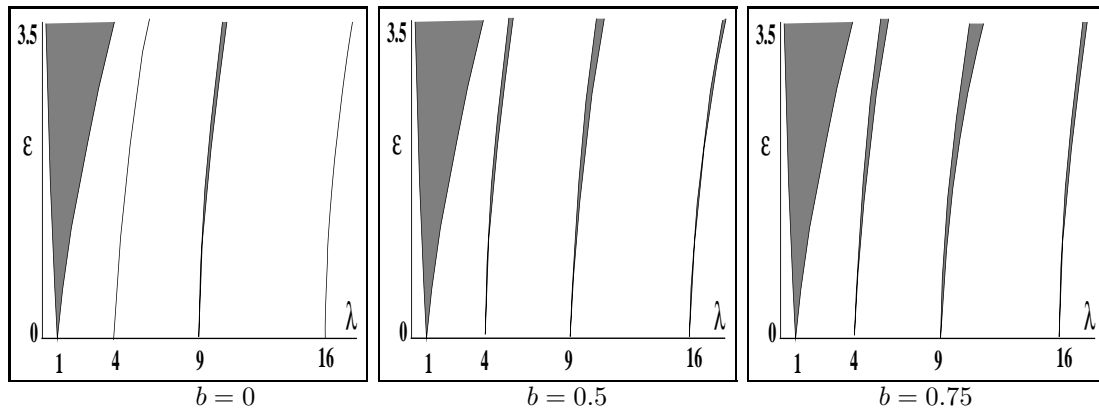


**Figure 3.2:** Stability diagram of equation (3.2.17) for various values of  $b$ . The shaded regions are areas of instability. When  $b = 0$  the instability areas have disappeared for  $\lambda = 4n^2$ .

dom system related to the dynamics of cable-stayed bridges. Firstly it will be shown how to model this problem in order to obtain a model equation of the form (3.1.1). Cable-stayed bridges are characterized by inclined stay cables connecting the bridge deck with one or more pylons. Usually the stay cables have a smooth polyurethane mantle and a cross section which is nearly circular. Under normal circumstances for such type of cables one would not expect galloping type of vibrations due to wind-forces. There are however exceptions: in the winter season ice accretion on the cable may induce aerodynamic instability resulting in vibrations with relatively large amplitudes. The instability mechanism for this type of vibrations is known and can be understood on the basis of quasi-steady modeling and analysis. In this analysis the so-called Den Hartog's criterion expressing a condition to have an unstable equilibrium state plays an important part. The other exception concerns vibrations excited by a wind-field containing raindrops. This phenomenon has probably been detected for the first time by Japanese researchers as can be derived from the papers by Matsumoto a.o. [17, 18]. As has been observed on scale models in wind-tunnels the raindrops that hit the inclined stay cable generate one or more rivulets on the surface of the cable. The presence of flowing water on the cable changes the cross section of the cable as experienced by the wind field. Accordingly the pressure distribution on the cable with respect to the direction of the (uniform) wind flow may become asymmetric, resulting in a lift force perpendicular to direction of the wind velocity.

It is of interest to remark that there is an important difference between the presence of ice accretion and rivulets as far as it concerns the dynamical behaviour. The ice accretion concerns an ice coating fixed to the surface of the cable whereas the rivulet concerns a flow of water on the surface of the cable where the position of the rivulet depends on the resulting wind velocity, the surface tension of the water and the adhesion between the water and polyurethane mantle of the cable.

For the interesting cases the thickness of the ice accretion is not uniform: the evolution process of ice accretion usually results in an ice coating involving a ridge of ice. The case with water rivulets can also be characterized by the presence of the ridge of water be it with the difference that this water ridge is not fixed to the surface of the

cable. As long as the water ridge is present, it may be blown off if the wind-speed exceeds a critical value, one may assume that the position of the ridge varies in time. Subsequently one may assume that this time-dependency has a similar character as the motion of the cable i.e. if the cable oscillates harmonically then one may expect that the water ridge moves accordingly. The observation of this complicated system of an inclined cable, connecting a bridge deck and a pylon, with a moving rivulet leads to the following conclusion.

The inclination of the cable is relevant for having a rivulet. The rivulet, however, can be viewed as a moving ridge which may be modeled by a solid state. According to this way of modeling the inclination of the cable is no longer relevant. Hence we consider as a prototype of an oscillator a one degree of freedom system consisting of a horizontal rigid cable supported by springs with a solid state ridge moving with small amplitude oscillations. From the point of view of the type of equation of motion, we arrive at a second order differential equation with external forcing. A more detailed description of the modeling is presented in the following section.

### 3.3.1 The Model Equation for Rain-Wind Induced Vibrations of a Prototype Oscillator

The modeling principles we use are closely related to the quasi-steady approach as given in [8, 27]. We consider a rigid cylinder with uniform cross-section supported by springs in a uniform rain-wind flow directed perpendicular to the axis of the cylinder. The oscillator is constructed in such a way that only vertical (one degree of freedom) oscillations are possible. The basic cross-section of the cylinder is circular, however, on the surface of the cylinder there is a ridge able to carry out small amplitude oscillations. To model the rain-wind forces on the cylinder a quasi-steady approach is used; the type of oscillations which can be studied on the respective assumptions are known as galloping. A more detailed description of the quasi-steady approach can be found in [27, 31]. The basic assumption of the quasi-steady approach is that at each moment in the dynamic situation the rain-wind force can be taken equal to the steady force exerted on the cylinder in static state. In the dynamic situation one should take into account that the flow-induced forces are based on the instantaneous flow velocity which is equal to the vector sum of flow velocity and the time varying vertical flow velocity induced by the (vertical) motion of the cylinder.

The steady rain-wind forces can be measured in a wind-tunnel and are expressed in the form of non-dimensional aerodynamic coefficients which depend on the angle of attack  $\alpha$ . This angle, an essential variable for the description of the dynamics of the oscillator, is defined as the angle between the resultant flow velocity and an axis of reference fixed to the cylinder; measured positive in clockwise direction. The system we will study in more detail is sketched in Figure 3.3.

The horizontal wind velocity is  $U$  and as the cylinder is supposed to move in the positive  $y$  direction, there is a virtual vertical wind velocity  $-\dot{y}$ . The drag force  $D$  is indicated in the direction of the resultant wind-velocity  $U_r$ , whereas the lift force  $L$  is perpendicular to  $D$  in anti clockwise direction. The ridge on the cylinder (shaded indicated in Figure 3.3) is able to carry out small amplitude oscillations. The aerodynamic force  $F_y$  in vertical direction can easily be derived from Figure 3.3



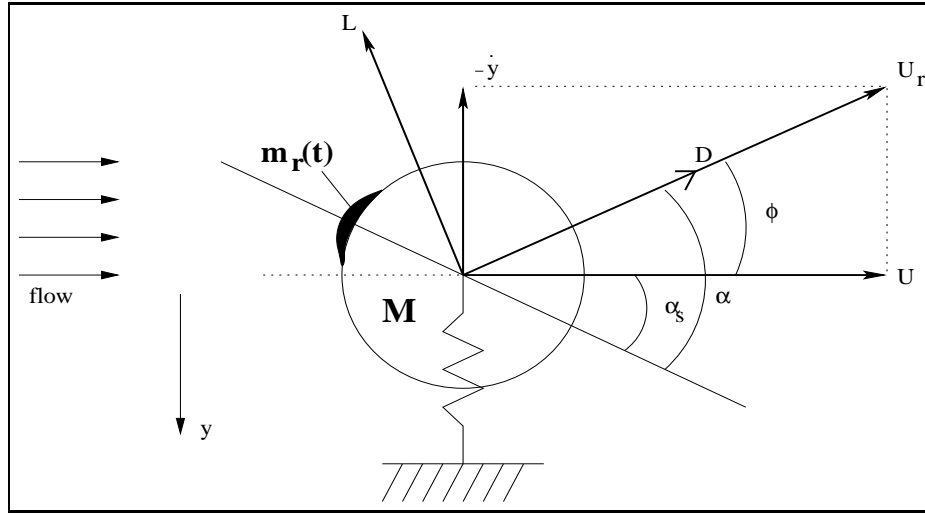


**Figure 3.3:** Cross-section of the cylinder-spring system, fluid flow with respect to the cylinder and wind forces on the cylinder

:

$$F_y = -D \sin \phi - L \cos \phi, \quad (3.3.1)$$

where  $\phi$  is the angle between  $U_r$  and  $U$ , positive in clockwise direction, with  $|\phi| \leq \pi/2$ .

The drag and lift force are given by the empirical relations:

$$\begin{aligned} D &= \frac{1}{2} \rho d l U_r^2 C_D(\alpha), \\ L &= \frac{1}{2} \rho d l U_r^2 C_L(\alpha), \end{aligned} \quad (3.3.2)$$

where  $\rho$  is the density of air,  $d$  the diameter of the cylinder,  $l$  the length of the cylinder,  $C_D(\alpha)$  and  $C_L(\alpha)$  are the drag and lift coefficient curves respectively, determined by measurements in a wind-tunnel. From Figure 3.3 it follows that :

$$\begin{aligned} \sin \phi &= \dot{y}/U_r, \\ \cos \phi &= U/U_r, \\ \alpha &= \alpha_s + \arctan(\dot{y}/U), \end{aligned} \quad (3.3.3)$$

where  $\alpha_s$  is the angle between the symmetry axis and the horizontal wind velocity. The equation of motion of the oscillator readily becomes :

$$m\ddot{y} + c_y\dot{y} + k_y y = F_y, \quad (3.3.4)$$

where  $m$  is the mass of the cylinder,  $c_y > 0$  the structural damping coefficient of the oscillator,  $k_y > 0$  the spring constant. By using (3.3.2) and (3.3.3) we obtain for  $F_y$ :

$$F_y = -\frac{1}{2} \rho d l \sqrt{U^2 + \dot{y}^2} (C_D(\alpha)\dot{y} + C_L(\alpha)U). \quad (3.3.5)$$

Setting  $\omega_y^2 = k_y/m$ ,  $\tau = \omega_y t$  and  $z = \omega_y y/U$  equation (3.3.4) becomes:

$$\begin{aligned}\ddot{z} + 2\beta\dot{z} + z &= -K\sqrt{1 + \dot{z}^2} (C_D(\alpha)\dot{z} + C_L(\alpha)), \\ \alpha &= \alpha_s + \arctan(\dot{z}),\end{aligned}\tag{3.3.6}$$

where  $2\beta = c_y/m\omega_y$  and  $K = \rho d lU/2m\omega_y$  are non-dimensional parameters, and  $\dot{z}$  now stands for differentiation with respect to  $\tau$ . We study the case where the drag and lift coefficient curve can be approximated by a constant and a cubic polynomial respectively:

$$\begin{aligned}C_D(\alpha) &= C_{D_o}, \\ C_L(\alpha) &= C_{L_1}(\alpha - \alpha_o) + C_{L_3}(\alpha - \alpha_o)^3,\end{aligned}\tag{3.3.7}$$

where  $C_{D_o} > 0$  and for the interesting cases  $C_{L_1} < 0$  and  $C_{L_3} > 0$ . As known in [27] that the aerodynamic drag and lift coefficient may be obtained from wind-tunnel experiments and have a typical result which can be approximated by (3.3.7) where  $\alpha_o$  is a special value such that the aerodynamic lift coefficient equals zero when  $\alpha = \alpha_o$ . By using  $\alpha = \alpha_s + \arctan(\dot{z})$  we obtain for  $C_L(\alpha)$ :

$$C_L(\alpha) = C_{L_1}(\alpha_s - \alpha_o + \arctan \dot{z}) + C_{L_3}(\alpha_s - \alpha_o + \arctan \dot{z})^3 \quad .\tag{3.3.8}$$

The cases that  $\alpha_s = \alpha_o$  and  $\alpha_s \neq \alpha_o$  where  $\alpha_s$  and  $\alpha_o$  are (time independent) parameters have been studied in [8]. Here we study the case that the position of the (water) ridge varies with time:

$$\alpha_s - \alpha_o = f(t) = f(\tau/\omega_y).\tag{3.3.9}$$

Substitution of (3.3.8) and (3.3.9) into (3.3.6) and expanding the right hand side with respect to  $\dot{z}$  in the neighbourhood of  $\dot{z} = 0$  yields:

$$\begin{aligned}\ddot{z} + z &= -K[C_{L_1}f(t) + C_{L_3}f^3(t) + \\ &(C_{D_o} + C_{L_1} + 2\beta/K + 3C_{L_3}f^2(t)) \dot{z} + \\ &(\frac{1}{2}C_{L_1}f(t) + \frac{1}{2}C_{L_3}f^3(t) + 3C_{L_3}f(t)) \dot{z}^2 + \\ &(\frac{1}{6}C_{L_1} + C_{L_3} + \frac{1}{2}C_{D_o} + \frac{1}{2}C_{L_3}f^2(t)) \dot{z}^3] + 0(\dot{z}^4).\end{aligned}\tag{3.3.10}$$

Inspection of this equation shows that for  $f(t) \equiv 0$  one obtains:

$$\ddot{z} + z = K[-(C_{D_o} + C_{L_1} + 2\beta/K) \dot{z} - (\frac{1}{6}C_{L_1} + C_{L_3} + \frac{1}{2}C_{D_o}) \dot{z}^3].\tag{3.3.11}$$

When the following conditions hold :

$$\begin{aligned}C_{D_o} + C_{L_1} + 2\beta/K &< 0 \text{ (Den Hartog's Criterion),} \\ \frac{1}{6}C_{L_1} + C_{L_3} + \frac{1}{2}C_{D_o} &> 0\end{aligned}\tag{3.3.12}$$

the equation can be reduced to the Rayleigh equation, which has, as is well-known, a unique periodic solution (limit-cycle). The linearized version of equation (3.3.11) has apart from  $z \equiv 0$  only unbounded solutions if Den Hartog's criterion applies.

Linearization of equation (3.3.10), however, leads to an equation which may have periodic solutions and is hence of interest to study in more detail. The nonlinear equation (3.3.10) will be studied further in subsection 3.3.2. The linearized version of (3.3.10) can be written as :

$$\begin{aligned} \ddot{z} + K(C_{D_o} + C_{L_1} + 2\beta/K + 3C_{L_3}f^2(t)) \dot{z} + z + \\ K(C_{L_1}f(t) + C_{L_3}f^3(t)) = 0. \end{aligned} \quad (3.3.13)$$

We consider the case that  $f(t) = A \cos(\frac{\omega}{\omega_y}\tau) = A \cos(\Omega\tau)$  where  $\Omega = \frac{\omega}{\omega_y}$ . With

$$\begin{aligned} f^2(t) &= \frac{1}{2}A^2(1 + \cos(2\Omega\tau)) \quad \text{and} \\ f^3(t) &= \frac{3}{4}A^3(\cos(\Omega\tau) + \frac{1}{3}\cos(3\Omega\tau)) \end{aligned}$$

(3.3.13) becomes:

$$\begin{aligned} \ddot{z} + (KA_o + KA_1 \cos(2\Omega\tau)) \dot{z} + z + \\ KA_2 \cos(\Omega\tau) + KA_3 \cos(3\Omega\tau) = 0, \end{aligned} \quad (3.3.14)$$

where

$$\begin{aligned} A_o &= C_{D_o} + C_{L_1} + 2\beta/K + \frac{3}{2}C_{L_3}A^2, \\ A_1 &= \frac{3}{2}C_{L_3}A^2, \\ A_2 &= C_{L_1}A + \frac{3}{4}C_{L_3}A^3, \\ A_3 &= \frac{1}{4}C_{L_3}A^3. \end{aligned}$$

For the oscillator we study the interesting case  $\Omega = 1 + \epsilon\eta$  where  $|\epsilon| \ll 1$ . By setting  $(1 + \epsilon\eta)\tau = \theta$  (3.3.14) becomes:

$$\begin{aligned} (1 + \epsilon\eta)^2 \ddot{z} + (1 + \epsilon\eta)(KA_o + KA_1 \cos(2\theta)) \dot{z} + z + \\ KA_2 \cos(\theta) + KA_3 \cos(3\theta) = 0, \end{aligned} \quad (3.3.15)$$

where a dot now stands for differentiation with respect to  $\theta$ . Let the coefficients  $KA_i$  for  $i = 0, 1, 2, 3$  be of  $O(\epsilon)$ . Then (3.3.15) can be written as:

$$\begin{aligned} \ddot{z} + (KA_o + KA_1 \cos(2\theta)) \dot{z} + (1 - 2\epsilon\eta)z + \\ KA_2 \cos(\theta) + KA_3 \cos(3\theta) + O(\epsilon^2) = 0. \end{aligned} \quad (3.3.16)$$

If one neglects the  $O(\epsilon^2)$  terms then the only difference between equation (3.3.16) and equation (3.1.1)(for  $m = 1$ ) is the term  $KA_3 \cos(3\theta)$ . This term can be regarded as a forcing term, but as the frequency is three times greater than the natural frequency it is not relevant for the  $O(\epsilon)$  approximation. Putting  $KA_o = a_o\epsilon$ ,  $KA_1 = a_1\epsilon$ ,  $KA_2 = a_2\epsilon$ , and  $KA_3 = a_3\epsilon$  and neglecting  $O(\epsilon^2)$  of (3.3.16) one obtains:

$$\ddot{z} + \epsilon(a_o + a_1 \cos(2\theta)) \dot{z} + (1 - 2\epsilon\eta)z + a_2 \cos(\theta) + a_3 \cos(3\theta) = 0. \quad (3.3.17)$$

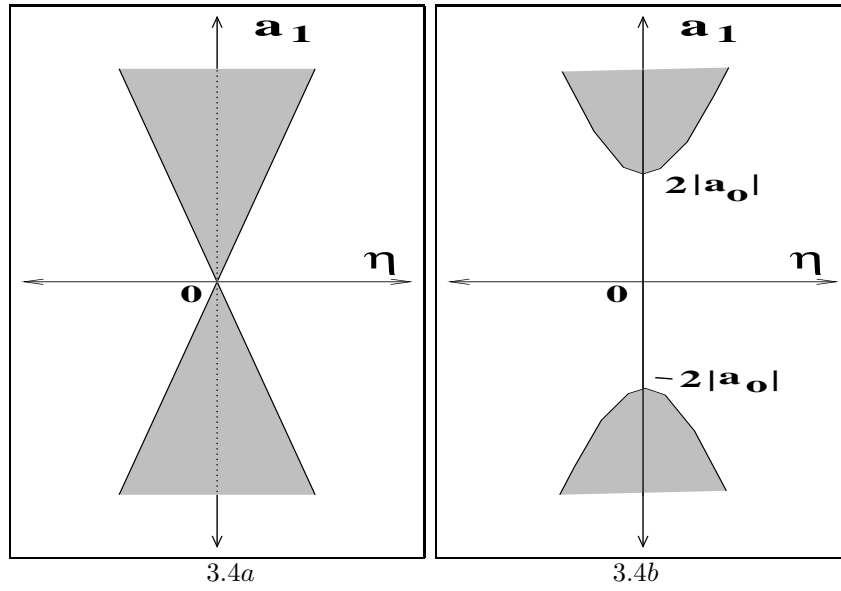


**Figure 3.4:** Separation of the instability tongue: Figure 3.4a:  $a_o = 0$ , Figure 3.4b:  $a_o \neq 0$

Transforming (3.3.17) by new variables  $y_1$  and  $y_2$  i.e.

$$\begin{aligned} z &= y_1 \cos \theta + y_2 \sin \theta, \\ \dot{z} &= -y_1 \sin \theta + y_2 \cos \theta, \end{aligned} \quad (3.3.18)$$

one obtains by first order averaging:

$$\begin{pmatrix} \dot{\bar{y}}_1 \\ \dot{\bar{y}}_2 \end{pmatrix} = \epsilon \begin{pmatrix} -\frac{1}{2}a_o + \frac{1}{4}a_1 & -\eta \\ \eta & -\frac{1}{2}a_o - \frac{1}{4}a_1 \end{pmatrix} \begin{pmatrix} \bar{y}_1 \\ \bar{y}_2 \end{pmatrix} + \epsilon \begin{pmatrix} 0 \\ -\frac{1}{2}a_1 \end{pmatrix}. \quad (3.3.19)$$

The critical point of (3.3.19) is

$$\left( \frac{\frac{1}{2}\eta a_2}{\frac{1}{4}a_o^2 - \frac{1}{16}a_1^2 + \eta^2}, \frac{\frac{1}{2}a_2(-\frac{1}{2}a_o + \frac{1}{4}a_1)}{\frac{1}{4}a_o^2 - \frac{1}{16}a_1^2 + \eta^2} \right).$$

If the determinant of the coefficient matrix of (3.3.19) is not equal to zero then (3.3.17) has a periodic solution and its stability depends on the eigenvalues of the coefficient matrix. The eigenvalues of the coefficient matrix are

$$\frac{1}{2}\epsilon \left( -a_o \pm \sqrt{\frac{1}{4}a_1^2 - 4\eta^2} \right).$$

By equating these eigenvalues to zero one obtains the transition curves between the stable and unstable regions  $a_o = \sqrt{\frac{1}{4}a_1^2 - 4\eta^2}$  in the  $a_1 - \eta$  plane. In case  $a_o = 0$  the stability diagram is depicted in Figure 3.4a, and if  $a_o > 0$  then the instability area separates from the  $\eta$ -axis with a distance  $2a_o$  as shown in Figure 3.4b.

### 3.3.2 The non-linear model

In this section we present some results on the analysis of the non-linear model equation (3.3.10) which can be written as:

$$\begin{aligned} \ddot{z} + z = & -K[A_2 \cos(\Omega\tau) + A_3 \cos(3\Omega\tau) + \\ & (A_o + A_1 \cos(2\Omega\tau)) \dot{z} - (2\epsilon\eta/K)z + \\ & (A_4 \cos(\Omega\tau) + \frac{1}{2}A_3 \cos(3\Omega\tau)) \dot{z}^2 + \\ & (A_5 + \frac{1}{6}A_1 \cos(2\Omega\tau)) \dot{z}^3], \end{aligned} \quad (3.3.20)$$

where  $A_o, A_1, A_2, A_3$  are defined in (3.3.14) and

$$\begin{aligned} A_4 &= \frac{1}{2}C_{L_1}A + 3C_{L_3}A + \frac{3}{8}C_{L_3}A^3, \\ A_5 &= \frac{1}{6}C_{L_1} + C_{L_3} + \frac{1}{2}C_{D_o} + \frac{1}{4}C_{L_3}A^2. \end{aligned}$$

We consider the case that  $\Omega = 1$ , i. e. the natural frequency of the oscillator is the same as the frequency of the motion of the water ridge. It seems natural that when the oscillator moves up and down then the water ridge along cylinder will be moving to the right and the left with the same frequency. By application of the transformation (3.3.18):

$$\begin{aligned} z &= y_1 \cos \tau + y_2 \sin \tau, \\ \dot{z} &= -y_1 \sin \tau + y_2 \cos \tau, \end{aligned} \quad (3.3.21)$$

we obtain after first order averaging:

$$\begin{aligned} \dot{\bar{y}}_1 &= K\left[-\frac{1}{2}A_o + \frac{1}{4}A_1\right]\bar{y}_1 + \left(\frac{1}{8}A_3 - \frac{1}{4}A_4\right)\bar{y}_1\bar{y}_2 - \\ & \quad \frac{3}{8}A_5\bar{y}_1\bar{y}_2^2 + \left(\frac{1}{24}A_1 - \frac{3}{8}A_5\right)\bar{y}_1^3, \\ \dot{\bar{y}}_2 &= -K\left[\frac{1}{2}A_2 + \left(\frac{1}{2}A_o + \frac{1}{4}A_1\right)\bar{y}_2 + \left(\frac{1}{8}A_4 - \frac{1}{16}A_3\right)\bar{y}_1^2 + \right. \\ & \quad \left. \left(\frac{3}{8}A_4 + \frac{1}{16}A_3\right)\bar{y}_2^2 + \frac{3}{8}A_5\bar{y}_1^2\bar{y}_2 + \left(\frac{3}{8}A_5 + \frac{1}{24}A_1\right)\bar{y}_2^3\right]. \end{aligned} \quad (3.3.22)$$

The linearized system (3.3.22) has the critical point  $(0, -\frac{A_2}{A_o + \frac{1}{2}A_1})$  which is unstable if  $A_o - \frac{1}{2}A_1 < 0$ . With the original variables this inequality reads:

$$C_{D_o} + C_{L_1} + 2\beta/K + \frac{3}{4}C_{L_3}A^2 < 0,$$

which can be considered as a modified Den Hartog criterion expressing that the instability is due to self-excitation combined with parametric excitation. Critical points of (3.3.22) may correspond to periodic solutions of equation (3.3.20). One important critical point can be found by setting  $\bar{y}_1 \equiv 0$ . The second coordinate can

be found by solving the cubical equation obtained from the right hand side of the second equation in (3.3.22) :

$$\begin{aligned} \left(\frac{1}{2}A_o + \frac{3}{8}A_5\bar{y}_2^2\right)\bar{y}_2 &= -\left\{\frac{1}{2}A_2 + \frac{1}{4}A_1\bar{y}_2 + \right. \\ &\quad \left. \left(\frac{3}{8}A_4 + \frac{1}{16}A_3\right)\bar{y}_2^2 + \frac{1}{24}A_1\bar{y}_2^3\right\}. \end{aligned} \quad (3.3.23)$$

The right hand side of this equation can be made arbitrary small by letting  $A \rightarrow 0$ . Accordingly a solution can be found by setting :

$$\bar{y}_2 = y_{20} + Ay_{21}, \quad (3.3.24)$$

where

$$y_{20}^2 = -\frac{1}{2}A_o/\frac{3}{8}A_5, \quad A_o < 0 \quad \text{and} \quad A_5 > 0. \quad (3.3.25)$$

$y_{21}$  can be computed by substitution of (3.3.24) into (3.3.23) and by applying a straight forward elementary perturbation procedure. It can be shown that the critical point  $(0, \bar{y}_2)$  corresponds with a stable periodic solution (limit cycle) of equation (3.3.22) in the sense of an approximation accurate up to  $O(A)$ .

If  $A = 0$  the critical points  $(\bar{y}_{10}, \bar{y}_{20})$  of (3.3.22) are on the circle  $\bar{y}_1^2 + \bar{y}_2^2 = -\frac{1}{2}A_o/\frac{3}{8}A_5$ , implying that the original equation has periodic solutions which can be approximated by time harmonic functions of constant amplitude  $\sqrt{-\frac{1}{2}A_o/\frac{3}{8}A_5}$  and arbitrary phase. If  $A = O(1)$  equation (3.3.23) may have one, two or three real zeros.

The other critical points of (3.3.22) can be found by assuming that  $\bar{y}_1 \neq 0$ . In this case the right hand side of the first equation (3.3.22) can be written as

$$K\bar{y}_1\left[\left(-\frac{1}{2}A_o + \frac{1}{4}A_1\right) + \left(\frac{1}{8}A_3 - \frac{1}{4}A_4\right)\bar{y}_2 - \frac{3}{8}A_5\bar{y}_2^2 + \left(\frac{1}{24}A_1 - \frac{3}{8}A_5\right)\bar{y}_1^2\right],$$

and it then follows that

$$\bar{y}_1^2 = -\left[\left(-\frac{1}{2}A_o + \frac{1}{4}A_1\right) + \left(\frac{1}{8}A_3 - \frac{1}{4}A_4\right)\bar{y}_2 - \frac{3}{8}A_5\bar{y}_2^2\right]/\left(\frac{1}{24}A_1 - \frac{3}{8}A_5\right). \quad (3.3.26)$$

Substituting (3.3.26) into the right hand side of the second equation of (3.3.22) one obtains a cubical polynomial in  $\bar{y}_2$ . Thus to find the zeros of this polynomial we can use Cardano's formula. As an example the case is considered where  $A$  varies and where the other parameters are given the following numerical values:  $C_{D_o} = 0.5$ ,  $C_{L_1} = -6.0$ ,  $\beta/K = 2.0$ , and  $C_{L_3} = 2.0$ . In case  $\bar{y}_1 \equiv 0$ , by using Cardano's formula one finds that for  $A = 0.1420$  there are two real zeros. Whereas for  $0 < A < 0.1420$  three real zeros exist and for  $A > 0.1420$  only one. However, in case  $\bar{y}_1 \neq 0$  we do not find critical points. The phase portraits for these three cases are given in Figure 3.5 including the case  $A = 0$ . These portraits are drawn by using the DSTOOL software package.

It is of interest to consider the case  $\Omega \neq 1$ , implying that the frequency ratio of the natural frequency of the oscillator and the frequency of the motion of the

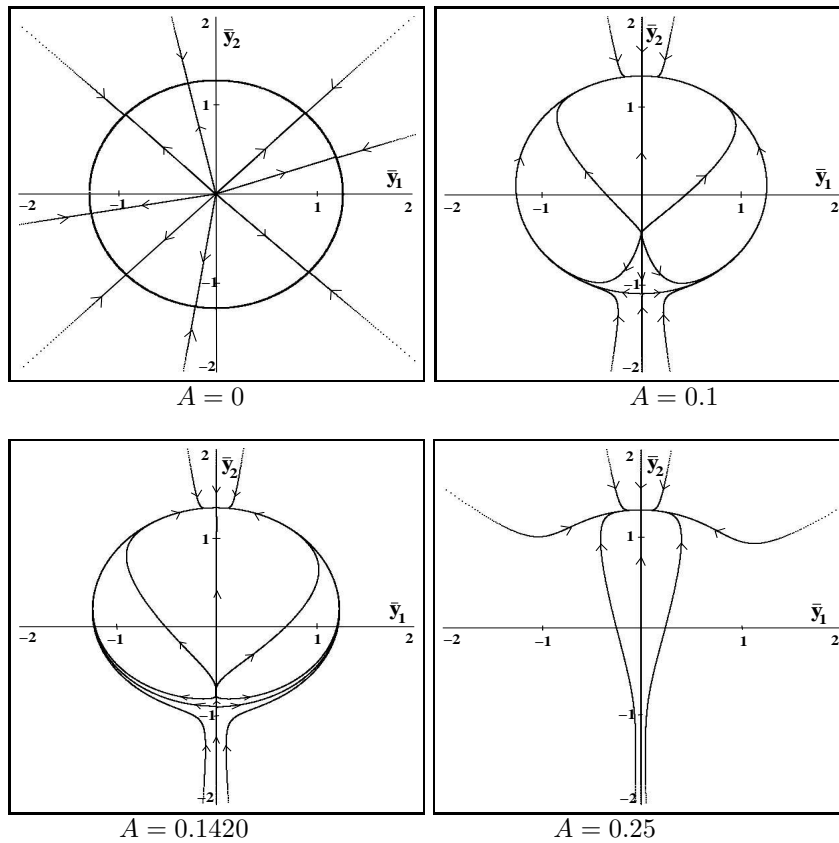


**Figure 3.5:** Orbits of equation (3.3.22) for  $A=0$ ,  $A=0.1$ ,  $A=0.1420$  and  $A=0.25$ . Vertical axis is  $\bar{y}_2$  and horizontal axis is  $\bar{y}_1$

ridge differs (slightly) from 1. By setting  $\Omega = 1 + \epsilon\eta$  one obtains after first order averaging:

$$\begin{aligned}
 \dot{\bar{y}}_1 &= K\left[\left(-\frac{1}{2}A_o + \frac{1}{4}A_1\right)\bar{y}_1 + \left(\frac{1}{8}A_3 - \frac{1}{4}A_4\right)\bar{y}_1\bar{y}_2 - \right. & (3.3.27) \\
 &\quad \left. \frac{3}{8}A_5\bar{y}_1\bar{y}_2^2 + \left(\frac{1}{24}A_1 - \frac{3}{8}A_5\right)\bar{y}_1^3\right] - \epsilon\eta\bar{y}_2, \\
 \dot{\bar{y}}_2 &= -K\left[\frac{1}{2}A_2 + \left(\frac{1}{2}A_o + \frac{1}{4}A_1\right)\bar{y}_2 + \left(\frac{1}{8}A_4 - \frac{1}{16}A_3\right)\bar{y}_1^2 + \right. \\
 &\quad \left. \left(\frac{3}{8}A_4 + \frac{1}{16}A_3\right)\bar{y}_2^2 + \frac{3}{8}A_5\bar{y}_1^2\bar{y}_2 + \left(\frac{3}{8}A_5 + \frac{1}{24}A_1\right)\bar{y}_2^3\right] + \epsilon\eta\bar{y}_1.
 \end{aligned}$$

Let now additionally  $A = 0.1$  and consider  $\eta$  as a parameter. By using a Gröbner basis algorithm one can show that for  $\eta = 0.194$  there are two real critical points of (3.3.27), and for  $0 < \eta < 0.194$  three real critical points exist, and for  $\eta > 0.194$  only one. In Figure 3.6 a sketch is given of this result, that is, how the number of critical points depends on  $\eta$ . In Figure 3.7 the phase portraits are given for  $\eta = 0.1$  and  $\eta = 0.2$ . For  $\eta = 0.1$  there is a stable critical point corresponding with a limit cycle. Furthermore, for  $\eta = 0.2$  there exists a periodic orbit corresponding with slowly varying amplitudes i.e. modulated oscillations.

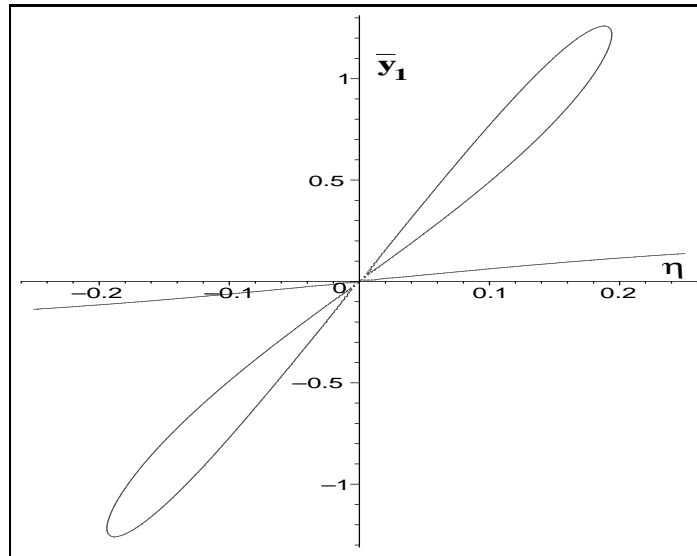


**Figure 3.6:** Curve relation between  $\bar{y}_1$  and  $\eta$  after using Gröbner basis algorithm. Vertical axis is  $\bar{y}_1$  and horizontal axis is  $\eta$

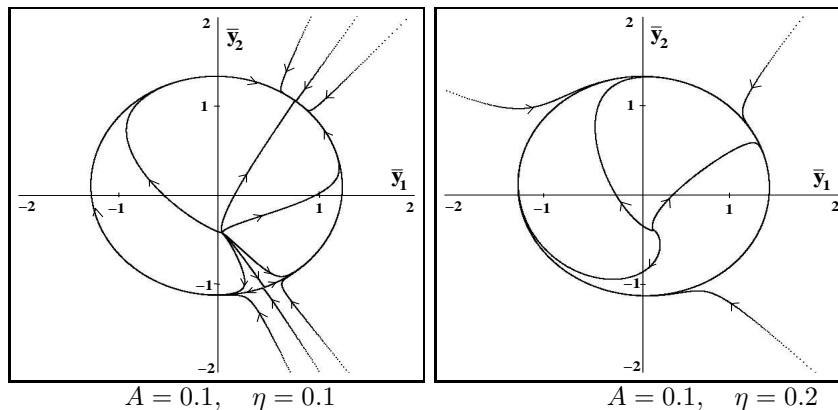


**Figure 3.7:** Orbits of equation (3.3.27) for  $A = 0.1$  and  $\eta = 0.1, \eta = 0.2$ . Vertical axis is  $\bar{y}_2$  and horizontal axis is  $\bar{y}_1$

### 3.4 Conclusions and Remarks

In this chapter a linear second order equation with time-periodic damping coefficient is investigated. It is shown that the equation can be used as a model for the study of rain-wind induced vibrations of a simple oscillator. The equation is a special case of Ince's equation. It is known that this equation displays coexistence, corresponding with curves in the stability diagram on which two linearly independent periodic solutions exist. These curves can be considered as a limiting case of the closure of the instability gaps. Although this phenomenon has been described in [16] in a qualitative sense, little quantitative results such as stability diagrams have been obtained. A new remarkable stability diagram is presented in Figure 2.1b; for small values of  $\epsilon$  the (transition) curves are additionally given by (truncated) power series in  $\epsilon$ . As far as it concerns the application it seems that only one application in [24] has been published yet. The application presented here seems to be new and is of



practical relevance. Problems with a time-varying damping coefficient play a role in the dynamics of rain-wind induced vibrations of elastic structures and are hence of considerable interest.

Furthermore, in this chapter a model equation for the study of rain-wind induced vibrations of a simple oscillator has been introduced. Both for the linear model equation as for the non-linear one periodic solutions are presented. For the linear equation the excitation mechanism may be ordinary forcing as well as combined parametrical and ordinary forcing. In both cases intermittent periodic self-excitation may additionally be present. For the non-linear model equation all three excitation mechanisms play a part in the excitation of a periodic motion as can be derived from equation (3.3.23) where all coefficients  $A_i$   $i = 0, 1, 2, 3, 4, 5$  are present. In case that  $\Omega \neq 1$  the averaged system may have a periodic orbit corresponding to modulated oscillations of the original equation.

### 3.5 Appendix

As described in section 3.2 by equating the coefficients of the sine and cosine terms in system (3.2.7) to zero we obtain a system of infinitely many equations for  $a_n$  and  $b_n$ . This system is given by:

$$\begin{aligned}
\frac{1}{2}(\lambda - \frac{1}{8}\epsilon^2)a_o + \frac{1}{2}\epsilon b_2 - \frac{1}{16}\epsilon^2 a_4 &= 0, \\
-\frac{1}{16}\epsilon^2 a_3 + \frac{1}{2}\epsilon b_1 + (\lambda - 1 - \frac{1}{8}\epsilon^2)a_1 + \frac{1}{2}\epsilon b_3 - \frac{1}{16}\epsilon^2 a_5 &= 0, \\
\frac{1}{16}\epsilon^2 b_3 + \frac{1}{2}\epsilon a_1 + (\lambda - 1 - \frac{1}{8}\epsilon^2)b_1 - \frac{1}{2}\epsilon a_3 - \frac{1}{16}\epsilon^2 b_5 &= 0, \\
(\lambda - 4 - \frac{3}{16}\epsilon^2)a_2 + \frac{1}{2}\epsilon b_4 - \frac{1}{16}\epsilon^2 a_6 &= 0, \\
\frac{1}{2}\epsilon a_o + (\lambda - 4 - \frac{1}{16}\epsilon^2)b_2 - \frac{1}{2}\epsilon a_4 - \frac{1}{16}\epsilon^2 b_6 &= 0, \\
-\frac{1}{16}\epsilon^2 a_1 - \frac{1}{2}\epsilon b_1 + (\lambda - 9 - \frac{1}{8}\epsilon^2)a_3 + \frac{1}{2}\epsilon b_5 - \frac{1}{16}\epsilon^2 a_7 &= 0, \\
\frac{1}{16}\epsilon^2 b_1 + \frac{1}{2}\epsilon a_1 + (\lambda - 9 - \frac{1}{8}\epsilon^2)b_3 - \frac{1}{2}\epsilon a_5 - \frac{1}{16}\epsilon^2 b_7 &= 0, \\
-\frac{1}{16}\epsilon^2 a_{n-4} - \frac{1}{2}\epsilon b_{n-2} + & \\
(\lambda - n^2 - \frac{1}{8}\epsilon^2)a_n + \frac{1}{2}\epsilon b_{n+2} - \frac{1}{16}\epsilon^2 a_{n+4} &= 0, \quad n \geq 4 \\
-\frac{1}{16}\epsilon^2 b_{n-4} + \frac{1}{2}\epsilon a_{n-2} + & \\
(\lambda - n^2 - \frac{1}{8}\epsilon^2)b_n - \frac{1}{2}\epsilon a_{n+2} - \frac{1}{16}\epsilon^2 b_{n+4} &= 0, \quad n \geq 4.
\end{aligned} \tag{3.5.1}$$

This system can be split up into two independent systems which contain odd indices and even indices respectively. In this way we have two systems  $\mathbf{A}\mathbf{v} = \mathbf{0}$  and  $\mathbf{B}\mathbf{w} = \mathbf{0}$ , where

$$\mathbf{v} = (a_1 \quad b_1 \quad a_3 \quad b_3 \quad a_5 \quad b_5 \quad \dots)^T, \quad \mathbf{w} = (a_o \quad a_2 \quad b_2 \quad a_4 \quad b_4 \quad \dots)^T,$$

$$\mathbf{A} = \begin{pmatrix} 1 & \mu_1 & \nu_1 & \mu_1 & \nu_1 & 0 & 0 & 0 & 0 & 0 & \dots \\ \mu_1 & 1 & -\mu_1 & -\nu_1 & 0 & \nu_1 & 0 & 0 & 0 & 0 & \dots \\ \nu_3 & -\mu_3 & 1 & 0 & 0 & \mu_3 & \nu_3 & 0 & 0 & 0 & \dots \\ \mu_3 & -\nu_3 & 0 & 1 & -\mu_3 & 0 & 0 & \nu_3 & 0 & 0 & \dots \\ \nu_5 & 0 & 0 & -\mu_5 & 1 & 0 & 0 & \mu_5 & \nu_5 & 0 & \dots \\ 0 & \nu_5 & \mu_5 & 0 & 0 & 1 & -\mu_5 & 0 & 0 & \nu_5 & \dots \\ 0 & 0 & \nu_7 & 0 & 0 & -\mu_7 & 1 & 0 & 0 & \mu_7 & \dots \\ 0 & 0 & 0 & \nu_7 & \mu_7 & 0 & 0 & 1 & -\mu_7 & 0 & \dots \\ 0 & 0 & 0 & 0 & \nu_9 & 0 & 0 & -\mu_9 & 1 & 0 & \dots \\ 0 & 0 & 0 & 0 & 0 & \nu_9 & \mu_9 & 0 & 0 & 1 & \dots \\ \vdots & \vdots & \vdots & \vdots & \vdots & \vdots & \vdots & \vdots & \vdots & \vdots & \ddots \end{pmatrix}$$

with

$$\mu_n = \frac{\frac{1}{2}\epsilon}{\lambda - n^2 - \frac{1}{8}\epsilon^2}, \quad \nu_n = -\frac{\frac{1}{16}\epsilon^2}{\lambda - n^2 - \frac{1}{8}\epsilon^2}, \quad n = 1, 3, 5, \dots, \text{ and}$$

$$\mathbf{B} = \begin{pmatrix} 1 & 0 & \sigma_o & \tau_o & 0 & 0 & 0 & 0 & 0 & 0 & \dots \\ 0 & 1 & 0 & 0 & 0 & \sigma_1 & \tau_1 & 0 & 0 & 0 & \dots \\ \sigma_2 & 0 & 1 & -\sigma_2 & 0 & 0 & \tau_2 & 0 & 0 & 0 & \dots \\ \tau_3 & 0 & -\sigma_3 & 1 & 0 & 0 & \sigma_3 & \tau_3 & 0 & 0 & \dots \\ 0 & \sigma_3 & 0 & 0 & 1 & -\sigma_3 & 0 & 0 & \tau_3 & 0 & \dots \\ 0 & \tau_4 & 0 & 0 & -\sigma_4 & 1 & 0 & 0 & \sigma_4 & \tau_4 & \dots \\ 0 & 0 & \tau_4 & \sigma_4 & 0 & 0 & 1 & -\sigma_4 & 0 & 0 & \dots \\ 0 & 0 & 0 & \tau_5 & 0 & 0 & -\sigma_5 & 1 & 0 & 0 & \dots \\ 0 & 0 & 0 & 0 & \tau_5 & \sigma_5 & 0 & 0 & 1 & -\sigma_5 & \dots \\ 0 & 0 & 0 & 0 & 0 & \tau_6 & 0 & 0 & -\sigma_6 & 1 & \dots \\ \vdots & \vdots & \vdots & \vdots & \vdots & \vdots & \vdots & \vdots & \vdots & \vdots & \ddots \end{pmatrix}$$

with

$$\begin{aligned} \sigma_o &= \frac{\frac{1}{2}\epsilon}{\frac{\lambda}{2} - \frac{1}{16}\epsilon^2}, & \tau_o &= -\frac{\frac{1}{16}\epsilon^2}{\frac{\lambda}{2} - \frac{1}{16}\epsilon^2}, \\ \sigma_1 &= \frac{\frac{1}{2}\epsilon}{\lambda - 4 - \frac{3}{16}\epsilon^2}, & \tau_1 &= -\frac{\frac{1}{16}\epsilon^2}{\lambda - 4 - \frac{3}{16}\epsilon^2}, \\ \sigma_2 &= \frac{\frac{1}{2}\epsilon}{\lambda - 4 - \frac{1}{16}\epsilon^2}, & \tau_2 &= -\frac{\frac{1}{16}\epsilon^2}{\lambda - 4 - \frac{1}{16}\epsilon^2}, \\ \sigma_{n+1} &= \frac{\frac{1}{2}\epsilon}{\lambda - 4n^2 - \frac{1}{8}\epsilon^2}, & \tau_{n+1} &= -\frac{\frac{1}{16}\epsilon^2}{\lambda - 4n^2 - \frac{1}{8}\epsilon^2}, \quad n \geq 2. \end{aligned}$$

To find the  $\pi$ -periodic solution(s) of (3.2.3) we expand  $y$  in the following way :

$$y = \frac{\tilde{a}_o}{2} + \sum_{n=1}^{\infty} (\tilde{a}_n \cos(2nt) + \tilde{b}_n \sin(2nt)). \quad (3.5.2)$$

Substituting (3.5.2) into (3.2.3), and observing that

$$\begin{aligned} 2 \cos(2t) \sin(2nt) &= \sin((2n+2)t) + \sin((2n-2)t), \\ 2 \cos(2t) \cos(2nt) &= \cos((2n+2)t) + \cos((2n-2)t) \end{aligned}$$

it follows that

$$\begin{aligned} &(\lambda - \frac{1}{8}\epsilon^2)\frac{\tilde{a}_o}{2} + \epsilon\frac{\tilde{a}_o}{2}\sin(2t) - \frac{1}{16}\epsilon^2\tilde{a}_o\cos(4t) + \\ &\sum_{n=1}^{\infty}(\lambda - \frac{1}{8}\epsilon^2 - 4n^2)[\tilde{a}_n\cos(2nt) + \tilde{b}_n\sin(2nt)] + \\ &\frac{1}{2}\epsilon\sum_{n=1}^{\infty}[\tilde{a}_n\sin((2n+2)t) - \tilde{a}_n\sin((2n-2)t) - \\ &\tilde{b}_n\cos((2n+2)t) + \tilde{b}_n\cos((2n-2)t)] - \\ &\frac{1}{16}\epsilon^2\sum_{n=1}^{\infty}[\tilde{a}_n\cos((2n+4)t) + \tilde{a}_n\cos((2n-4)t) + \\ &\tilde{b}_n\sin((2n+4)t) + \tilde{b}_n\sin((2n-4)t)] = 0. \end{aligned} \tag{3.5.3}$$

By equating the coefficients of sine and cosine terms in this system to zero, one obtain the following infinite system of linear equations :

$$\begin{aligned} &\frac{1}{2}(\lambda - \frac{1}{8}\epsilon^2)\tilde{a}_o + \frac{1}{2}\epsilon\tilde{b}_1 - \frac{1}{16}\epsilon^2\tilde{a}_2 = 0, \\ &(\lambda - 4 - \frac{3}{16}\epsilon^2)\tilde{a}_1 + \frac{1}{2}\epsilon\tilde{b}_2 - \frac{1}{16}\epsilon^2\tilde{a}_3 = 0, \\ &\frac{1}{2}\epsilon\tilde{a}_o + (\lambda - 4 - \frac{1}{16}\epsilon^2)\tilde{b}_1 - \frac{1}{2}\epsilon\tilde{a}_2 - \frac{1}{16}\epsilon^2\tilde{b}_3 = 0, \\ &\quad -\frac{1}{16}\epsilon^2\tilde{a}_{n-2} - \frac{1}{2}\epsilon\tilde{b}_{n-1} + \\ &(\lambda - 4n^2 - \frac{1}{8}\epsilon^2)\tilde{a}_n + \frac{1}{2}\epsilon\tilde{b}_{n+1} - \frac{1}{16}\epsilon^2\tilde{a}_{n+2} = 0, \quad n \geq 2, \\ &\quad -\frac{1}{16}\epsilon^2\tilde{b}_{n-2} + \frac{1}{2}\epsilon\tilde{a}_{n-1} + \\ &(\lambda - 4n^2 - \frac{1}{8}\epsilon^2)\tilde{b}_n - \frac{1}{2}\epsilon\tilde{a}_{n+1} - \frac{1}{16}\epsilon^2\tilde{b}_{n+2} = 0, \quad n \geq 2. \end{aligned} \tag{3.5.4}$$

This system can be written as  $\mathbf{B}\mathbf{u} = \mathbf{0}$ , where

$$\mathbf{u} = (\tilde{a}_o \quad \tilde{a}_1 \quad \tilde{b}_1 \quad \tilde{a}_2 \quad \tilde{b}_2 \quad \tilde{a}_3 \quad \tilde{b}_3 \cdots)^T.$$

To get the nontrivial periodic solutions of (3.2.3), one should set the determinant of matrix  $\mathbf{A}$ ,  $\det\mathbf{A}$ , or the determinant of matrix  $\mathbf{B}$ ,  $\det\mathbf{B}$ , equal to zero. The values of  $\lambda$  and  $\epsilon$  which satisfy  $\det\mathbf{A} = 0$  are related to the  $2\pi$ -periodic solutions and those values related to  $\det\mathbf{B} = 0$  are the  $\pi$ -periodic solutions. To evaluate the convergence of the infinite determinants of the matrices  $\mathbf{A}$  and  $\mathbf{B}$ , we will use the following definition and theorem.

*Definition.* An infinite matrix  $\mathbf{H} = (h_{ij}), i, j = 1, 2, 3, \dots$  is called an infinite matrix of Hill-type if

$$\sum_{i,j} |h_{ij} - \theta_{ij}| < \infty$$

where

$$\theta_{ij} = \begin{cases} 1, & i = j \\ 0, & i \neq j \end{cases} .$$

Thus, according to this definition the infinite matrices  $\mathbf{A}$  and  $\mathbf{B}$  are of Hill-type because all series  $\sum_i |\mu_i|$ ,  $\sum_i |\nu_i|$ ,  $\sum_i |\sigma_i|$  and  $\sum_i |\tau_i|$  are convergent.

*Theorem* (Th 1.1 [19]). Suppose  $\mathbf{H} = (h_{ij}), i, j = 1, 2, 3, \dots$  is an infinite matrix of Hill-type and  $\mathbf{H}_N = (h_{ij}), i, j = 1, 2, 3, \dots, N$ . Then the infinite determinant  $\det \mathbf{H}$  exist,  $|\det \mathbf{H}| \leq P < \infty$  and

$$|\det \mathbf{H}_N - \det \mathbf{H}_{N-1}| \leq P \{ |h_{NN} - 1| + (\sum_{i=1}^{N-1} |h_{iN}|) (\sum_{i=1}^{N-1} |h_{Ni}|) \}$$

where

$$P = \prod_{i=1}^{\infty} (1 + \sum_{j=1}^{\infty} |h_{ij} - \theta_{ij}|) .$$

So this theorem guarantees the existence of the infinite determinant of the infinite matrix of Hill-type. Furthermore, based on this theorem we can determine not only the upper bound of the absolute value of the determinant but also we can estimate the error truncating the infinite determinant.

Now consider the infinite matrix  $\mathbf{B} = (b_{ij}), i, j = 1, 2, 3, \dots$ . Let

$$\begin{aligned} K_B &= \prod_{i=1}^{\infty} (1 + \sum_{j=1}^{\infty} |b_{ij} - \theta_{ij}|) \\ &= (1 + |\sigma_o| + |\tau_o|)(1 + |\sigma_1| + |\tau_1|)(1 + |2\sigma_2| + |\tau_2|) \\ &\quad (1 + |2\sigma_3| + |2\tau_3|)(1 + |2\sigma_3| + |\tau_3|) \prod_{n=4}^{\infty} (1 + |2\sigma_n| + |2\tau_n|)^2. \end{aligned} \tag{3.5.5}$$

Because  $\sum_n (|2\sigma_n| + |2\tau_n|)$  is convergent it follows that  $K_B < \infty$ . Furthermore, using the theorem above we can write

$$\begin{aligned} |\det \mathbf{B}_{2n+1} - \det \mathbf{B}_{2n}| &\leq K_B \{ 0 + (\sum_{i=1}^{2n} |b_{i,2n+1}|) (\sum_{i=1}^{2n} |b_{2n+1,i}|) \} \\ &= K_B (|\sigma_n| + |\tau_{n-1}|) (|\sigma_{n+1}| + |\tau_{n+1}|) \\ &= O(n^{-4}) . \end{aligned} \tag{3.5.6}$$

Similarly, for matrix  $\mathbf{A} = (a_{ij}), i, j = 1, 2, 3, \dots$  we have

$$\begin{aligned} |\det \mathbf{A}_{2n+1} - \det \mathbf{A}_{2n}| &\leq K_A (|\nu_{2n-3}| + |\mu_{2n-1}|) (|\nu_{2n+1}| + |\mu_{2n+1}|) \\ &= O(n^{-4}) , \end{aligned} \tag{3.5.7}$$

where

$$\begin{aligned} K_A &= \prod_{i=1}^{\infty} (1 + \sum_{j=1}^{\infty} |a_{ij} - \theta_{ij}|) \\ &= \prod_{n=1}^{\infty} (1 + |2\mu_{2n-1}| + |2\nu_{2n-1}|)^2 \quad . \end{aligned} \tag{3.5.8}$$



# Chapter 4

## A New Model for the Study of Rain-wind Induced Vibrations of a Simple Oscillator <sup>†</sup>

**Abstract.** In this chapter a model equation is presented for the study of rain-wind induced vibrations of a simple oscillator. As will be shown the presence of raindrops in the wind-field may have an essential influence on the dynamic stability of the oscillator. In this model equation the influence of the variation of the mass of the oscillator due to an incoming flow of raindrops hitting the oscillator and a mass flow which is blown and shaken off, is investigated. The time-varying mass is modeled by a time harmonic function whereas simultaneously also time-varying lift and drag forces are considered.

### 4.1 Introduction

Inclined stay cables of bridges are fixed on one end to a pylon and on the other end to the bridge-deck. Usually the stay cables have a polyurethane mantle and a cross section which is nearly circular. With low structural damping of the bridge, a wind-field containing raindrops may induce vibrations of the cables.

As an example one can refer to Erasmus bridge in Rotterdam of which the stay cables vibrated heavily on November 4, 1996 less then two months after its opening. The problem of rain-wind induced vibrations of stay cables has been reported and studied experimentally for the first time in [13]. Additional experimental studies can be found in [17, 18] and [33]. In these papers it is remarked that regrettfully calculation models are not available. A first attempt to model this problem can be found in [28] where in particular time-varying lift and drag forces are modeled. Time-varying lift and drag forces are due to the movement of the water rivulet on the

---

<sup>†</sup>This chapter is a revised version of [30], A New Model for the Study of Rain-wind Induced Vibrations of a Simple Oscillator, submitted for publication.

cable. In recent years some authors [26, 36, 35] have studied models for rain-wind induced vibrations of cables. In [36], an analytical study of wind-rain induced cable vibrations was presented by considering the influence of a moving upper rivulet on the cable. However, the varying mass of rain water on the cables has not been taken into account by these authors.

In this chapter a possible additional effect is taken into account namely the variation of the quantity of rainwater located on the cable. In terms of modeling one can say that the vibrating mass of rainwater on the cable is time-dependent, and is modeled by a time harmonic function, whereas simultaneously also time-varying lift and drag forces are considered. The attention is mainly focused on the interaction of the rain with the oscillator, assuming that this interaction is an instability mechanism. Raindrops hitting the oscillator, may form a rivulet or a water ridge on the oscillator. However in a stationary situation the mass flow of incoming raindrops hitting the oscillator and the mass flow of raindrops shaken off will be equal. If these mass flows are not equal then the mass of raindrops attached to the oscillator varies with time.

One may conclude that the following mechanisms may be relevant for the study of the instability of the oscillator.

- the assumption that the mass of the ridge and hence the mass of oscillator may vary in time, seems realistic,
- drag and lift forces vary usually in the dynamic situation, however due to the fact that the position of the ridge on the oscillator is not fixed but varies with time, the aerodynamic coefficients additionally depend on time.

As the second mechanism has been studied in [28] it looks of interest to include the additional effect of time-varying mass. It should be stressed that the dynamics of the mass of the rivulets will not be modeled by a separate equation of motion in this stage: in the modeling we assume that either the position of the rivulets is fixed or varies harmonically in time in the same way as the oscillator.

## 4.2 A model equation with time-varying mass and lift and drag forces

In this section we use the modeling principles as given in [8] or [31]. Consider a horizontal rigid cylinder with uniform circular cross section supported by springs. A rain-wind flow is directed to the axis of the cylinder. The cylinder with springs is constructed in such a way that only vertical oscillations i.e. oscillations in cross-flow are possible. The raindrops that hit the cable may stay on the surface of the cylinder for some time and may form a ridge of water of which the position varies with time. Due to the variation of the acceleration of the cable and the aerodynamic forces, part of the water will be blown and or shaken off and hence the mass of the water ridge varies in time. The system which will be studied is sketched in Figure 4.1.  $U$  is the horizontal uniform velocity of the wind containing raindrops. When the cylinder moves in the positive  $y$  direction a virtual wind velocity  $-y$  is induced, i.e. a



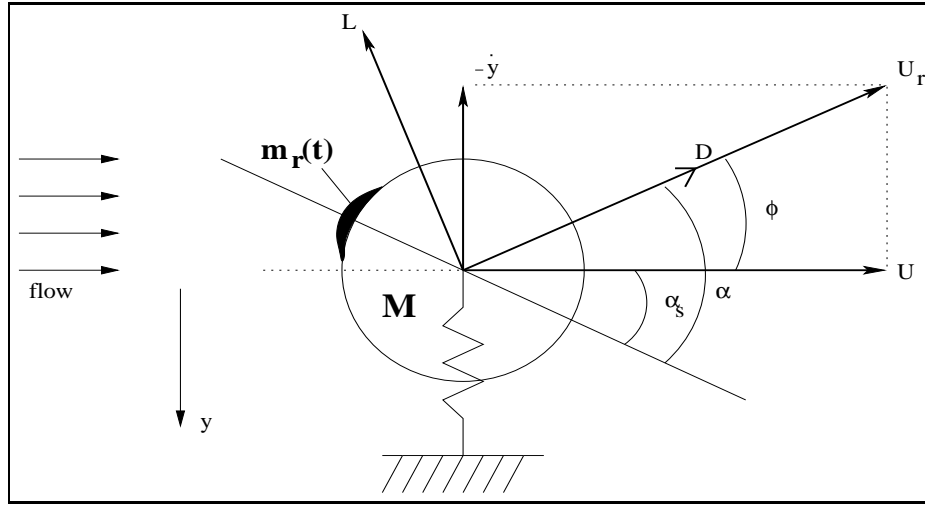


**Figure 4.1:** Cross-section of the cylinder-spring system, fluid flow with respect to the cylinder and wind forces on the cylinder

wind flow with velocity  $\dot{y}$  in opposite direction. The drag force  $D$  is indicated in the direction of the resultant wind-velocity  $U_r$ , whereas the lift force  $L$  is perpendicular to  $D$  in anti clockwise direction. The water ridge on the cylinder, boldly indicated in Figure 4.1, is assumed to carry out harmonic oscillations with small amplitude on the surface of the cylinder whereas the mass of the water ridge  $m_r(t)$  is supposed to vary harmonically in time as well. The aerodynamic force  $F_y$  in vertical direction follows from Figure 4.1 :

$$F_y = -D \sin \phi - L \cos \phi, \quad (4.2.1)$$

where  $\phi$  is the angle between  $U_r$  and  $U$ , positive in clockwise direction:  $|\phi| < \pi/2$ . The drag and lift forces are given by the empirical relations:

$$\begin{aligned} D &= \frac{1}{2} \rho d l U_r^2 C_D(\alpha), \\ L &= \frac{1}{2} \rho d l U_r^2 C_L(\alpha), \end{aligned} \quad (4.2.2)$$

where  $\rho$  is the density of the flowing medium (air with raindrops),  $d$  the diameter of the cylinder,  $l$  the length of the cylinder,  $C_D(\alpha)$  and  $C_L(\alpha)$  are the drag and lift coefficient curves respectively, determined by measurements in a wind-tunnel.

From Figure 4.1 it follows that :

$$\begin{aligned} \sin \phi &= \dot{y}/U_r, \\ \cos \phi &= U/U_r, \\ \alpha &= \alpha_s + \arctan(\dot{y}/U). \end{aligned} \quad (4.2.3)$$

The equation of motion of the oscillator readily becomes :

$$\frac{d}{dt}[(M + m_r(t)) \frac{dy}{dt}] + c_y \frac{dy}{dt} + k_y y = F_y, \quad (4.2.4)$$

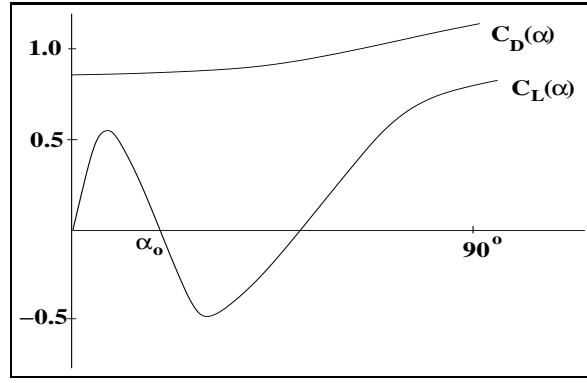


**Figure 4.2:** Aerodynamic drag and lift coefficients

where  $M$  is the mass of the cylinder,  $m_r(t)$  the time-varying mass of the raindrops on the cylinder,  $c_y > 0$  the structural damping coefficient of the oscillator, and  $k_y > 0$  the spring constant. By using (4.2.1), (4.2.2) and (4.2.3) we obtain for  $F_y$  :

$$F_y = -\frac{1}{2}\rho d l \sqrt{U^2 + \dot{y}^2} (C_D(\alpha) \frac{dy}{dt} + C_L(\alpha)U). \quad (4.2.5)$$

Let  $m_r(t)/M = \epsilon m(t)$ , where  $\epsilon > 0$  is a small parameter, (4.2.4) becomes :

$$(1 + \epsilon m(t)) \frac{d^2 y}{dt^2} + \left( \frac{c_y}{M} + \epsilon \frac{dm}{dt} \right) \frac{dy}{dt} + \omega_y^2 y = F_y/M, \quad (4.2.6)$$

where  $\omega_y^2 = k_y/M$ . The case is studied where the drag and lift coefficient curves can be approximated by :

$$\begin{aligned} C_D(\alpha) &= C_{D_o}, \\ C_L(\alpha) &= C_{L_1}(\alpha - \alpha_o) + C_{L_3}(\alpha - \alpha_o)^3, \end{aligned} \quad (4.2.7)$$

where  $C_{D_o} > 0$ ,  $C_{L_1} < 0$ ,  $C_{L_3} > 0$  and  $\alpha_o > 0$ ,  $\alpha_o$  is any angle in the domain of the  $\alpha$ -axis of the  $C_L(\alpha)$  curve where the slope is negative i. e.  $C_{L_1} < 0$ . The approximations (4.2.7) fit as a first step with typical curves obtained from wind tunnel experiments as indicated in Figure 4.2 (see also [3]). By using (4.2.3), (4.2.7) can be written as:

$$C_L(\alpha) = C_{L_1}(\alpha_s - \alpha_o + \arctan(\dot{y}/U)) + C_{L_3}(\alpha_s - \alpha_o + \arctan(\dot{y}/U))^3. \quad (4.2.8)$$

Now the variation of the position of the water ridge can be modeled by  $\alpha_s - \alpha_o = f(t)$ . Substitution of this variation in (4.2.8) using (4.2.5) and (4.2.7) one obtains for (4.2.6) the following linearized model equation (around  $\dot{y} = 0$ ):

$$\begin{aligned} (1 + \epsilon m(t)) \frac{d^2 y}{dt^2} + \left( \bar{K}(C_{D_o} + C_{L_1}) + \frac{c_y}{M} + 3C_{L_3} \bar{K} f^2(t) + \epsilon \frac{dm}{dt} \right) \frac{dy}{dt} \\ + \omega_y^2 y = -\bar{K}(C_{L_1} f(t) + C_{L_3} f^3(t))U, \end{aligned} \quad (4.2.9)$$

where  $\bar{K} = \rho d l U / 2M$ . Let  $c_y/M = 2\epsilon\beta$  and  $\bar{K} = \epsilon K\omega$ , then by dividing  $(1 + \epsilon m(t))$  one obtains :

$$\frac{d^2 y}{dt^2} + (\epsilon\omega q(t)) \frac{dy}{dt} + \omega_y^2 (1 - \epsilon m(t)) y = \epsilon K\omega (C_{L_1} f(t) + C_{L_3} f^3(t))U + O(\epsilon^2), \quad (4.2.10)$$

where  $\omega q(t) = K\omega(C_{D_o} + C_{L_1}) + 2\beta + 3C_{L_3}K\omega f^2(t) + \frac{dm}{dt}$ , and where  $\omega$  is defined in the expressions for  $f(t)$  and  $m(t)$  below. Consider the following model variations of the water ridge and  $m(t)$  :

$$\begin{aligned} f(t) &= c_1 \cos(\omega t) + d_1 \sin(\omega t), \\ m(t) &= a_2 \cos(2\omega t) + b_2 \sin(2\omega t), \\ f^2(t) &= c_o + c_2 \cos(2\omega t) + d_2 \sin(2\omega t), \end{aligned} \quad (4.2.11)$$

where

$$c_o = \frac{1}{2}(c_1^2 + d_1^2), \quad c_2 = \frac{1}{2}(c_1^2 - d_1^2), \quad d_2 = c_1 d_1. \quad (4.2.12)$$

By introducing the new variables  $z = \omega y/U$  and  $\omega t = \tau$  one obtains:

$$\frac{d^2 z}{d\tau^2} + (\epsilon q(\tau/\omega)) \frac{dz}{d\tau} + \frac{\omega_y^2}{\omega^2} (1 - \epsilon m(\tau/\omega)) z = \epsilon K (C_{L_1} f(\tau/\omega) + C_{L_3} f^3(\tau/\omega)) + O(\epsilon^2). \quad (4.2.13)$$

For the main resonance case as studied in this chapter one should consider :

$$\frac{\omega_y^2}{\omega^2} = 1 - 2\epsilon\eta, \quad (4.2.14)$$

where  $\eta$  is a detuning parameter. By using (4.2.14), (4.2.13) can be written as :

$$\ddot{z} + z = \epsilon H(z, \dot{z}, \tau), \quad (4.2.15)$$

where  $H(z, \dot{z}, \tau) = K(C_{L_1} f(\tau/\omega) + C_{L_3} f^3(\tau/\omega)) - q(\tau/\omega)\dot{z} + (2\eta + m(\tau/\omega))z + O(\epsilon)$ . Let

$$\begin{aligned} z &= y_1 \cos(\tau) + y_2 \sin(\tau), \\ \dot{z} &= -y_1 \sin(\tau) + y_2 \cos(\tau). \end{aligned} \quad (4.2.16)$$

Then (4.2.15) becomes :

$$\begin{aligned} \dot{y}_1 &= -\epsilon H \sin(\tau), \\ \dot{y}_2 &= \epsilon H \cos(\tau). \end{aligned} \quad (4.2.17)$$

By averaging one obtains :

$$\begin{aligned} \begin{pmatrix} \dot{\bar{y}}_1 \\ \dot{\bar{y}}_2 \end{pmatrix} &= \begin{pmatrix} s + \frac{1}{4}b_2 + \frac{1}{4}\bar{c}_2 & \frac{1}{4}\bar{d}_2 - \frac{1}{4}a_2 - \eta \\ \frac{1}{4}\bar{d}_2 - \frac{1}{4}a_2 + \eta & s - \frac{1}{4}b_2 - \frac{1}{4}\bar{c}_2 \end{pmatrix} \begin{pmatrix} \bar{y}_1 \\ \bar{y}_2 \end{pmatrix} + \\ &\quad \begin{pmatrix} \frac{1}{2}KC_{L_1}d_1 + \frac{1}{8}d_1\bar{c}_o \\ -\frac{1}{2}KC_{L_1}c_1 - \frac{1}{8}c_1\bar{c}_o \end{pmatrix}, \end{aligned} \quad (4.2.18)$$

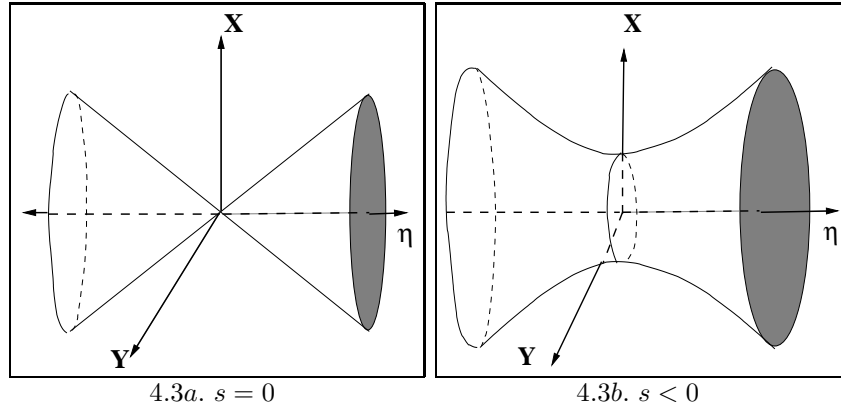


**Figure 4.3:** Inside the cone and hyperboloid the critical point is stable .

where  $s = -(\beta/\omega + \frac{1}{2}K(C_{D_o} + C_{L_1}) + \frac{1}{2}\bar{c}_o)$ ,  $\bar{c}_o = 3c_oKC_{L_3}$ ,  $\bar{c}_2 = 3c_2KC_{L_3}$  and  $\bar{d}_2 = 3d_2KC_{L_3}$ . The stability of the critical point of (4.2.18) depends on the eigenvalues  $\lambda$  of the matrix in the equation (4.2.18) and follows from:

$$(s - \lambda)^2 - \left(\frac{1}{4}b_2 + \frac{1}{4}\bar{c}_2\right)^2 - \left(\frac{1}{4}\bar{d}_2 - \frac{1}{4}a_2\right)^2 + \eta^2 = 0. \quad (4.2.19)$$

For  $s = 0$ , implying that the constant damping coefficient vanishes, the transition curve (or manifold in a higher dimensional parameter space) separating stable and unstable regions in the relevant parameter space follows from:

$$\eta^2 = \frac{1}{16}(b_2 + \bar{c}_2)^2 + \frac{1}{16}(\bar{d}_2 - a_2)^2 \quad (4.2.20)$$

When one sets  $b_2 + \bar{c}_2 = X$  and  $\bar{d}_2 - a_2 = Y$  in (4.2.20) then the equation represents a cone in the  $(\eta, X, Y)$  space, with the  $\eta$ -axis as central axis. The domain inside the cone corresponds with a regime of parameters where all solutions are stable. For  $\eta = 0$  i.e.  $\omega = \omega_y$  and  $s = 0$  only unstable solutions are found. Apparently for  $\eta = 0$  stable solutions only exist if both eigenvalues which follow from (4.2.19) are negative. For this case it is clear that  $s < 0$  and that the right hand side of (4.2.20) should be sufficiently small.

Result (4.2.20) describes an interesting property. If for instance  $\bar{c}_2 = \bar{d}_2 = 0$  which implies by using (4.2.12) that  $f(t) \equiv 0$  (the position of the water ridge on the surface is fixed), by varying the amplitude  $r_1 = \sqrt{a_2^2 + b_2^2}$  one can control the stability of the trivial solution i.e. pass through the surface of the cone for  $\eta \neq 0$  fixed. However, if  $\bar{c}_2 \neq 0$  and  $\bar{d}_2 \neq 0$  the right hand side of (4.2.20) can be written in terms of amplitudes and phases as follows :

$$\frac{1}{16}[(b_2 + \bar{c}_2)^2 + (\bar{d}_2 - a_2)^2] = \frac{1}{16}[r_1^2 + r_2^2 + 2r_1r_2 \sin(\varphi_1 - \varphi_2)], \quad (4.2.21)$$

where  $r_1^2 = a_2^2 + b_2^2$ ,  $r_2^2 = \bar{c}_2^2 + \bar{d}_2^2$ ,  $\varphi_1 = \arctan(b_2/a_2)$  and  $\varphi_2 = \arctan(\bar{d}_2/\bar{c}_2)$ . From (4.2.21) it follows that by keeping  $r_1$  and  $r_2$  constant but by varying the phase difference  $(\varphi_1 - \varphi_2)$  between  $f(t)$  and  $m(t)$  one can pass through the surface of the cone separating the stable and unstable regime of parameters.

### 4.3 The non-linear model

According to the previous section, by introducing the new variables  $z = \omega y/U$  and  $\omega t = \tau$  one obtains :

$$\ddot{z} + \left(\epsilon \frac{dm}{d\tau} + \epsilon 2\beta/\omega\right)\dot{z} + \frac{\omega_y^2}{\omega^2}(1 - \epsilon m(\tau/\omega))z = -\epsilon K \sqrt{1 + \dot{z}^2} \quad (4.3.1)$$

$$(C_D(\alpha)\dot{z} + C_L(\alpha)) + O(\epsilon^2),$$

where  $K = \rho dlU/2M\omega$ ,  $\epsilon 2\beta = c_y/M$ ,  $\omega_y^2 = k_y/M$ ,  $\dot{z} = dz/d\tau$ , and

$$C_D(\alpha) = C_{D_o},$$

$$C_L(\alpha) = C_{L_1}(f(\tau/\omega) + \arctan \dot{z}) + C_{L_3}(f(\tau/\omega) + \arctan \dot{z})^3.$$

Substituting (4.2.14) into (4.3.1), expanding the right hand side of (4.3.1) with respect to  $\dot{z}$  (up to cubical terms), using (4.2.16) one obtains after first order averaging:

$$\begin{aligned} \dot{\bar{y}}_1 &= \epsilon \left[ \frac{1}{2} K C_{L_1} d_1 + \frac{1}{8} d_1 \bar{c}_o + \left(s + \frac{1}{4} b_2 + \frac{1}{4} \bar{c}_2\right) \bar{y}_1 + \left(\frac{1}{4} \bar{d}_2 - \frac{1}{4} a_2 - \eta\right) \bar{y}_2 \right] \quad (4.3.2) \\ &+ d_1 \left(3q + \frac{1}{12} \bar{c}_o - \frac{1}{48} \bar{c}_2\right) \bar{y}_1^2 + d_1 \left(q + \frac{1}{24} \bar{c}_o + \frac{1}{48} \bar{c}_2\right) \bar{y}_2^2 - \\ &c_1 \left(2q + \frac{1}{12} \bar{c}_o - \frac{1}{24} \bar{c}_2\right) \bar{y}_1 \bar{y}_2 + \left(p - \frac{1}{16} \bar{c}_o + \frac{1}{24} \bar{c}_2\right) \bar{y}_1^3 + \\ &\frac{1}{48} \bar{d}_2 \bar{y}_2^3 + \frac{1}{16} \bar{d}_2 \bar{y}_1^2 \bar{y}_2 + \left(p - \frac{1}{16} \bar{c}_o\right) \bar{y}_1 \bar{y}_2^2, \\ \dot{\bar{y}}_2 &= \epsilon \left[ -\frac{1}{2} K C_{L_1} c_1 - \frac{1}{8} c_1 \bar{c}_o + \left(\frac{1}{4} \bar{d}_2 - \frac{1}{4} a_2 + \eta\right) \bar{y}_1 + \left(s - \frac{1}{4} b_2 - \frac{1}{4} \bar{c}_2\right) \bar{y}_2 \right] \\ &- c_1 \left(q + \frac{1}{24} \bar{c}_o - \frac{1}{48} \bar{c}_2\right) \bar{y}_1^2 - c_1 \left(3q + \frac{1}{12} \bar{c}_o + \frac{1}{48} \bar{c}_2\right) \bar{y}_2^2 + \\ &d_1 \left(2q + \frac{1}{12} \bar{c}_o + \frac{1}{24} \bar{c}_2\right) \bar{y}_1 \bar{y}_2 + \frac{1}{48} \bar{d}_2 \bar{y}_1^3 + \left(p - \frac{1}{16} \bar{c}_o - \frac{1}{24} \bar{c}_2\right) \bar{y}_2^3 + \\ &\left(p - \frac{1}{16} \bar{c}_o\right) \bar{y}_1^2 \bar{y}_2 + \frac{1}{16} \bar{d}_2 \bar{y}_1 \bar{y}_2^2, \end{aligned}$$

where  $p = -K(\frac{3}{16}C_{D_o} + \frac{1}{16}C_{L_1} + \frac{3}{8}C_{L_3})$  and  $q = K(\frac{1}{16}C_{L_1} + \frac{3}{8}C_{L_3})$ . The signs of  $p$  and  $q$  depend on the values of the aerodynamic coefficients which are for instance given in [6]. System (4.3.2) is a general cubical system, which includes the linear terms from equation (4.2.18). In the cases where in linear approximation unstable solutions are found the non-linear terms in system (4.3.2) may provide stable solutions. In what follows some special cases of the general system (4.3.2) are studied.

#### 4.3.1 Fixed position of water ridge and time-varying mass

System (4.3.2) describes both the effect of the time-varying position of the ridge of water as well as the time-varying mass of rain water on the oscillator. These effects can be studied separately by first considering the case that the position of the water

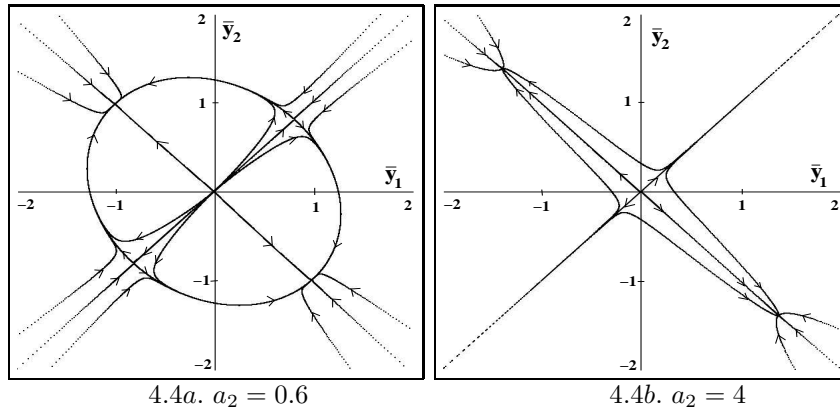


**Figure 4.4:** The phase portrait of (4.3.3) for  $a_2 = 0.6$  and  $a_2 = 4$ ,  $b_2 = 0$ ,  $\eta = 0$ ,  $C_{L_3} = 2$ ,  $C_{L_1} = -6$ ,  $C_{D_o} = 1/2$ ,  $\beta/\omega = 2$  and  $K = 1$ .

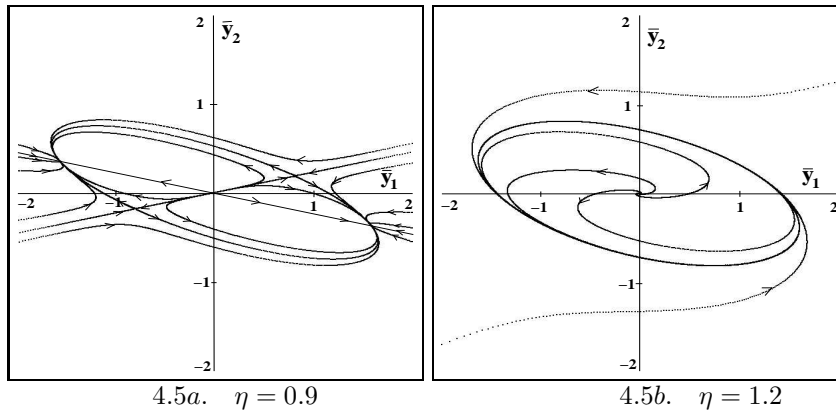


**Figure 4.5:** The phase portraits of equation (4.3.3) for several values of  $\eta$ , the detuning parameter,  $a_2 = 4$ ,  $b_2 = 0$ ,  $C_{L_3} = 2$ ,  $C_{L_1} = -6$ ,  $C_{D_o} = 1/2$ ,  $\beta/\omega = 2$  and  $K = 1$ .

ridge does not vary in time i.e.  $\bar{c}_2 = \bar{d}_2 = 0$ . In this case (4.3.2) becomes :

$$\begin{aligned}\dot{\bar{y}}_1 &= \epsilon\left[\left(\bar{s} + \frac{1}{4}b_2\right)\bar{y}_1 - \left(\frac{1}{4}a_2 + \eta\right)\bar{y}_2 + p\bar{y}_1^3 + p\bar{y}_1\bar{y}_2^2\right], \\ \dot{\bar{y}}_2 &= \epsilon\left[-\left(\frac{1}{4}a_2 - \eta\right)\bar{y}_1 + \left(\bar{s} - \frac{1}{4}b_2\right)\bar{y}_2 + p\bar{y}_2^3 + p\bar{y}_1^2\bar{y}_2\right],\end{aligned}\quad (4.3.3)$$

where  $\bar{s} = -(\beta/\omega + \frac{1}{2}K(C_{D_o} + C_{L_1}))$ . By using the transformation

$$\bar{y}_1 = r \cos \theta, \quad \bar{y}_2 = r \sin \theta, \quad (4.3.4)$$

(4.3.3) becomes :

$$\begin{aligned}\dot{r} &= \epsilon r \left[ \frac{1}{4}b_2 \cos(2\theta) - \frac{1}{4}a_2 \sin(2\theta) + \bar{s} + pr^2 \right], \\ \dot{\theta} &= \epsilon \left[ -\frac{1}{4}a_2 \cos(2\theta) - \frac{1}{4}b_2 \sin(2\theta) + \eta \right].\end{aligned}\quad (4.3.5)$$

The non trivial critical points of (4.3.5) are solutions of :

$$\begin{aligned} \frac{1}{4}b_2 \cos(2\theta) - \frac{1}{4}a_2 \sin(2\theta) + \bar{s} + pr^2 &= 0, \\ -\frac{1}{4}a_2 \cos(2\theta) - \frac{1}{4}b_2 \sin(2\theta) + \eta &= 0. \end{aligned} \quad (4.3.6)$$

By elimination of  $\theta$  in (4.3.6) one obtains:

$$\frac{1}{16}a_2^2 + \frac{1}{16}b_2^2 = \eta^2 + (\bar{s} + pr^2)^2, \quad (4.3.7)$$

or

$$r^2 = \frac{1}{p} \left( -\bar{s} \pm \sqrt{\frac{1}{16}a_2^2 + \frac{1}{16}b_2^2 - \eta^2} \right). \quad (4.3.8)$$

Thus (4.3.5) has only one critical point i.e. the origin if  $\frac{1}{16}a_2^2 + \frac{1}{16}b_2^2 < \eta^2$ , implying that (4.3.3) has only one critical point. In case  $\frac{1}{16}a_2^2 + \frac{1}{16}b_2^2 > \eta^2$  (4.3.5) may have three or five critical points. To evaluate the stability of these critical points one can linearize the system around each critical point. Jacobi's matrix of (4.3.5) evaluated at its critical point  $(r_o, \theta_o)$  is

$$\begin{pmatrix} 2pr_o^2 & -\frac{1}{2}r_o(b_2 \sin 2\theta_o + a_2 \cos 2\theta_o) \\ 0 & 2\bar{s} + 2pr_o^2 \end{pmatrix}. \quad (4.3.9)$$

The eigenvalues of (4.3.9) are

$$\lambda_1 = 2pr_o^2 \text{ and } \lambda_2 = 2\bar{s} + 2pr_o^2.$$

If for instance  $a_2 = 0.6$  or  $a_2 = 4$ ,  $b_2 = 0$ ,  $\eta = 0$ ,  $C_{L_3} = 2$ ,  $C_{L_1} = -6$ ,  $C_{D_o} = 1/2$ ,  $\beta/\omega = 2$  and  $K = 1$  five or three critical points are found respectively, and these phase portraits of system (4.3.3) are given in Figure 4.4a, 4.4b. In Figure 4.4b there are two stable critical points corresponding with two stable periodic solution of (4.3.1) having equal amplitudes but a phase difference of  $\pi$ .

In case that the detuning parameter,  $\eta$ , is not equal to zero, for instance  $\eta = 0.9$  and  $\eta = 1.2$ , these phase portraits are depicted in Figure 4.5a and 4.5b. In these phase portraits the value of  $a_2$  is 4. We can observe that the variation of the detuning parameter  $\eta$ , leads to a change in the number of the critical points, and when  $\eta > 1$  a limit cycle occurs. The change in the number of the critical points can be easily understood by evaluating formula (4.3.8). In that case the formula (4.3.8) become :

$$r^2 = -\frac{32}{15} \left( -\frac{3}{4} \pm \sqrt{1 - \eta^2} \right). \quad (4.3.10)$$

The graph of  $r$  as a function of  $\eta$  is depicted in Figure 4.6. If  $0 < \sqrt{1 - \eta^2} < \frac{3}{4}$  then we obtain four values of  $r$ . This results implies that equation (4.3.3) has five critical points as the origin is also a critical point. If  $\sqrt{1 - \eta^2} = \frac{3}{4}$  then three values of  $r$  are obtained (one of them is zero) and if  $\frac{3}{4} < \sqrt{1 - \eta^2} < 1$  then we obtain two values for  $r$ .

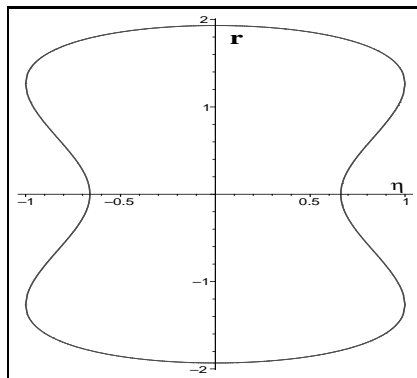


Figure 4.6: Relation between  $r$  and  $\eta$  of formula (4.3.10).

### 4.3.2 Constant mass and varying position of water ridge

Secondly, we consider the case that the position of the ridge of water varies in time and that there is no mass variation due to the rain, i.e.  $a_2 = b_2 = 0$ , implying that the mass flow of rain water hitting the cylinder is equal to the mass flow of rain water which is blown off the cylinder. As is known  $f(t) = f(\tau/\omega) = c_1 \cos(\tau) + d_1 \sin(\tau)$  can be written as  $A \cos(\tau + \psi_o)$ . It is no essential limitation to put  $\psi_o = 0$  in other words  $c_1 \neq 0, d_1 = 0$ . In this case (4.3.2) becomes :

$$\begin{aligned} \dot{\bar{y}}_1 &= \epsilon \left[ \left( s + \frac{1}{4} \bar{c}_2 \right) \bar{y}_1 - \eta \bar{y}_2 - c_1 \left( 2q + \frac{1}{12} \bar{c}_o - \frac{1}{24} \bar{c}_2 \right) \bar{y}_1 \bar{y}_2 \right. \\ &\quad \left. + \left( p - \frac{1}{16} \bar{c}_o + \frac{1}{24} \bar{c}_2 \right) \bar{y}_1^3 + \left( p - \frac{1}{16} \bar{c}_o \right) \bar{y}_1 \bar{y}_2^2 \right], \\ \dot{\bar{y}}_2 &= \epsilon \left[ -\frac{1}{2} K C_{L_1} c_1 - \frac{1}{8} c_1 \bar{c}_o + \eta \bar{y}_1 + \left( s - \frac{1}{4} \bar{c}_2 \right) \bar{y}_2 \right. \\ &\quad \left. - c_1 \left( q + \frac{1}{24} \bar{c}_o - \frac{1}{48} \bar{c}_2 \right) \bar{y}_1^2 - c_1 \left( 3q + \frac{1}{12} \bar{c}_o + \frac{1}{48} \bar{c}_2 \right) \bar{y}_2^2 \right. \\ &\quad \left. + \left( p - \frac{1}{16} \bar{c}_o - \frac{1}{24} \bar{c}_2 \right) \bar{y}_2^3 + \left( p - \frac{1}{16} \bar{c}_o \right) \bar{y}_1^2 \bar{y}_2 \right], \end{aligned} \quad (4.3.11)$$

where  $\bar{c}_o = \bar{c}_2 = \frac{3}{2} c_1^2 K C_{L_3}$ . One can observe that when  $\eta = 0$ ,  $\bar{y}_1 = 0$  is a solution of the first equation of (4.3.11). Thus to find the critical points of (4.3.11) one can substitute  $\bar{y}_1 = 0$  into the second equation of (4.3.11) and the result is a cubical equation in  $\bar{y}_2$ . If for instance  $C_{L_3} = 2, C_{L_1} = -6, C_{D_o} = 1/2, \beta/\omega = 2, K = 1$  and  $c_1 = A$  the relation between  $A$  and  $\bar{y}_2$  is depicted in Figure 4.7a. Clearly when  $A$  varies from 0 to 1 the number of real zeros of the cubical equation for  $\bar{y}_2$  varies from 3 to 2 and finally to 1, and similar results for the critical points of (4.3.11). For  $A = 0.1$  and the values of the other parameters as given above, the phase portrait of (4.3.11) is shown in Figure 4.7b. The coordinates of the critical points in Figure 4.7b correspond with the values of  $\bar{y}_2$  along line  $A = 0.1$  in Figure 4.7a. From Figure 4.7b one can observe that there are three critical points one stable and two unstable. It follows that there are three periodic solutions in the original system: one asymptotically stable and the others unstable. In the case that  $\eta \neq 0$ ,  $\bar{y}_1 = 0$  is not a solution of the first equation of (4.3.11). When  $\eta$  increases from  $\eta = 0$  than the three critical points (in Figure 4.7b) are moving into the positive direction of



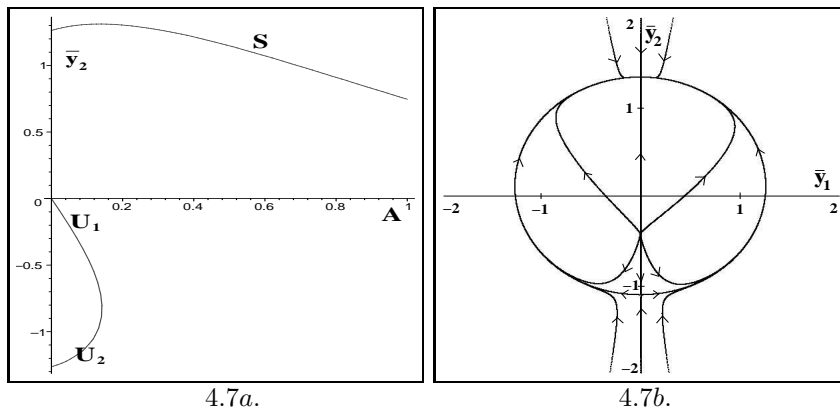


**Figure 4.7:** 4.7a. Critical points  $(0, \bar{y}_2)$  of (4.3.11) as a function of  $A$  for  $\eta = 0$ . 4.7b. The phase portrait of (4.3.11) for  $A = 0.1$  and  $\eta = 0$ .

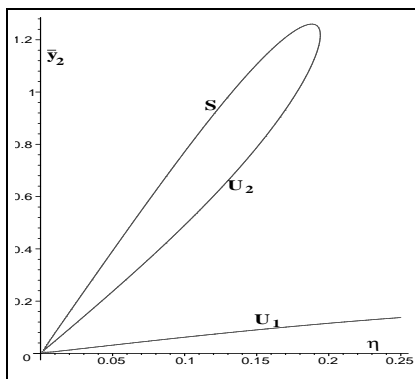


**Figure 4.8:** Relation between  $\bar{y}_2$  and  $\eta$  by using a Gröbner basis algorithm.

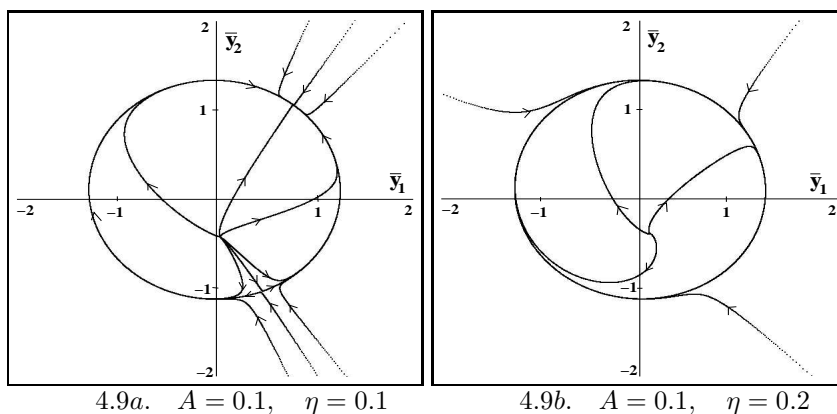


**Figure 4.9:** Orbits of equation (4.3.11) for  $A = 0.1$  and  $\eta = 0.1, \eta = 0.2$ .

the  $\bar{y}_1$ -axis as is shown in Figure 4.9a. Further, following Figure 4.8 when the value of  $\eta$  is around 0.2 there will be a saddle node bifurcation and a limit cycle occurs. The limit cycle corresponds with a modulated oscillation in the original system. For more details one can consult [29].

### 4.3.3 Mass and position of water ridge vary both with time

Now we discuss the situation that both effects are included. The effect of the varying position of the ridge of water is indicated by the parameters  $c_1$  and  $d_1$ , and the effect of the varying mass is indicated by  $a_2$  and  $b_2$ . By observing system (4.3.2) it follows that  $a_2$  and  $b_2$  affect only the coefficients of the linear terms of the system. Hence by varying  $a_2$  and  $b_2$  the structure of the solutions near the origin may vary. However  $c_1$  and  $d_1$  affect both the coefficients of the linear as the non linear terms and hence this variation has a local and non-local influence on the behaviour of the solutions. Clearly the coefficients of the non-linear terms define the structure of the solutions of the critical points away from the origin implying their non-local relevance. Note that  $s$  depends on  $c_1$  and  $d_1$  and are involved in some of the coefficients of the linear terms. We study the situation that both effects are included in two ways, the first one is keeping  $a_2$  and  $b_2$  fixed and vary  $c_1$  and  $d_1$ , and the other one is keeping  $c_1$  and  $d_1$  fixed and vary  $a_2$  and  $b_2$ . It is known that  $f(t) = f(\tau/\omega) = c_1 \cos \tau + d_1 \sin \tau$  can be written as  $A \cos(\tau + \psi_o)$ . It is no essential limitation to put  $\psi_o = 0$  in other words  $c_1 \neq 0, d_1 = 0$ , which reduces system (4.3.2) to :

$$\begin{aligned} \dot{\bar{y}}_1 &= \epsilon \left[ \left( \bar{s} + \frac{1}{4}b_2 - \frac{3}{8}KC_{L_3}c_1^2 \right) \bar{y}_1 + \left( -\frac{1}{4}a_2 - \eta \right) \bar{y}_2 + c_1(2q + \right. & (4.3.12) \\ &\quad \left. \frac{1}{16}KC_{L_3}c_1^2) \bar{y}_1 \bar{y}_2 + \left( p - \frac{1}{32}KC_{L_3}c_1^2 \right) \bar{y}_1^3 + \left( p - \frac{3}{32}KC_{L_3}c_1^2 \right) \bar{y}_1 \bar{y}_2^2 \right], \\ \dot{\bar{y}}_2 &= \epsilon \left[ -\frac{1}{2}KC_{L_1}c_1 - \frac{3}{8}KC_{L_3}c_1^3 + \left( -\frac{1}{4}a_2 + \eta \right) \bar{y}_1 + \left( \bar{s} - \frac{1}{4}b_2 - \right. \right. \\ &\quad \left. \frac{9}{8}KC_{L_3}c_1^2) \bar{y}_2 - c_1 \left( q + \frac{1}{32}KC_{L_3}c_1^2 \right) \bar{y}_1^2 - c_1 \left( 3q + \frac{5}{32}KC_{L_3}c_1^2 \right) \bar{y}_2^2 + \right. \\ &\quad \left. \left( p - \frac{5}{32}KC_{L_3}c_1^2 \right) \bar{y}_2^3 + \left( p - \frac{3}{32}KC_{L_3}c_1^2 \right) \bar{y}_1^2 \bar{y}_2 \right]. \end{aligned}$$

The critical points of (4.3.12) for relevant values of the coefficients can be analyzed by using a Gröbner basis algorithm. Keep all parameters fixed except  $c_1 = A$ , for instance  $a_2 = 4, b_2 = 0, \eta = 0, C_{L_3} = 2, C_{L_1} = -6, C_{D_o} = 1/2, \beta/\omega = 2$  and  $K = 1$ . Then one can obtain a relation between  $A$  and  $\bar{y}_1, \bar{y}_2$  as shown in Figure 4.10. The number of critical points of (4.3.12) varies from three to one if  $A$  varies from 0 to 1 and the phase portraits are depicted in Figure 4.11a, 4.11b, 4.11c and 4.11d for several values of  $A$ . In Figure 4.9 the vertical axis is  $\bar{y}_2$  and the horizontal axis is  $\bar{y}_1$ . The coordinates of the critical points in Figure 4.11 correspond with the value of  $\bar{y}_1$  and  $\bar{y}_2$  in Figure 4.10 for the given value of  $A$ . Corresponding (parts of) curves in Figure 4.10a, 4.10b are indicated with  $S_1, U$ , and  $S_2$  where  $S$  stands for stable and  $U$  stands for unstable. If for example  $A = 0.1$  the coordinates of the stable critical point  $(\bar{y}_1, \bar{y}_2)$  follow from Figure 4.10a by using the upper  $S_2$  curve to obtain  $\bar{y}_1$  and from Figure 4.10b the lower  $S_2$  curve to obtain  $\bar{y}_2$ . Further one can observe that a saddle-node bifurcation occurs for  $A$  in the neighbourhood of 0.52.

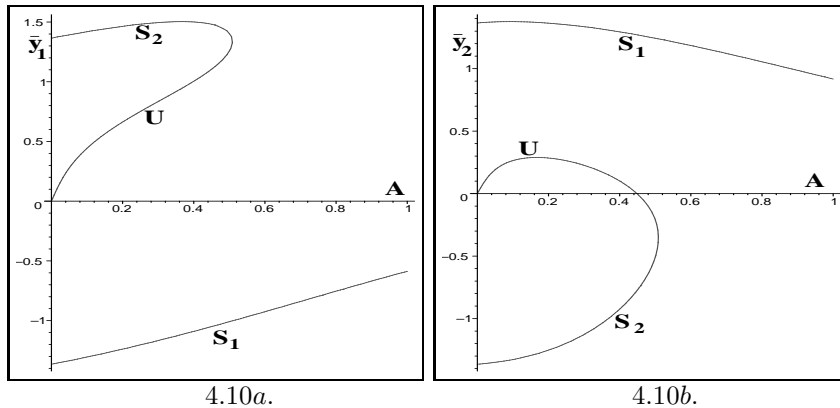


**Figure 4.10:** Critical points  $(\bar{y}_1, \bar{y}_2)$  of system (4.3.12) as a function of  $A$  where  $d_1 = 0$ ,  $a_2 = 4$ ,  $b_2 = 0$  and  $\eta = 0$ .

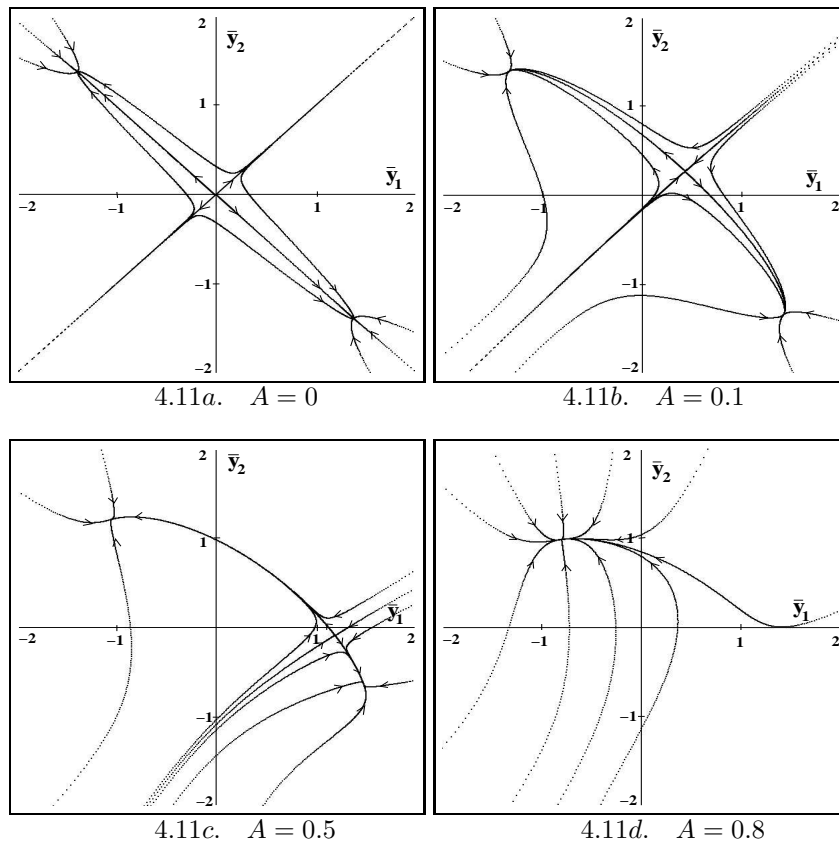


**Figure 4.11:** The phase portraits of equation (4.3.12) for several values of  $A$ , the amplitude of the variation of the position of the water ridge. The variation of the mass of rainwater has in this case a constant amplitude  $a_2 = 4$ ,  $b_2 = 0$ .

Further we study the situation  $c_1 = A = 0.1$ ,  $d_1 = 0$  and vary  $a_2$  with  $b_2 = 0$ . By keeping the other parameters fixed as before implying that only  $a_2$  varies in equation (4.3.12), then by using the Gröbner basis algorithm one can find the number of critical points as shown in Figure 4.12a, 4.12b. From the diagram in Figure 4.12a one can observe that the number of critical points varies as follows

$$3 \rightarrow 4 \rightarrow 5 \rightarrow 4 \rightarrow 3,$$

when  $a_2$  varies from 0 to 5. For example when  $a_2 = 4$  the number of critical points is three. The phase portraits are depicted in Figure 4.13 for several values of  $a_2$ . In Figure 4.13 the vertical axis is  $\bar{y}_2$  and the horizontal axis is  $\bar{y}_1$ .

In comparing the phase portraits in Figures 4.11 and 4.13 one can verify that Figure 4.11b and Figure 4.13d are qualitatively equivalent although the values of  $a_2$  differ : 4 in Figure 4.11b and 1.3 in Figure 4.13d. This is in accordance with the qualitative behaviour of the critical points in Figures 4.12a, 4.12b for  $a_2 > 1.3$ . Clearly in both phase portraits there are two stable critical points corresponding with stable periodic solutions with approximately the same amplitude but with different phases. Increasing  $A$  in Figure 4.11 and decreasing  $a_2$  in Figure 4.13 leads to Figures 4.11d and 4.13a with one stable critical point. However, the phase portraits are qualitatively rather different.

Finally the number and the stability of the critical points of system (4.3.12) for several values of  $A$  and  $a_2$  are summarized in Table 4.1. In general the variation of the position of the water ridge and the variation of the mass of rain water on the oscillator give different effects to the system. The presence of the variation of the position of the water ridge in the system implies that the origin is not a critical point of the system. In other words the system does not have a trivial solution. Further, if we increase the amplitude of the variation of the position of the water ridge then the system has only one stable critical point. However, if we increase the amplitude of the variation of the mass of rain water on the oscillator then the system can have three critical points of which two are stable and one unstable. Considering the magnitude of the amplitude of the two variations, it seems that in a number of cases the variation of the position of the water ridge leads to bifurcation of critical points. In Figure 4.10c for example (  $a_2 = 4$  and  $A = 0.5$  ) the system has three critical points and in Figure 4.11d (  $a_2 = 4$  and  $A = 0.8$  ) the system has only one stable critical point, thus between  $A = 0.5$  and  $A = 0.8$  a saddle node bifurcation occurs. Because a critical point corresponds with a periodic solution in the original system then according to the Figure 4.11c the original system has three periodic solutions, two stable and one unstable. The influence of increasing the amplitude of the position of the water ridge of the system is that the two critical points vanish due to saddle node bifurcation and only one stable critical point remains.

The results which are described in Table 4.1 do not include the influence of the detuning parameter  $\eta$ . Now, we will see the effect of the detuning parameter  $\eta$  by keeping all other parameters fixed. When the value of  $\eta$  is "large" then we will have in the phase plane of equation (4.3.12) an unstable critical point and a stable limit cycle around this point. For instance, when we fix the parameters,  $a_2 = 4$ ,  $b_2 = 0$ ,

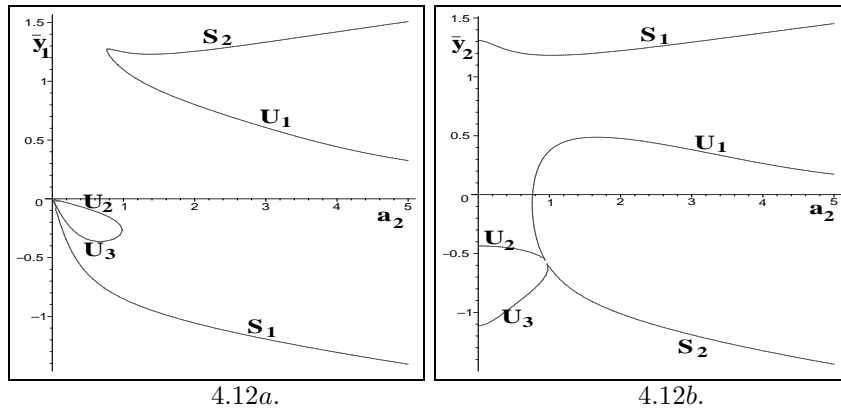


**Figure 4.12:** Critical points  $(\bar{y}_1, \bar{y}_2)$  of system (4.3.12) as a function of  $a_2$ , where  $c_1 = A = 0.1$ ,  $d_1 = 0$ ,  $b_2 = 0$  and  $\eta = 0$ .

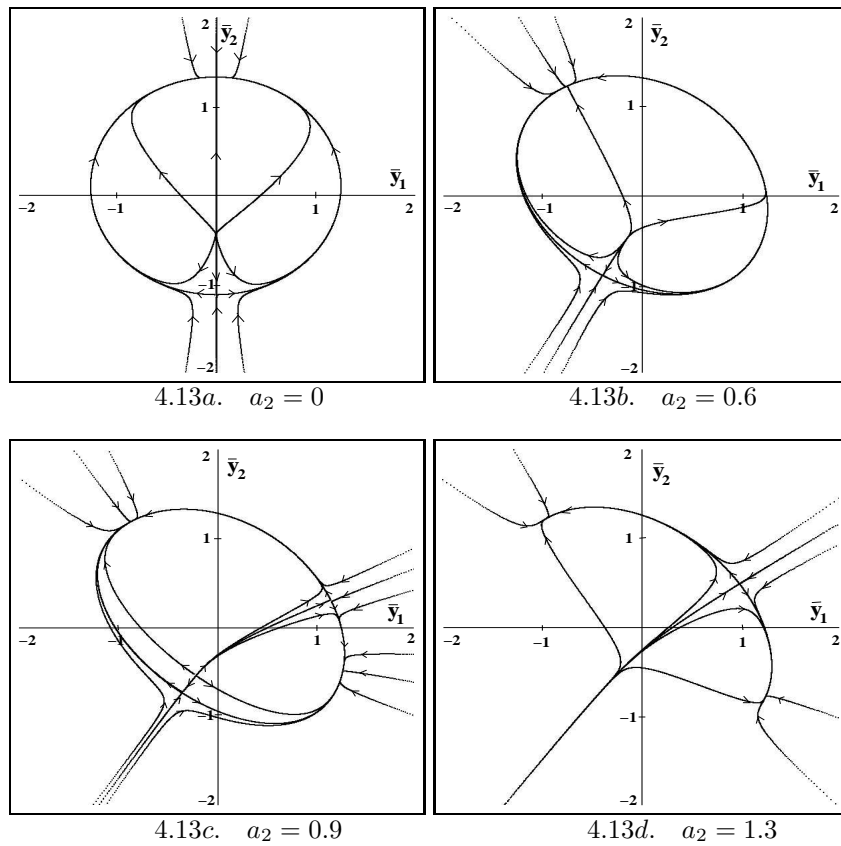


**Figure 4.13:** The phase portraits of system (4.3.12) for several values of  $a_2$ , the amplitude of the variation of the mass of rain water. The variation of the position of the water ridge has constant amplitude  $A = 0.1$ .

**Table 4.1:** The number of critical points and their stability of system (4.3.12) for several values of  $A$  and  $a_2$ , where  $A$  = the amplitude of the variation of the position of the water ridge,  $a_2$  = the amplitude of the variation of the mass of rain water, s = stable and u = unstable, c.p.= critical point, o.n.s.=origin is not a solution.

$\eta = 0, C_{L_3} = 2$ $C_{L_1} = -6$ $C_{D_o} = 1/2$ $\beta/\omega = 2, K = 1$ $b_2 = 0, d_1 = 0$	$A = 0$	$A = 0.1$	$A = 0.14$	$A = 0.5$	$A = 0.8$
$a_2 = 0$	Origin is an unstable node.  Infinitely many stable c.p. on a circle.	o.n.s.  3 c. p. (1s, 2u)	o.n.s.  saddle node bifurcation.	o.n.s.  1s c.p.	o.n.s.  1s c.p.
$a_2 = 0.6$	Origin is an unstable node.  5 c.p. (2s, 3u)	o.n.s.  3 c.p. (1s, 2u)	o.n.s.  1s c.p.	o.n.s.  1s c.p.	o.n.s.  1s c.p.
$a_2 = 0.9$	Origin is an unstable node.  5 c.p. (2s, 3u)	o.n.s.  5 c.p. (2s, 3u)	o.n.s.  1s c.p.	o.n.s.  1s c.p.	o.n.s.  1s c.p.
$a_2 = 1.3$	Origin is an unstable node.  5 c.p. (2s, 3u)	o.n.s.  3 c.p. (2s, 1u)	o.n.s.  3 c.p. (2s, 1u)	o.n.s.  1s c.p.	o.n.s.  1s c.p.
$a_2 = 4$	Origin is a saddle point.  3 c.p. (2s, 1u)	o.n.s.  3 c.p. (2s, 1u)	o.n.s.  3 c.p. (2s, 1u)	o.n.s.  3 c.p. (2s, 1u)	o.n.s.  1s c.p.

$C_{L_3} = 2, C_{L_1} = -6, C_{D_o} = 1/2, \beta/\omega = 2, K = 1$  and  $A = 0.1$  and when we vary  $\eta$  we will find the following. When  $\eta = 0$  the phase portrait is shown in Figure 4.14a. By increasing  $\eta$  the two critical points come closer to each other and finally collapse when the value of  $\eta$  is between 0.8 and 1 (see Figure 4.14b and 4.14c).

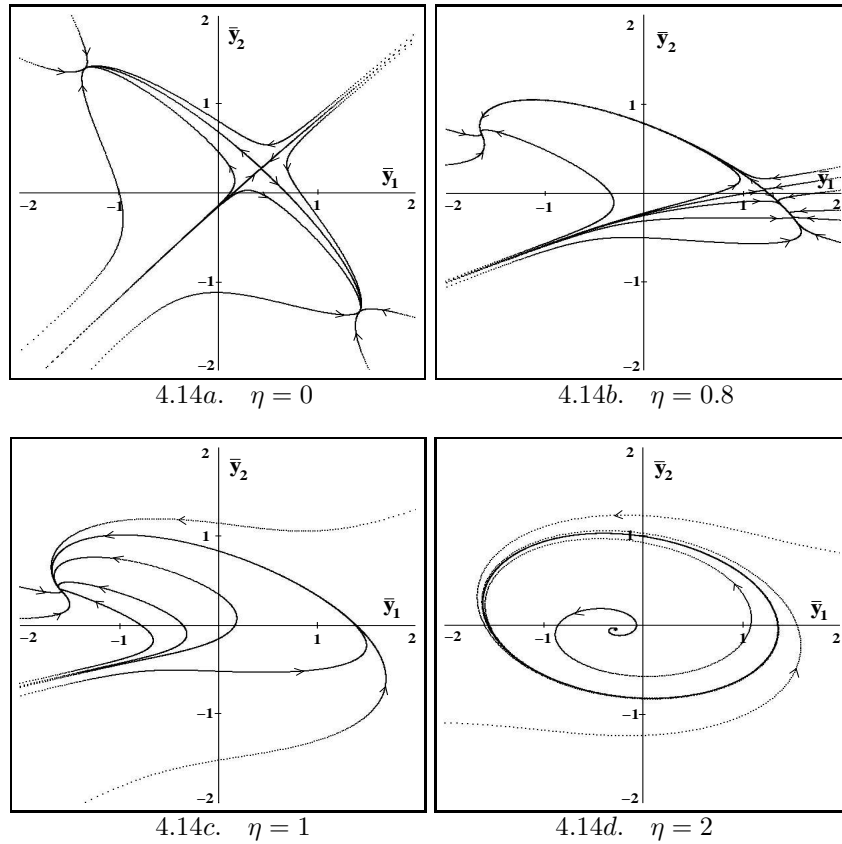


**Figure 4.14:** The phase portraits of equation (4.3.12) for several values of  $\eta$ , the detuning parameter,  $a_2 = 4$ ,  $b_2 = 0$ ,  $C_{L_3} = 2$ ,  $C_{L_1} = -6$ ,  $C_{D_o} = 1/2$ ,  $\beta/\omega = 2$ ,  $K = 1$  and  $A = 0.1$ .

This phenomenon is known as a saddle node bifurcation. When the values of  $\eta$  are between 1.24 and 1.25 the Hopf bifurcation occurs, initiating the occurrence of a limit cycle. For  $\eta = 2$  the phase portrait is given in Figure 4.14d.

## 4.4 Conclusions

From the model equation describing the interaction of a wind-field containing rain drops and a simple oscillator it follows that both the time-varying mass of rain drops attached to the oscillator and the time-varying lift and drag force coefficients are mechanisms leading to an unstable equilibrium position. From physical point of view it can be understood that regular adding and removing of a marginal quantity of raindrops attached to a mass spring system defined as a Hamiltonian system, may lead to an unstable equilibrium.

On the other hand the time varying position of the water ridge leads to time varying lift and drag forces as an instability mechanism. When the position of the water ridge is fixed ( $A = 0$ , Figure 4.11a) the unstable equilibrium position as evolution of three unstable critical points and two stable critical points corresponding with two periodic solutions are found. In absence of variation of mass of rain water on the oscillator ( $a_2 = 0$ , Figure 4.13a) only one stable critical point i.e. one periodic

solution is found. Apparently the first mechanism displays a certain symmetry which the second mechanism does not show. In general the variation of position of the water ridge and the variation of mass of rain water on the oscillator give different effects to the system. Increasing the amplitude of the variation of the position of the water ridge it turns out that the system has one stable periodic solution, but when the amplitude of the variation of the mass of rain water increases the system will have three periodic solutions ( two stable and one unstable). Variations of the detuning parameter will lead to saddle node and Hopf bifurcations in the system. From a practical point of view one may conclude that in order to avoid instabilities one should design the oscillator in such a way that rain water accumulation and variation is not be possible.

## 4.5 Appendix

To illustrate what a Gröbner basis algorithm is, one can consider as an example the following system of linear equations:

$$\begin{aligned} x + y - 2z &= 0, \\ 2x - y + 5z &= 0, \\ 6x + z &= 0. \end{aligned} \tag{4.5.13}$$

By using Gauss elimination one obtains as an equivalent system ( that is, a system which has the same set of solutions)

$$\begin{aligned} x + y - 2z &= 0, \\ 3x + 3z &= 0, \\ - 5z &= 0, \end{aligned} \tag{4.5.14}$$

and this system is "easier" to solve than the system (4.5.13). Now the problem is if we have a system of equations with nonlinear polynomials then how do we obtain an equivalent system which is "easier" to solve. To find this system turns out to be equivalent with finding a Gröbner basis.

It should be observed that system (4.5.13) can be written as  $f_1 = 0$ ,  $f_2 = 0$ ,  $f_3 = 0$ , where  $f_1 = x + y - 2z$ ,  $f_2 = 2x - y + 5z$  and  $f_3 = 6x + z$  are in  $k[x, y, z]$ , that is, the set of all polynomials in the variables  $x, y, z$  with coefficients in the field  $k$  (in this case  $k = \mathbf{R}$  the set of all real numbers).  $k[x, y, z]$  is a *commutative ring* under the operations of addition and multiplication of polynomials. The set

$$\langle f_1, f_2, f_3 \rangle = \{u_1 f_1 + u_2 f_2 + u_3 f_3 \mid u_1, u_2, u_3 \in k[x, y, z]\}$$

is an *ideal* in  $k[x, y, z]$ . If we denote  $f_4 = 3x + 3z$  and  $f_5 = -5z$  then  $\langle f_1, f_2, f_3 \rangle = \langle f_1, f_4, f_5 \rangle$  because  $f_4 = f_1 + f_2$  and  $f_5 = -2f_3 + f_4$ .

Furthermore, for a given  $f \in k[x, y, z]$  we define the *variety*  $V(f)$  to be the set of all solutions of the equation  $f = 0$ , i. e.

$$V(f) = \{(x, y, z) \in \mathbf{R}^3 \mid f = 0\}.$$

The variety  $V(f_1, f_2)$  is the set of all solutions of the system of equations  $f_1 = 0$ ,  $f_2 = 0$ . More generally, if  $S \subseteq k[x, y, z]$  then the variety  $V(S)$  is

$$V(S) = \{(x, y, z) \in \mathbf{R}^3 \mid f = 0 \text{ for all } f \in S\}.$$



Evidently  $V(f_1, f_2, f_3) = V(f_1, f_4, f_5)$  and  $V(f_1, f_2, f_3) = V(\langle f_1, f_2, f_3 \rangle)$ . Generally, if we have an ideal  $I$  in  $k[x_1, x_2, \dots, x_n]$  ( a set of all polynomials in  $n$  variables) which is generated by  $f_1, f_2, \dots, f_m$  then  $V(I) = V(f_1, f_2, \dots, f_m)$ .

An ideal may have many different generating sets with different number of elements. Suppose  $I = \langle f_1, f_2, \dots, f_m \rangle = \langle \bar{f}_1, \bar{f}_2, \dots, \bar{f}_l \rangle$  then  $V(f_1, f_2, \dots, f_m) = V(I) = V(\bar{f}_1, \bar{f}_2, \dots, \bar{f}_l)$ . It means that the variety is determined by an ideal and not by a particular set of equations. Thus the problem above becomes : "if we have an ideal  $I = \langle f_1, f_2, \dots, f_r \rangle$  how can we find another generating set for the ideal  $I$  such that we can "easier" evaluate its variety". Such a generating set will be called a Gröbner basis for the ideal  $I$ . To find it we need an "ordering" in  $k[x_1, x_2, \dots, x_n]$ . The existence of the finite generating sets of an ideal  $I$  in  $k[x_1, x_2, \dots, x_n]$  is guaranteed by Hilbert's basis theorem, i. e. if  $I$  is any ideal in the ring  $k[x_1, x_2, \dots, x_n]$  then there exist polynomials  $f_1, f_2, \dots, f_s \in k[x_1, x_2, \dots, x_n]$  such that  $I = \langle f_1, f_2, \dots, f_s \rangle$ . As is well known,  $k[x_1, x_2, \dots, x_n]$  is a vector space over the field  $k$  with a basis set  $\mathbf{T}^n$ , of all power products,

$$\mathbf{T}^n = \{x_1^{\alpha_1} x_2^{\alpha_2} \dots x_n^{\alpha_n} \mid \alpha_i \in \mathbf{N} = \{0, 1, 2, \dots\}, i = 1, 2, \dots, n\}.$$

For simplicity,  $x_1^{\alpha_1} x_2^{\alpha_2} \dots x_n^{\alpha_n}$  is denoted as  $\mathbf{x}^\alpha$ , where  $\alpha = (\alpha_1, \alpha_2, \dots, \alpha_n) \in \mathbf{N}^n$ . Many definitions of the order can be defined on  $\mathbf{T}^n$ , one of them is a lexicographical order (which is used in this thesis).

*Definition 1.* The lexicographical order on  $\mathbf{T}^n$  with  $x_1 > x_2 > \dots > x_n$  is defined as follows: For  $\alpha = (\alpha_1, \alpha_2, \dots, \alpha_n)$  and  $\beta = (\beta_1, \beta_2, \dots, \beta_n) \in \mathbf{N}^n$ ,  $\mathbf{x}^\alpha < \mathbf{x}^\beta$  if and only if the first coordinates  $\alpha_i$  and  $\beta_i$  in  $\alpha$  and  $\beta$  from the left, which are different, satisfy  $\alpha_i < \beta_i$ .

We have an order on  $k[x_1, x_2, \dots, x_n]$  if we have an order on  $\mathbf{T}^n$ . Thus, for example in the case of two variables  $x_1, x_2$  with  $x_1 > x_2$  then in  $k[x_1, x_2]$  we have

$$1 < x_2 < x_2^2 < x_2^3 < \dots < x_1 < x_2 x_1 < x_2^2 x_1 < \dots < x_1^2 < \dots.$$

If we write a polynomial  $f$  in  $k[x_1, x_2, \dots, x_n]$  as

$$f = a_1 \mathbf{x}^{\alpha_1} + a_2 \mathbf{x}^{\alpha_2}, \dots + a_s \mathbf{x}^{\alpha_s},$$

where  $0 \neq a_1 \in k$  and  $\mathbf{x}^{\alpha_1} > \mathbf{x}^{\alpha_2} > \dots > \mathbf{x}^{\alpha_s}$ ,  $\mathbf{x}^{\alpha_i} \in \mathbf{T}^n$ , then we define

- $lp(f) = \mathbf{x}^{\alpha_1}$ , the leading power product of  $f$ ,
- $lc(f) = a_1$ , the leading coefficient of  $f$ ,
- $lt(f) = a_1 \mathbf{x}^{\alpha_1}$ , the leading term of  $f$ .

*Definition 2.* Let  $f, g, h$  be polynomials in  $k[x_1, x_2, \dots, x_n]$  with  $g \neq \mathbf{0}$ . Polynomial  $f$  reduces to  $h$  modulo  $g$  in one step, denoted,  $f \xrightarrow{g} h$ , if and only if  $lp(g)$  divides a non-zero term  $X$  that appears in  $f$  and  $h = f - \frac{X}{u(g)}g$ .

*Definition 3.* Let  $f, h$  and  $f_1, f_2, \dots, f_s$  be polynomials in  $k[x_1, x_2, \dots, x_n]$  with  $f_i \neq \mathbf{0}, i = 1, 2, \dots, s$  and  $F = \{f_1, f_2, \dots, f_s\}$ . The polynomial  $f$  reduces to  $h$  modulo  $F$ , denoted,  $f \xrightarrow{F}_+ h$  if and only if there exists a sequence of indices  $i_1, i_2, \dots, i_t$  in

$\{1, 2, \dots, s\}$  and a sequence of polynomials  $h_1, h_2, \dots, h_{t-1}$  in  $k[x_1, x_2, \dots, x_n]$  such that

$$f \frac{f_{i_1}}{h_1} \frac{f_{i_2}}{h_2} \frac{f_{i_3}}{h_3} \dots \frac{f_{i_{t-1}}}{h_{t-1}} \frac{f_{i_t}}{h_{t-1}} h.$$

*Definition 4.* A polynomial  $r$  is called reduced with respect to  $F = \{f_1, f_2, \dots, f_s\}$  if  $r = \mathbf{0}$  or no power product that appears in  $r$  is divisible by any one of the  $lp(f_i)$ ,  $i = 1, 2, \dots, s$ . Furthermore, if  $f \frac{F}{+} r$  and  $r$  reduced with respect to  $F$ , then  $r$  is a remainder for  $f$  with respect to  $F$ .

Now we define what is a Gröbner basis.

*Definition 5.* Let  $I$  be an ideal in  $k[x_1, x_2, \dots, x_n]$ .  $G = \{g_1, g_2, \dots, g_t\} \subseteq I$  is called a Gröbner basis for  $I$  if and only if for all  $f \in I$  ( $f \neq \mathbf{0}$ ) there exist  $i \in \{1, 2, \dots, t\}$  such that  $lp(g_i)$  divides  $lp(f)$ .

*Definition 6.* Let  $f, g$  be non-zero polynomials in  $k[x_1, x_2, \dots, x_n]$  and  $L = lcm(lp(f), lp(g))$  be a least common multiple of  $lp(f)$  and  $lp(g)$ . The polynomial

$$S(f, g) = \frac{L}{lt(f)} f - \frac{L}{lt(g)} g$$

is called the  $S$ -polynomial of  $f$  and  $g$ .

*Theorem (Buchberger).* Let  $G = \{g_1, g_2, \dots, g_t\}$  be a set of non-zero polynomials in  $k[x_1, x_2, \dots, x_n]$ . Then  $G$  is a Gröbner basis for the ideal  $I = \langle g_1, g_2, \dots, g_t \rangle$  if and only if for all  $i \neq j$ ,  $S(g_i, g_j) \frac{G}{+} \mathbf{0}$ .

The Gröbner basis can be found by the following algorithm (called Buchberger's Algorithm):

**INPUT :**  $F = \{f_1, f_2, \dots, f_s\} \subset k[x_1, x_2, \dots, x_n]$ ,  $f_i \neq \mathbf{0}$  for all  $i \in \{1, 2, \dots, s\}$

**OUTPUT :**  $G = \{g_1, g_2, \dots, g_t\}$  a Gröbner basis for ideal  $\langle f_1, f_2, \dots, f_s \rangle$

**INITIALIZATION :**  $G := F$ ,  $\mathcal{G} = \{ \{f_i, f_j\} \mid f_i \neq f_j \in G \}$

**WHILE**  $\mathcal{G} \neq \emptyset$  **DO**

- Choose any  $\{f, g\} \in \mathcal{G}$
- $\mathcal{G} := \mathcal{G} - \{\{f, g\}\}$
- $S(f, g) \frac{G}{+} h$ , where  $h$  is reduced with respect to  $G$

**IF**  $h \neq \mathbf{0}$  **THEN**

- $\mathcal{G} := \mathcal{G} \cup \{ \{u, h\} \mid \text{for all } u \in G \}$
- $G := G \cup \{h\}$

Thus if one gives a set of non-zero polynomials  $\{f_1, f_2, \dots, f_s\}$  then based on Buchberger's algorithm one can produce a Gröbner basis for the ideal  $\langle f_1, f_2, \dots, f_s \rangle$ . Finally the existence of a Gröbner basis is guaranteed by Buchberger's theorem, i. e. :

*Theorem.* Given  $F = \{f_1, f_2, \dots, f_s\}$  with  $f_i \neq \mathbf{0}$  for all  $i$ . Buchberger's algorithm will produce a Gröbner basis for the ideal  $I = \langle f_1, f_2, \dots, f_s \rangle$ .

*Example.* Consider equation (4.3.12) Keep all parameters fixed except  $c_1 = A$ , for instance  $a_2 = 4$ ,  $b_2 = 0$ ,  $\eta = 0$ ,  $C_{L_3} = 2$ ,  $C_{L_1} = -6$ ,  $C_{D_o} = 1/2$ ,  $\beta/\omega = 2$  and  $K = 1$ ,

then equation (4.3.12) becomes:

$$\begin{aligned}\dot{\bar{y}}_1 &= \epsilon \left[ \left( \frac{3}{4} - \frac{3}{4}A^2 \right) \bar{y}_1 - \frac{6}{5} \bar{y}_2 - \left( \frac{3}{4}A + \frac{1}{8}A^3 \right) \bar{y}_1 \bar{y}_2 - \left( \frac{15}{32} + \frac{1}{8}A^2 \right) \bar{y}_1^3 - \right. \\ &\quad \left. \left( \frac{15}{32} + \frac{3}{16}A^2 \right) \bar{y}_1 \bar{y}_2^2 \right], \\ \dot{\bar{y}}_2 &= \epsilon \left[ 3A - \frac{3}{8}A^3 - \frac{4}{5} \bar{y}_1 + \left( \frac{3}{4} - \frac{9}{4}A^2 \right) \bar{y}_2 - \left( \frac{3}{8} + \frac{1}{16}A^2 \right) \bar{y}_1^2 - \right. \\ &\quad \left. \left( \frac{9}{8}A + \frac{5}{48}A^3 \right) \bar{y}_2^2 - \left( \frac{15}{32} + \frac{5}{48}A^2 \right) \bar{y}_2^3 - \left( \frac{5}{32} + \frac{3}{16}A^2 \right) \bar{y}_1^2 \bar{y}_2 \right].\end{aligned}\quad (4.5.15)$$

For simplicity we will write  $x$  for  $\bar{y}_1$  and  $y$  for  $\bar{y}_2$ . So equation (4.5.15) can be written as

$$\dot{x} = \epsilon f_1, \quad \dot{y} = \epsilon f_2, \quad (4.5.16)$$

where

$$\begin{aligned}f_1 &= \left( \frac{3}{4} - \frac{3}{4}A^2 \right) x - \frac{6}{5}y - \left( \frac{3}{4}A + \frac{1}{8}A^3 \right) xy - \left( \frac{15}{32} + \frac{1}{8}A^2 \right) x^3 - \\ &\quad \left( \frac{15}{32} + \frac{3}{16}A^2 \right) xy^2, \\ f_2 &= 3A - \frac{3}{8}A^3 - \frac{4}{5}x + \left( \frac{3}{4} - \frac{9}{4}A^2 \right) y - \left( \frac{3}{8} + \frac{1}{16}A^2 \right) x^2 - \\ &\quad \left( \frac{9}{8}A + \frac{5}{48}A^3 \right) y^2 - \left( \frac{15}{32} + \frac{5}{48}A^2 \right) y^3 - \left( \frac{5}{32} + \frac{3}{16}A^2 \right) x^2 y.\end{aligned}$$

To find all critical points of equation (4.5.15) is equivalent to solve the system of equations  $f_1 = 0$ ,  $f_2 = 0$  or to find the variety  $V(f_1, f_2)$ . Now we consider the ideal  $I$  which is generated by  $f_1$  and  $f_2$ , that is,  $I = \langle f_1, f_2 \rangle$ . By using the Gröbner basis algorithm in the software package Maple with ordering  $x > y$ , we obtain a Gröbner basis of ideal  $I$ , that is,  $\{\bar{f}_1, \bar{f}_2\}$ , where

$$\begin{aligned}\bar{f}_1 &= -149299200 y^3 + 496125 y^9 A^4 - 46448640 y + 11560 A^{10} y^9 + \\ &\quad 431550 A^6 y^9 + 1111283712 A^4 y + 123420 A^8 y^9 - 597196800 A^5 + \\ &\quad 16329600 y^6 A^3 - 36920448 A^7 + 15968016 A^9 + 93312000 y^5 + \\ &\quad 159751764 y^3 A^6 + 42840 A^{12} y^7 + 27880 A^{13} y^6 + 9600 A^{14} y^5 + \\ &\quad 1440 A^{15} y^4 - 2068632 y^2 A^9 + 60480 y^3 A^{14} + 5145120 y^2 A^{11} + \\ &\quad 75064320 A^3 y^4 + 51763968 A^4 y^3 + 205641504 A^5 y^4 + 238878720 A - \\ &\quad 6562944 A^{10} y + 575424 A^{12} y + 245520 A^{13} y^4 - 103680 A^{13} y^2 + \\ &\quad 769800672 A^6 y - 7597800 A^4 y^7 + 7721568 A^{10} y^3 - 17721180 A^5 y^6 + \\ &\quad 123310080 A^4 y^5 - 1859436 A^7 y^6 - 182448 A^{11} y^4 + 89370360 A^8 y^3 - \\ &\quad 249540048 A^7 y^2 + 57378816 A^7 y^4 + 864252 A^{10} y^7 + \\ &\quad 5184 A^{15} y^2 + 872544 A^{11} y^6 + 577872 A^{12} y^5 + 2552040 A^6 y^7 + \\ &\quad 3865320 A^8 y^7 + 1697040 A^{10} y^5 - 9384336 A^8 y^5 + 4068576 A^9 y^6 - \\ &\quad 489888 y^3 A^{12} + 82944000 A^2 y^5 - 1643760 A^9 y^4 - 1039564800 y A^2 + \\ &\quad 688435200 y^3 A^2 + 580939776 y^2 A^3 - 776355840 y^2 A + 70655328 y A^8 -\end{aligned}$$

$$\begin{aligned}
& 320924160 A^5 y^2 - 1065000960 A^3 + 2778300 A^5 y^8 + 298598400 A y^4 + \\
& 34680 A^{11} y^8 + 2069550 A^7 y^8 + 485928 A^9 y^8 - 1716336 A^6 y^5, \\
\bar{f}_2 &= bx + cg(y),
\end{aligned}$$

with  $g(y)$  a polynomial in  $y$ ;  $b$  and  $c$  depend on  $A$ .

We know that  $V(f_1, f_2) = V(\bar{f}_1, \bar{f}_2)$ . Fix  $A$ , then  $\bar{f}_1$  becomes a polynomial in the single variable  $y$ . To find the zeros of the polynomial  $\bar{f}_1$  is then relatively simple. Substituting these values into  $\bar{f}_2 = bx + cg(y) = 0$ , then gives  $x$ . So the variety  $V(\bar{f}_1, \bar{f}_2)$  has been determined. Furthermore, the relation between  $A$  and  $y$  can be given by implicitly plotting  $\bar{f}_1(A, y) = 0$ . The result is depicted in Figure 4.10b. For more details about the Gröbner basis one can consult [1].

# Chapter 5

## Rain-wind Induced Vibrations of a Seesaw Oscillator <sup>†</sup>

**Abstract.** In this chapter the rain-wind induced vibrations of a seesaw oscillator will be studied. The model equations will be derived under the assumption that the position of the rivulet of water on the oscillator varies in time. The eigenfrequency of the oscillator and the frequency of the movement of the water rivulet on the oscillator are assumed to be close to each other. Several Hopf and saddle node bifurcations will occur when the amplitude of the movement of the water rivulet on the oscillator is varied.

### 5.1 Introduction

There are many examples of rain-wind induced vibrations of elastic structures such as cables or bridges. The Erasmus bridge in Rotterdam and the Meikonishi bridge in the Nagoya Harbor in Japan are examples of such elastic structures. The cables of these bridge are stable under dry wind condition (no rain), but can become unstable when it is raining (see also [13]). Another instability mechanism can be caused by torsional flutter as for instance described in [21]. This instability mechanism might have been the cause of the collapse of the Tacoma Narrows bridge. The first instability mechanism can be described by spring type oscillators, and the torsional instability mechanism can be modelled by seesaw type oscillators (see also [7, 8]). In [7, 8] a rather complete analysis of the vibrations of a spring type oscillator and of a seesaw type oscillator with a fixed position of the water-rivulet on the oscillators has been presented. And in [29] an analysis for the spring oscillator has been given when the position of the water ridge on the oscillator varies in time.

In this chapter the vibrations of a seesaw oscillator with a time-varying position of a water ridge on the surface of the oscillator will be studied. In Figure 5.1 a sketch

---

<sup>†</sup>This chapter is a revised version of [12], On Rain-wind Induced Vibrations of a Seesaw Oscillator, submitted for publication.

is given of the circular cross-section of the seesaw oscillator with such a water ridge (in black) on the surface. In fact the seesaw oscillator consists of a circular cylinder connected to a rigid bar. At the other end of the bar a hinge-axis is connected such that the bar-cylinder can rotate around this axis (see also Figure 5.1). It is assumed that for each cross-section of the cylinder the time-varying position of the water ridge is the same.

This chapter is organized as follows. In section 2 the equations describing the vibrations of the seesaw oscillator will be derived. In section 3 and in section 4 the effect of the amplitude of the variation in the position of the water rivulet will be studied for different values of the parameters. Finally in section 5 some conclusions will be drawn.

## 5.2 Derivation of the equation of motion

The angle  $\theta$ , measured positive in clockwise direction, describes the angle between the arm holding the cylinder and the horizontal line. The angle  $\alpha_s$  denotes the angle between the rotation arm and a symmetry axis of the cylinder's cross-section, counted positive in clock wise direction, see Figure 5.1. Further,  $R$  is the distance from the cylinder's axis to the pivot  $O$ . It is assumed that a quasi-steady theory can be used to model the windforces acting on the cylinder. The quasi-steady theory implies that for the description of the dynamics of the elastic structure with the flowing medium one may use data which describes the static situation. More precisely one assumes that the fluid forces on the structure are determined solely by the instantaneous resultant flow velocity [7, 31]. The aerodynamic moment  $M$  exerted on the structure can be modeled by using the aerodynamic forces exerted on the cylinder. A moment coefficient curve  $C_M(\alpha)$  for the structure will be used to describe  $M$ .

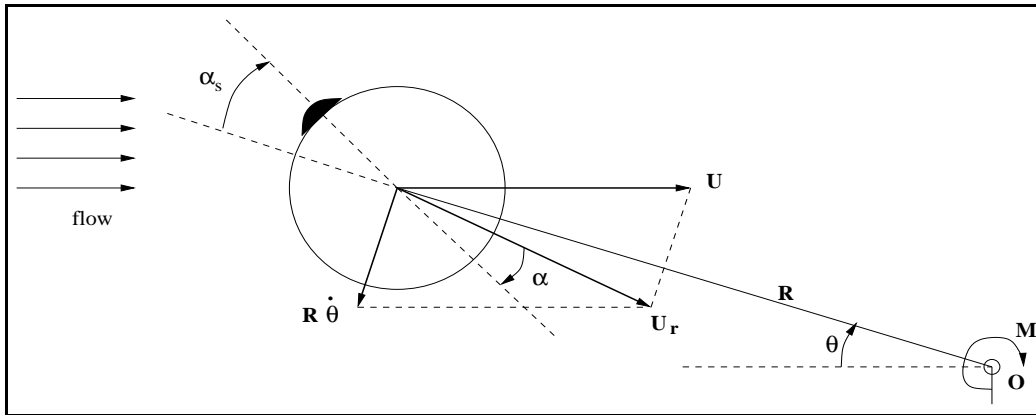


**Figure 5.1:** The cross-section of the seesaw oscillator, the fluid flow with respect to the cylinder, and the definitions of the angles  $\alpha$ ,  $\alpha_s$ , and  $\theta$ .

In the dynamic situation the aerodynamic moment is assumed to be given by

$$M(\alpha) = \frac{1}{2} \rho d l R U_r^2 C_M(\alpha), \quad (5.2.1)$$

where  $\rho$  is the density of air,  $d$  the diameter of the cylinder,  $l$  the length of the cylinder and

$$\alpha = \alpha_s + \theta - \arctan\left(\frac{R\dot{\theta} \cos \theta}{U - R\dot{\theta} \sin \theta}\right), \quad (5.2.2)$$

the angle between the instantaneous velocity vector  $U_r$  of the flow relative to the cylinder and the symmetry axis, measured positive in clockwise direction, and

$$U_r^2 = (U - R\dot{\theta} \sin \theta)^2 + (R\dot{\theta} \cos \theta)^2. \quad (5.2.3)$$

The equation of motion is given by :

$$I\ddot{\theta} + c_\theta\dot{\theta} + k_\theta\theta = M(\alpha), \quad (5.2.4)$$

where  $I$  is the structural moment of inertia,  $k_\theta > 0$  the linear torsional spring constant, and  $c_\theta > 0$  the structural damping coefficient of the oscillator. Defining the dimensionless parameters  $\omega_\theta^2 = k_\theta/I$  and  $\mu = U/R\omega_\theta$  and introducing the transformation  $\tau = \omega_\theta t$ , the following equation is obtained from (5.2.4) :

$$\frac{d^2\theta}{d\tau^2} + \frac{c_\theta}{\omega_\theta I} \frac{d\theta}{d\tau} + \theta = \frac{\rho dl R^3}{2I} \left( \mu^2 - 2\mu \frac{d\theta}{d\tau} \sin \theta + \left( \frac{d\theta}{d\tau} \right)^2 \right) C_M(\alpha), \quad (5.2.5)$$

where  $\alpha = \alpha_s + \theta - \arctan\left(\frac{\frac{d\theta}{d\tau} \cos \theta}{\mu - \frac{d\theta}{d\tau} \sin \theta}\right)$ . By assuming that both damping and aerodynamic moments are small, i.e. :

$$\frac{\rho dl R^3}{2I} = \epsilon, \quad \frac{c_\theta}{\omega_\theta I} = 2\beta_\theta \epsilon, \quad (5.2.6)$$

where  $0 < \epsilon \ll 1$  it follows from (5.2.5) that

$$\frac{d^2\theta}{d\tau^2} + \theta = \epsilon \left[ \left( \mu^2 - 2\mu \frac{d\theta}{d\tau} \sin \theta + \left( \frac{d\theta}{d\tau} \right)^2 \right) C_M(\alpha) - 2\beta_\theta \frac{d\theta}{d\tau} \right]. \quad (5.2.7)$$

A similar derivation of this equation also can be found in [7]. As described in [27] the  $C_M(\alpha)$  curves may be obtained from wind tunnel experiments, and some typical results obtained from measurements in a wind tunnel are sketched in Figure 5.2. Now the  $C_M(\alpha)$  curves will be approximated by cubical polynomials in  $\alpha$  near those values of  $\alpha$  for which aerodynamic instabilities occur, that is, near  $\alpha = \alpha_o$  for which  $C_M(\alpha_o) = 0$ . So, it is assumed that

$$C_M(\alpha) = c_1(\alpha - \alpha_o) + c_3(\alpha - \alpha_o)^3, \quad (5.2.8)$$

where  $c_1 < 0$  and  $c_3 > 0$ . Further it is assumed that the position of the water ridge on the oscillator varies in time according to the following formula

$$\alpha_s - \alpha_o = f(t) = A \cos(\omega t) = A \cos\left(\frac{\omega}{\omega_\theta} \tau\right), \quad (5.2.9)$$

where  $A$  is an amplitude related to the position of the water ridge, and  $\omega$  is the frequency of the movement of the water ridge. By putting  $\frac{\omega}{\omega_\theta} = \Omega = 1 + \epsilon\eta$ , where

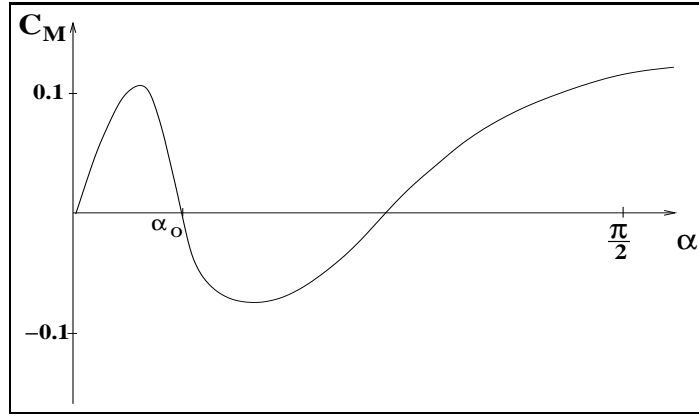


**Figure 5.2:** The aerodynamic torsion coefficient  $C_M(\alpha)$ .

$\eta$  is a detuning parameter and by introducing the transformation  $\Omega\tau = \sigma$  it follows that (5.2.7) can be rewritten in

$$\frac{d^2\theta}{d\sigma^2} + \Omega^{-2}\theta = \epsilon\left[\frac{\mu^2}{\Omega^2} - 2\frac{\mu}{\Omega}\frac{d\theta}{d\sigma}\sin\theta + \left(\frac{d\theta}{d\sigma}\right)^2\right]C_M(\alpha) - 2\frac{\beta_\theta}{\Omega}\frac{d\theta}{d\sigma} \quad (5.2.10)$$

or in

$$\frac{d^2\theta}{d\sigma^2} + \theta = \epsilon\left[\mu^2 - 2\mu\frac{d\theta}{d\sigma}\sin\theta + \left(\frac{d\theta}{d\sigma}\right)^2\right]C_M(\alpha) - 2\beta_\theta\frac{d\theta}{d\sigma} + 2\eta\theta] + O(\epsilon^2) \quad (5.2.11)$$

with

$$\alpha - \alpha_o = A\cos\sigma + \theta - \arctan\left(\frac{\frac{d\theta}{d\sigma}\cos\theta}{\mu\Omega^{-1} - \frac{d\theta}{d\sigma}\sin\theta}\right). \quad (5.2.12)$$

It should be observed that in (5.2.10) and in (5.2.11) it has been assumed that the frequency  $\omega$  of the position of the water ridge on the surface of the oscillator and the frequency  $\omega_\theta$  of the oscillator itself are close to each other. Furthermore, it is assumed that  $\theta$  and  $\frac{d\theta}{d\sigma}$  are small such that (5.2.12) can be expanded in a Taylor series in  $\theta$  and  $\frac{d\theta}{d\sigma}$  (around  $\theta = 0$  and  $\frac{d\theta}{d\sigma} = 0$ ). Then by substituting (5.2.8) into (5.2.11) and by setting

$$\begin{aligned} \theta(\sigma) &= y_1(\sigma)\cos(\sigma) + y_2(\sigma)\sin(\sigma), \\ \frac{d\theta(\sigma)}{d\sigma} &= -y_1(\sigma)\sin(\sigma) + y_2(\sigma)\cos(\sigma), \end{aligned} \quad (5.2.13)$$

and by using the Taylor expansion of (5.2.12) a system of two first order ordinary differential equations for  $y_1$  and  $y_2$  is obtained. In this system for  $y_1$  and  $y_2$  all terms of degree four and higher are neglected. Then, by applying the first order averaging method to the so-obtained equations for  $y_1$  and  $y_2$ , one finally obtains

$$\begin{aligned} \dot{\bar{y}}_1 &= \epsilon\left[(-\mu p_1 - \beta_\theta)\bar{y}_1 - \mu^2 p_1 \bar{y}_2 - 2\mu A p_2 \bar{y}_1^2 + 2\mu A p_2 \bar{y}_2^2 + \right. \\ &\quad \left. 2A(p_2 - 3p_5)\bar{y}_1\bar{y}_2 - \frac{1}{\mu}(p_3 + 3p_4 + \frac{1}{2}p_o(9\mu^2 + 4))\bar{y}_1^3 - \right. \\ &\quad \left. (p_3 + 6p_o)\bar{y}_2^3 - (p_3 - 6p_o)\bar{y}_1^2\bar{y}_2 - \right] \end{aligned} \quad (5.2.14)$$



$$\begin{aligned}
& \frac{1}{\mu}(p_3 + 3p_4 - \frac{1}{2}p_o(9\mu^2 - 12))\bar{y}_1\bar{y}_2^2] - \epsilon\eta\bar{y}_2, \\
\dot{\bar{y}}_2 = & \epsilon[\mu^2 Ap_1 + \mu^2(p_1 + 12p_o)\bar{y}_1 - (\mu(p_1 + 12p_o) + \beta_\theta)\bar{y}_2 + \\
& A(p_2 + 9p_5)\bar{y}_1^2 - A(3p_2 + 3p_5 + 2p_o)\bar{y}_2^2 - 4\mu A(p_2 + p_o)\bar{y}_1\bar{y}_2 + \\
& (p_3 + 6p_o)\bar{y}_1^3 - \frac{1}{\mu}(p_3 + 3p_4 + \frac{1}{2}p_o(9\mu^2 + 20))\bar{y}_2^3 - \\
& \frac{1}{\mu}(p_3 + 3p_4 + \frac{1}{2}p_o(27\mu^2 + 6))\bar{y}_1^2\bar{y}_2 + (p_3 + 18p_o)\bar{y}_1\bar{y}_2^2] + \epsilon\eta\bar{y}_1,
\end{aligned}$$

where  $\bar{y}_1$  and  $\bar{y}_2$  are order  $\epsilon$  accurate approximations of  $y_1$  and  $y_2$  respectively on time-scales of order  $\frac{1}{\epsilon}$ , and where

$$\begin{aligned}
p_o &= \frac{1}{16}c_3A^2, \quad p_1 = \frac{1}{2}c_1 + \frac{3}{8}c_3A^2, \quad p_2 = \frac{1}{8}c_1 + \frac{3}{8}c_3 + \frac{1}{16}c_3A^2, \\
p_3 &= \frac{1}{4}c_1 + \frac{3}{8}c_3 + \frac{3}{8}c_3\mu^2, \quad p_4 = \frac{1}{16}c_1\mu^2, \quad p_5 = \frac{1}{8}c_3\mu^2.
\end{aligned}$$

For a water ridge with a fixed position (that is, for  $f(t) \equiv 0$  and so  $A = 0$ ) system (5.2.14) can be rewritten in a more simple form by introducing the polar coordinates  $\bar{y}_1 = r \cos \varphi$  and  $\bar{y}_2 = r \sin \varphi$ , yielding

$$\begin{aligned}
\dot{r} &= \epsilon r[q_1 - q_2 r^2], \\
\dot{\varphi} &= \epsilon[\eta + \frac{1}{2}\mu^2 c_1 + p_3 r^2],
\end{aligned} \tag{5.2.15}$$

where  $q_1 = -\frac{1}{2}\mu c_1 - \beta_\theta$  and  $q_2 = \frac{1}{\mu}(p_3 + 3p_4)$ . It is obvious from (5.2.15) that a limit cycle will occur when  $q_1$  and  $q_2$  have the same sign. When  $q_1$  and  $q_2$  have different signs it is also obvious that no limit cycles will occur, and that the origin can be the only critical point of (5.2.15). In the next two sections the influence of the movement of the water ridge on the surface of the cylinder will be studied for the following two cases : case I with  $q_1 < 0$  and  $q_2 < 0$  and case II with  $q_1 < 0$  and  $q_2 > 0$ .

### 5.3 Case I : $q_1 < 0$ and $q_2 < 0$

In this section the following choice for the parameters has been made  $\mu = 1$ ,  $c_1 = -3$ ,  $c_3 = 2$ ,  $\beta_\theta = 1$ ,  $\eta = 0$  or  $\eta \neq 0$  and  $A$  is a parameter. This choice turned out to be representative for the behaviour of the solution of system (5.2.14), that is, for other values of the parameters the behaviour of the solutions is more or less similar. Firstly it is assumed that  $\eta = 0$ . It is obvious that the number of critical point of (5.2.14) is a function of  $A$ . By using a Gröbner basis algorithm in the software package Maple the relation between  $A$  and the critical points  $(\bar{y}_1, \bar{y}_2)$  of system (5.2.14) can be determined, and is given in Figure 5.3. For some values of  $A$  the phase portraits of the system (5.2.14) are given in Figure 5.4, where the horizontal axis is the  $\bar{y}_1$ -axis, and the vertical axis is the  $\bar{y}_2$ -axis. The label  $S$  and  $U$  in Figure 5.3 are related to the stable and unstable critical points respectively. Part of the curve in Figure 5.3a with label  $U_1$  should be combined with that part of the curve in Figure 5.3b

with label  $U_1$  and so on. The end points of each labeled curve are determined by  $\frac{d\bar{y}_i}{dA} = \pm\infty$ . From Figure 5.3 and from Figure 5.4 it can be seen that the number of critical points of system (5.2.14) varies when the value of  $A$  is varied. In fact for increasing  $A$  the following can be observed :

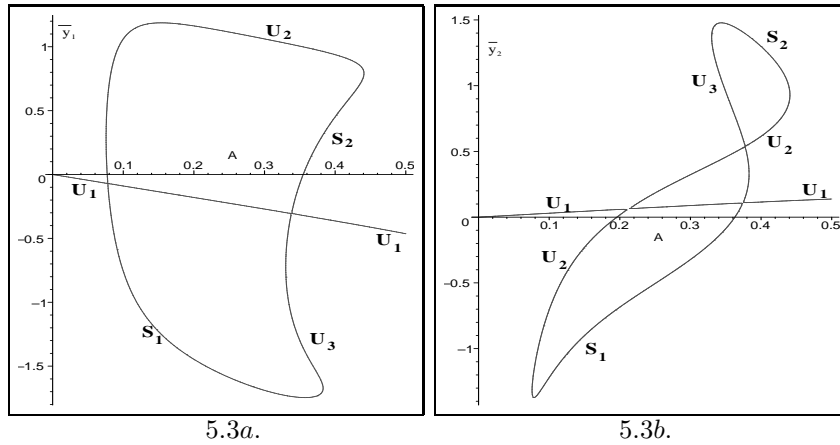


**Figure 5.3:** Critical points  $(\bar{y}_1, \bar{y}_2)$  of system (5.2.14) as function of  $A$ , where  $\mu = 1$ ,  $c_1 = -3$ ,  $c_3 = 2$ ,  $\beta_\theta = 1$  and  $\eta = 0$ .

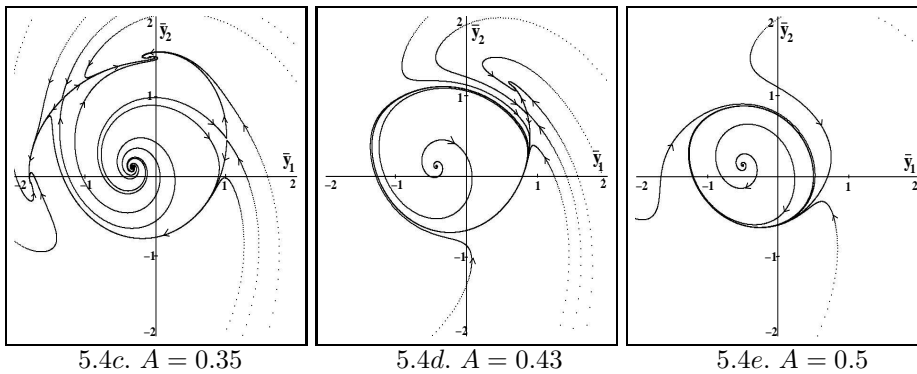
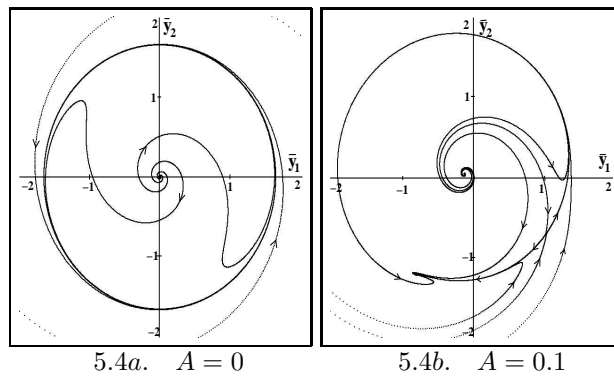


**Figure 5.4:** The phase portraits of system (5.2.14) for several values of  $A$ , and  $\mu = 1$ ,  $c_1 = -3$ ,  $c_3 = 2$ ,  $\beta_\theta = 1$  and  $\eta = 0$ .

$(1cp + \text{a stable limit cycle}) \rightarrow 2cp \rightarrow 3cp \rightarrow 4cp \rightarrow 5cp \rightarrow 4cp \rightarrow$   
 $(3cp + \text{a stable limit cycle}) \rightarrow (2cp + \text{a stable limit cycle})$   
 $\rightarrow (1cp + \text{a stable limit cycle}),$

where 'cp' is an abbreviation for critical point(s). When  $A = 0$  there is one unstable critical point (the origin) and one stable limit cycle. By increasing  $A$  the limit cycle will disappear, but for larger values of  $A$  it will re-appear. A stable or unstable critical point corresponds with a stable or unstable periodic solution in the original equation (5.2.11) and a limit cycle corresponds with a modulated oscillation in the original equation.

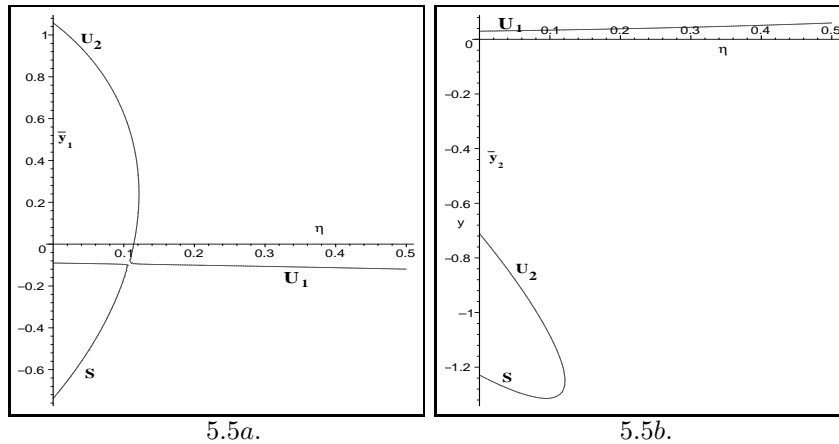


**Figure 5.5:** Critical points  $(\bar{y}_1, \bar{y}_2)$  of system (5.2.14) as a function of  $\eta$ , where  $\mu = 1$ ,  $c_1 = -3$ ,  $c_3 = 2$ ,  $\beta_\theta = 1$  and  $A = 0.1$ .

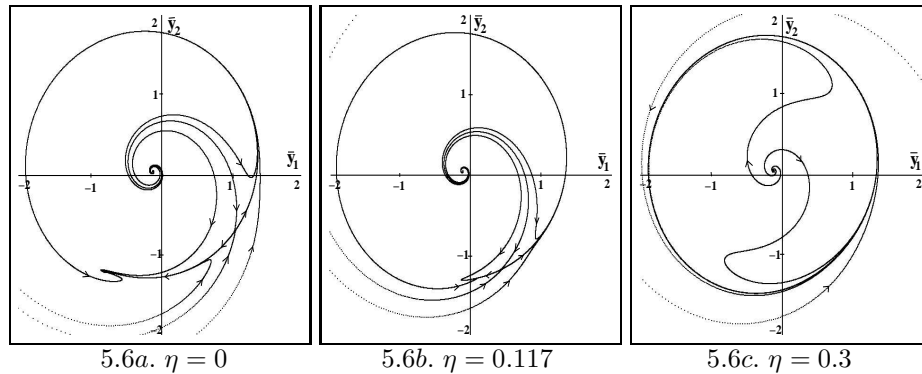


**Figure 5.6:** The phase portraits of system (5.2.14) for several values of  $\eta$ , where  $\mu = 1$ ,  $c_1 = -3$ ,  $c_3 = 2$ ,  $\beta_\theta = 1$  and  $A = 0.1$ .

Now the effect of the detuning parameter will be studied, and the other parameters are kept fixed, that is, the following choice is made  $\mu = 1$ ,  $c_1 = -3$ ,  $c_3 = 2$ ,  $\beta_\theta = 1$ ,  $A = 0.1$  and  $\eta$  is varied. It is obvious that the number of critical points of system (5.2.14) will depend on  $\eta$ . Again by using the Gröbner basis algorithm the dependence of the number of critical points on  $\eta$  can be determined and is given in Figure 5.5. It can be observed from Figure 5.5 that the number of critical points of system (5.2.14) now decreases from 3 to 1 when  $\eta$  increases from 0. The phase portraits of system (5.2.14) for several values of  $\eta$  are given in Figure 5.6. It can be observed from Figure 5.5 and Figure 5.6 that a saddle-node bifurcation occurs when the value of  $\eta$  is around 0.125. For smaller values of  $\eta$  there will be 3 critical points, and for larger values there will be one critical point and a limit cycle. For the original equation (5.2.11) this implies that for  $0 \leq \eta < 0.125$  three periodic solutions

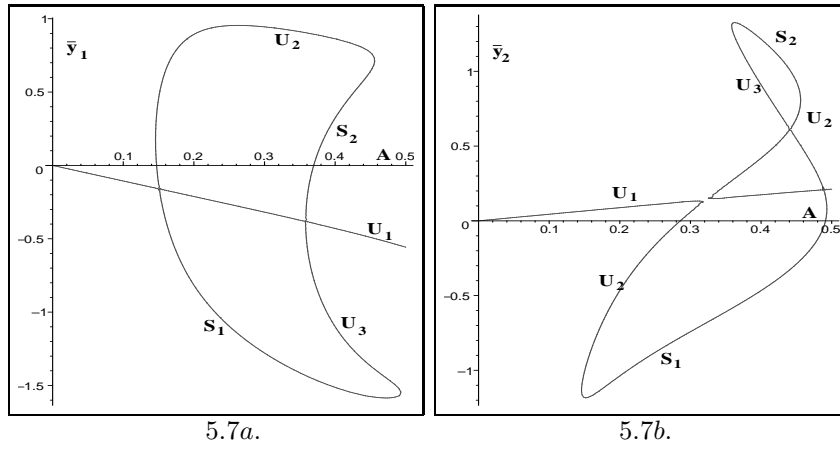


**Figure 5.7:** Critical points  $(\bar{y}_1, \bar{y}_2)$  of system (5.2.14) as a function of  $A$  where  $\mu = 1$ ,  $c_1 = -3$ ,  $c_3 = 2$ ,  $\beta_\theta = 1$  and  $\eta = 0.3$ .

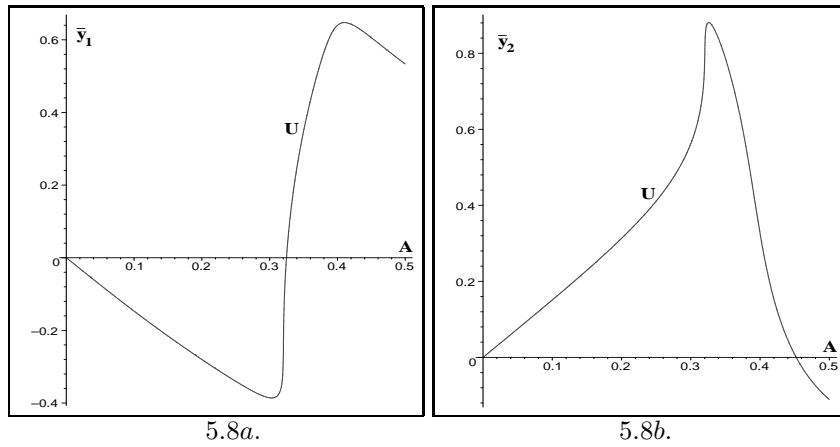


**Figure 5.8:** Critical points  $(\bar{y}_1, \bar{y}_2)$  of system (5.2.14) as a function of  $A$  where  $\mu = 1$ ,  $c_1 = -3$ ,  $c_3 = 2$ ,  $\beta_\theta = 1$  and  $\eta = 1$ .

will exist ( two unstable and one stable), that for  $\eta$  approximately equal to 0.125 a stable and an unstable periodic solution will coincide, and that for  $\eta$  larger than 0.125 one unstable periodic solution and a modulated solution will exist. The effect of the detuning parameter  $\eta$  on the positions of the critical points in system (5.2.14) can also be seen in Figure 5.7 and in Figure 5.8. In Figure 5.7  $\eta$  taken to be equal to 0.3, and the results on the position of the critical points can readily be compared with those obtained in Figure 5.3 for  $\eta = 0$ .

## 5.4 Case II : $q_1 < 0$ and $q_2 > 0$

For  $A = 0$  there is only one critical point (stable) of system (5.2.14) as has been shown at the end of section 5.2. In this section the following choice for the parameters has been made  $\mu = 1$ ,  $c_1 = -2$ ,  $c_3 = 2$ ,  $\beta_\theta = 2$  and  $A$  is a parameter. By using a Gröbner basis algorithm in the software package Maple the relation between  $A$  and the critical points  $(\bar{y}_1, \bar{y}_2)$  of system (5.2.14) can be determined, and is given in

Figure 5.9 for  $\eta = 0$  and in Figure 5.10 for  $\eta = 3$ . Also for some values of  $A$  the phase portraits of system (5.2.14) are given in Figure 5.11. The results as given in these figures imply that for the given set of parameters only one critical point will occur, which is stable. For the original equation (5.2.11) these results imply that a stable periodic solution will exist.

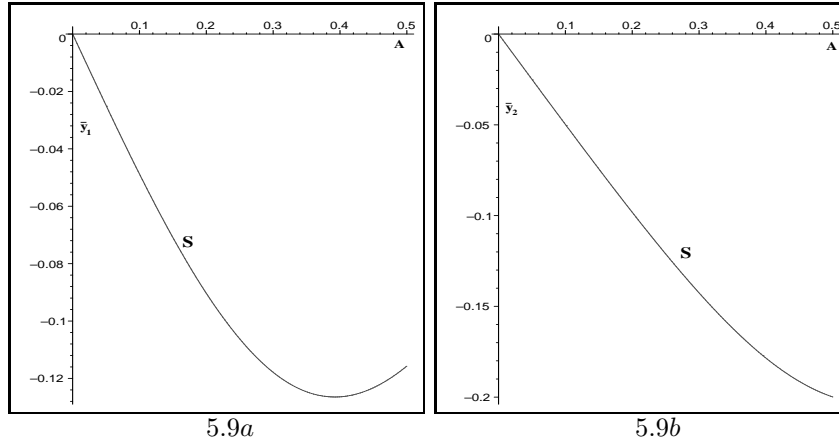


**Figure 5.9:** Critical points  $(\bar{y}_1, \bar{y}_2)$  of system (5.2.14) as a function of  $A$ , where  $\mu = 1$ ,  $c_1 = -2$ ,  $c_3 = 2$ ,  $\beta_\theta = 2$  and  $\eta = 0$ .

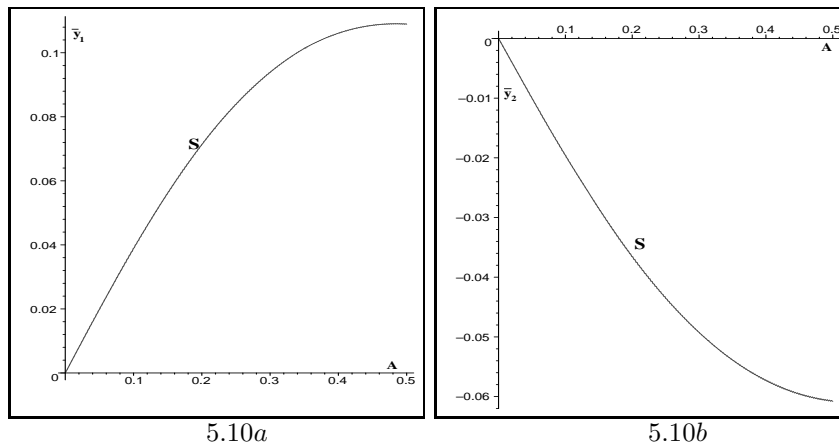


**Figure 5.10:** Critical points  $(\bar{y}_1, \bar{y}_2)$  of system (5.2.14) as a function of  $A$ , where  $\mu = 1$ ,  $c_1 = -2$ ,  $c_3 = 2$ ,  $\beta_\theta = 2$ ,  $\eta = 3$ .

## 5.5 Conclusion

In this chapter the rain-wind induced vibration of a seesaw oscillator have been studied. The model equations have been derived under the assumption that the position of the rivulet of water on the oscillator varies harmonically in time. The eigenfrequency of the oscillator and the frequency of the movement of the water rivulet on the oscillator are assumed to be close to each other. In case  $I$  that is in

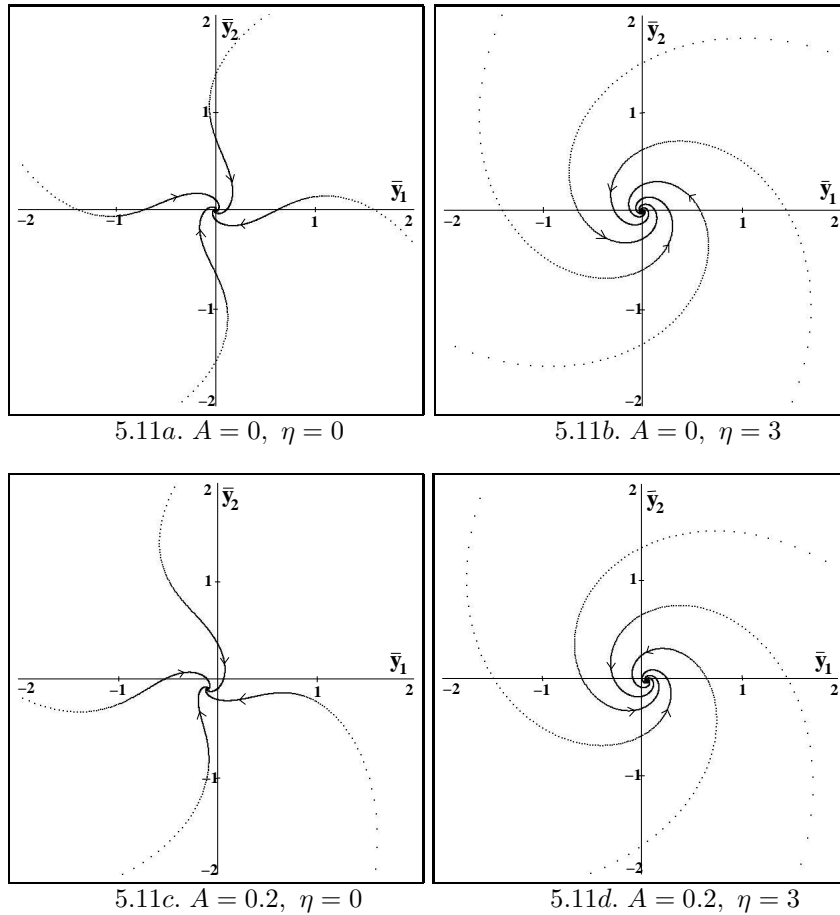


**Figure 5.11:** The phase portraits of system (5.2.14) for  $\mu = 1$ ,  $c_1 = -2$ ,  $c_3 = 2$ ,  $\beta_\theta = 2$ , and for different values of  $A$  and  $\eta$ .

case that the system has a limit cycle when  $A = 0$ , several Hopf and saddle-node bifurcations occur when  $A$  (the amplitude of the movement of the water rivulet on the oscillator) and  $\eta$  (a detuning parameter) are varied. When  $\eta$  is large a limit cycle occurs and it corresponds with a modulated oscillation in the original system. However, in case *II* no bifurcation occurs when  $A$  and  $\eta$  are varied. For some sets of the parameters in the model equations the existence and the stability of the periodic or of the modulated vibrations have been established.

# Bibliography

- [1] W.W. Adams and P. Loustau. *An Introduction to Grobner Bases*. American Mathematical Society, USA, 1994.
- [2] D. B. Batchelor. Parametric resonance of systems with time-varying dissipation. *Appl. Phys. Lett.*, 29:280–281, 1976.
- [3] R. D. Blevins. *Flow-induced vibrations*. Van Nostrand Reinhold Company, New York, 1977.
- [4] J. A. Ellison, A. W. Saenz, and H. S. Dumas. Improved  $n$ th order averaging theory for periodic systems. *J. Differential Equation*, 84:383–403, 1990.
- [5] R. Grimshaw. *Nonlinear Ordinary Differential Equations*. CRC Press Inc, Florida, 1993.
- [6] M. Gu and Q. Lu. Theoretical analysis of wind-rain-induced vibration of cables of cable-stayed bridges. *APCWE-5, J. Wind Eng*, 81:125–128, 2001.
- [7] T.I. Haaker. *Quasi-steady Modelling and Asymptotic Analysis of Aeroelastic Oscillators*. PhD thesis, Delft University of Technology, 1996.
- [8] T.I. Haaker and A.H.P. van der Burgh. On the dynamics of aeroelastic oscillators with one degree of freedom. *SIAM J. Appl. Math.*, 54:1033–1047, 1994.
- [9] Hartono and A. H. P. van der Burgh. Periodic solutions of an inhomogeneous second order equation with time-dependent damping coefficient. In *Proceedings of the 8th Biennial ASME Conference, Symposium on Dynamics and Control of Time-Varying Systems and Structures*, pages 1–9, Pittsburgh, Pennsylvania, USA, September 9-12, 2001. ASME.
- [10] Hartono and A.H.P. van der Burgh. Higher-order averaging: periodic solutions, linear systems and an application. *Nonlinear Analysis*, 52:1727–1744, 2003.
- [11] Hartono and A.H.P. van der Burgh. A linear differential equation with a time-periodic damping coefficient: stability diagram and an application. *Journal of Engineering Mathematics*, 49(2):99–112, 2004.

- [12] Hartono and W. T. Van Horssen. Rain-wind induced vibrations of a seesaw oscillator. *Submitted for publication*, 2004.
- [13] Y. Hikami and N. Shiraishi. Rain-wind induced vibrations of cables in cable stayed bridges. *Journal of Wind Engineering and Industrial Aerodynamics*, 29:409–418, 1988.
- [14] H. Hochstadt. A direct and inverse problem for a hill's equation with double eigenvalues. *Journal of Mathematical Analysis and Applications*, 66:507–513, 1978.
- [15] H. Lumbantobing and T. I. Haaker. Aeroelastic oscillations of seesaw-type oscillator under strong wind conditions. *Journal of Sound and Vibration*, 257(3):439–456, 2002.
- [16] W. Magnus and S. Winkler. *Hill's Equation*. John Wiley & Sons, Inc., New York, 1966.
- [17] M. Matsumoto, N. Shiraishi, M. Kitazawa, C. Knisely, H. Shirato, Y. Kim, and M. Tsujii. Aerodynamic behavior of inclined circular cylinders-cable aerodynamics. *Journal of Wind Engineering and Industrial Aerodynamics*, 33:63–72, 1990.
- [18] M. Matsumoto, M. Yamagishi, J. Aoki, and N. Shiraishi. Various mechanism of inclined cable aerodynamics. In *International Association for Wind Engineering Ninth International Conference on Wind Engineering*, pages 759–770, New Delhi, 1995.
- [19] R. Mennicken. On the convergence of infinite hill-type determinants. *Archive for Rational Mechanics and Analysis*, 29:12–37, 1968.
- [20] J. A. Murdock. *Perturbations: theory and methods*. John Wiley & Sons, Inc., New York, 1991.
- [21] Y. Nakamura and T. Mizota. Torsional flutter of rectangular prisms. *J. Engng. Mech. Div., ASCE*, 101:125–142, 1975.
- [22] A. H. Nayfeh and D. T. Mook. *Nonlinear Oscillations*. John Wiley & Sons, New York, 1985.
- [23] R.H. Rand and S.F. Tseng. On the stability of a differential equation with application to the vibrations of a particle in the plane. *Journal of Applied Mechanics*, pages 311–313, 1969.
- [24] R.H. Rand and S.F. Tseng. On the stability of the vibrations of a particle in the plane restrained by two non-identical springs. *Int. J. Non-Linear Mechanics*, 5:1–9, 1970.
- [25] J. A. Sanders and F. Verhulst. *Averaging Methods in Nonlinear Dynamical Systems*. Springer-Verlag New York Inc., New York, 1985.



- [26] C. Seidel and D. Dinkler. Regen-wind-induzierte schwingungen - ursache und dreibung. *Proc. Appl. Math. Mech.*, 2:76–77, 2003.
- [27] C.G.A. Van der Beek. *Asymptotic Analysis of Wind-Induced Vibrations*. PhD thesis, Delft University of Technology, 1989.
- [28] A. H. P. Van der Burgh. Rain-wind induced vibrations of a simple oscillator. In *Proceedings of the 8th Biennial ASME Conference, Symposium on Dynamics and Control of Time-Varying Systems and Structures*, pages 1–9, Pittsburgh, Pennsylvania, USA, September 9-12, 2001. ASME.
- [29] A. H. P. Van der Burgh and Hartono. Rain-wind induced vibrations of a simple oscillator. *International journal of non-linear mechanics*, 39:93–100, 2004.
- [30] A. H. P. Van der Burgh, Hartono, and A. K. Abramian. A new model for the study of rain-wind induced vibrations of a simple oscillator. *Submitted for publication*, 2004.
- [31] A.H.P. Van der Burgh. *Nonlinear Dynamics of Structures Excited by Flows: Quasi-steady Modeling and Asymptotic Analysis in Fluid-Structure Interactions in Acoustics, CISM Courses and Lectures No. 396*. Springer Wien New York, New York, 1999.
- [32] F. Verhulst. *Nonlinear Differential Equations and Dynamical Systems*. Springer-Verlag New York Inc., New York, 2000.
- [33] C. Verwiebe and H. Ruscheweyh. Recent research results concerning the exciting mechanism of rain-wind induced vibrations. In *Proc. 2nd European and African Conference on Wind Engineering, G.Solari (ed.)*, pages 1783–1790, SGE Padova, 1997.
- [34] S. B. Waluya and W. T. Van Horssen. Asymptotic approximations of first integrals for a nonlinear oscillator. *Nonlinear Analysis TMA*, 51(8):1327–1346, 2002.
- [35] K. Wilde and W. Witkowski. Simple model of rain-wind induced vibrations of stayed cables. *Journal of Wind Engineering and Industrial Aerodynamics*, 91:409–418, 2003.
- [36] Y. L. Xu and L. Y. Wang. Analytical study of wind-rain induced cable vibration: Sdof model. *Journal of Wind Engineering and Industrial Aerodynamics*, 91:27–40, 2003.



# Summary

In this thesis simple mathematical models are derived to describe the rain-wind induced vibrations of elastic structures such as cables or bridges. All models will be described by weakly nonlinear ordinary differential equations with time dependent coefficients. This time dependence is due to the assumption that the position and the mass of the water rivulet on the surface of the elastic structure varies in time. As models for these elastic structures oscillators of spring-type or of see-saw type are chosen. First order and higher order averaging techniques, strained parameter methods, and numerical methods are used to study the existence and the stability of time-periodic vibrations or of modulated vibrations for these oscillators. Several types of bifurcations will occur when for instance the amplitude of the position of the water rivulet on the surface of the oscillator is varied.



# Samenvatting

In dit proefschrift worden eenvoudige wiskundige modellen afgeleid om regen- en wind-geïnduceerde trillingen van elastische structuren, zoals kabels en bruggen, te beschrijven. Alle modellen worden beschreven door zwak niet-lineaire normale differentiaalvergelijkingen met tijdsafhankelijke coëfficiënten. Deze tijdsafhankelijkheid komt voort uit de aanname dat de positie en de massa van waterstroompjes aan het oppervlak van de structuren variëren in de tijd. Als model voor elastische structuren zijn oscillatoren van het veer- en het wip (“see-saw”) -type gekozen. Om het bestaan en de stabiliteit van oplossingen van periodieke of gemoduleerde trillingen van de oscillatoren te bestuderen, worden eerste- en hogere-orde middelingstechnieken, “strained parameter”- en numerieke methoden gebruikt. Verschillende typen bifurcaties treden op wanneer bijvoorbeeld de amplitude van de positie van het waterstroompje op het oppervlak van de oscillator wordt gevarieerd.



# Acknowledgments

As author of this thesis, I wish to thank the PGSM Jakarta and the CICAT organization of the TU Delft for financial support during my research project. I am indebted to my daily supervisor Dr. ir. A.H.P. van der Burgh (since october 1998 till december 2002) for his patience in guiding me to do research. I am also indebted to Dr. ir. Wim T. van Horsen (my daily supervisor since january 2003) for his guidance to finish this thesis and for being my adjunct promotor. Further, I wish to express my gratitude to my promotor Prof. dr. ir. A. W. Heemink for his careful reading of my thesis.

For many interesting discussions on mathematics and its applications I also would like to thank Prof. dr. F. Verhulst, Prof. dr. J. J. Duistermaat, Dr. ir. T. I. Haaker, and Prof. A. K. Abramian.

In addition, I would like to thank all members of the Department of Applied Mathematics, Delft University of Technology for their hospitality and especially Xander for his help to translate the summary and the propositions in Dutch.

Also all my friends ( of the PGSM group and of the Indonesian community in Delft) I would like to thank for their kindness and friendliness.

Finally, I thank my family for their patience during my stay in Delft, far away from you.





# Curriculum Vitae

Hartono was born on March 29, 1962 in Kediri, East Java, Indonesia. He finished his high school education in 1981 in Pare - Kediri and continued his study in the Department of Mathematics of the Gadjah Mada University Yogyakarta. He obtained his bachelor degree in 1986 and then since 1987 he was working as a lecturer at the Department of Mathematics IKIP Yogyakarta (nowadays known as State University of Yogyakarta). His master degree in mathematics was obtained from Bandung Institute of Technology in 1994. Since October 1998 till June 2004 he was on leave from Indonesia as a PhD researcher at the Department of Applied Mathematical Analysis, Delft University of Technology, The Netherlands.